



Technische Universität München

TUM School of Life Sciences

# **Maximizing risk prediction by synthesizing multiple data sets accommodating systematic missing data and heterogeneous scales**

Matthias Josef Philipp Neumair

Vollständiger Abdruck der von der TUM School of Life Sciences der Technischen Universität München zur Erlangung des akademischen Grades eines

Doktors der Naturwissenschaften (Dr. rer. nat.)

genehmigten Dissertation.

Vorsitz:

Prof. Aurélien Tellier

Prüfer\*innen der Dissertation:

1. Prof. Donna Ankerst, Ph.D.

2. Assoc. Prof. Jonathan Gelfond, Ph.D.

Die Dissertation wurde am 15. September 2022 bei der Technischen Universität München eingereicht und durch die TUM School of Life Sciences am 29. November 2022 angenommen.



# Summary

Statistical analyses highly depend on the data quality and sample size. A common approach to increasing the sample size in clinical trials is to include data from multiple institutions. Additionally, for lots of hypotheses, it is not sufficient to use only one data source. However, this approach creates new challenges since data is collected and reported differently. Data from different sources are often on a different scale and miss-aligned with the primary data. Treating this defiance additionally to high missing data and rare events were investigated in this thesis and were shown in three studies from different study areas: prostate cancer, forestry, and fatal mountain accidents.

The prostate cancer study was based on the risk factor and outcome data collected from January 2006 to December 2019 from trans-rectal systematic ten to twelve core biopsies. Biopsy data from ten Prostate Biopsy Collaborative Group (PBCG) cohorts spanning North America and Europe were used for training. One European PBCG cohort was used for validation. The study aimed to improve individualized risk predictions from the previous PBCG tool, which a broader range of patients could apply by allowing missing and additional risk factors at the user end. The previous risk tool included the six common risk factors: prostate-specific antigen, digital rectal exam, age, African ancestry, first-degree prostate cancer family history, and history of a prior negative prostate biopsy. The developed risk calculator additionally includes prostate volume, Hispanic ethnicity, 5-alpha-reductase inhibitor use, second-degree prostate cancer family history, and first-degree breast cancer family history. Four philosophically distinct approaches were applied to combine multiple cohorts with high missingness: available case analyses, ensembles of cohort-specific models, missing indicator methods, and imputation. Six variations of these multivariable logistic regression approaches were compared by internal leave-one-cohort-out cross-validation and one external cohort validation. We chose the available cases method for implementing the online risk tool since it showed the highest accuracy in calibration in external validation, where all six methods indicated an equivalent area under the receiver operating characteristic curve (AUC). AUC and calibration-in-the-large across the ten cohorts used as test sets in the internal leave-one-cohort-out cross-validation were also similar, and the available cases method had the lowest variability. The resulting risk calculator is published online at [riskcalc.org](http://riskcalc.org) to facilitate its use in daily routine.

The fatal mountain accidents study combined two data sets. The first data set comprised 3,285 fatal accidents in the Austrian mountains for twelve years, from November 2006 to October 2018. These data were combined with weather information of 43 weather stations located 900 meters above sea level to mirror regions typical for mountain sports. Four approaches were compared to combine the two data sets and handle the incomplete weather information and miss-alignment of locations. These approaches excluded too far cases, weather stations with high missing data, or imputed values from the next station. Results were similar in magnitude and significance, and the imputation approach was used

for analyses as it maximizes sample sizes. Weather information was analyzed by anomalies and comprised temperature, air pressure, relative humidity, radiation, precipitation, wind, cloudiness, and snow. Analyses were performed with data of all stations pooled by season, discipline, or activity. Multivariable logistic regression with the outcome of whether one or more fatal accidents occurred on a day versus not was used for detecting the risk of a fatal accident as a function of weather variables. Only the most predictive of similar weather variables was selected in the final models to avoid multi-collinearity. The weather characteristics underlined that warmer, sunnier, and dryer days with reduced wind speed and preferably higher air pressure were more associated with fatal accidents in summer. Associations between weather patterns and fatal mountain accidents detected in this observational study may be mediated by the influence of weather and its interaction with the season on visitor numbers. Skiers are less likely to visit mountains on low-snow days in the winter, which would reduce overall fatal accidents. Conversely, less mountain snow may favor spring hikes, leading to more visitors and accidents due to improper equipment.

Similarly, the forestry study combined weather data with tree mortality data of Europe's nine most common tree species (European beech, sessile oak, pedunculated oak, silver birch, black pine, Austrian oak, Scots pine, European hornbeam, and Norway spruce). Overall, 746,478 tree-year observations from 32 countries were analyzed. These observations came from 130,018 trees from 8,618 plots over ten years from 2011 to 2020. Information on stand age and aspect were combined with weather from the ClimateEU data, which adjusts for elevation at locations. Bioclimatic variables such as temperature, precipitation, and continentality were considered for different periods up to three years before tree death, as well as 30-year averages. Because tree death is only observed yearly, meaning that the specific date of the death is not observed and only the cumulative survival over the year, logistic regression can be used to approximate interval-censored survival data analysis. Multi-collinearity among risk factors was reduced by building variable groups according to similarity. For all species except sessile oak, higher 30-year-temperature averages were associated with higher odds of tree mortality. The effect size of other risk factors varied among species, with similar weather associations between Austrian and sessile oak on the one hand and Scots pine, Norway spruce, and pedunculate oak on the other hand. In particular, warmer winters reduced mortality for silver birch, sessile and Austrian oaks while having the opposite association for the other species. Sessile oak was most robust against drought effects and could serve as an important tree species under climate change scenarios.

# Zusammenfassung

Statistische Analysen hängen stark von der Datenqualität und Stichprobengröße ab. Ein gängiger Ansatz bei klinischen Studien zur Erhöhung der Stichprobengröße besteht darin, Daten aus mehreren Institutionen zusammen zufassen. Außerdem reicht es für viele Hypothesen nicht, nur eine Datenquelle heran zu ziehen. Dieser Ansatz führt jedoch zu neuen Herausforderungen, da Daten unterschiedlich gesammelt und gemeldet werden. Daten aus unterschiedlichen Quellen haben oft verschiedene Skalierungen, die nicht mit den Hauptdaten übereinstimmen. Der Umgang mit diesen Unstimmigkeiten, zusätzlich zu der Datenunvollständigkeit und seltenen Ereignissen, wurde in dieser Arbeit untersucht und an drei Studien aus verschiedenen Untersuchungsgebieten veranschaulicht: Prostatakrebs, Forstwirtschaft und tödliche Bergunfälle.

Die Prostatakrebsstudie basiert auf Risikofaktor- und Ergebnisdaten, wurden von Januar 2006 bis Dezember 2019 aus transrektalen systematischen Zehn bis Zwölf Kern Biopsien gesammelt. Für die Modellbildung wurden Zehn Kohorten der Prostate Biopsy Collaborative Group (PBCG) in Nordamerika und Europa verwendet, die auf einer europäischen Kohorte validiert wurden. Das Studienziel war, individualisierte Risikovorhersagen aus dem vorherigen Tool zu verbessern, um eine breitere Zielgruppe von Patienten zu erreichen indem fehlende und zusätzliche Risikofaktoren auf der Benutzeroberfläche zugelassen wurden. Das bisherige Risikotool umfasste die sechs Standardrisikofaktoren: Prostata-spezifisches Antigen, rektale Abtastuntersuchung, Alter, afrikanische Abstammung, Prostatakrebs ersten Grades in der Familienanamnese und Vorgeschichte einer früheren negativen Prostatabiopsie. Der entwickelte Risikorechner umfasst zusätzlich das Prostatavolumen, die hispanische Herkunft, die Verwendung von 5-Alpha-Reduktasehemmer, die familiäre Vorgeschichte von Prostatakrebs zweiten Grades und von Brustkrebs ersten Grades. Um mehrere Kohorten mit vielen fehlenden Werten zu kombinieren, wurden vier methodisch unterschiedliche Ansätze angewandt: verfügbare Fälle, Ensemble von Kohorten spezifischen Modellen, fehlende Indikatormethoden und Imputation. Sechs Variationen dieser multivariablen logistischen Regression Ansätze wurden durch interne Lass-eine-Kohorte-weg-Kreuzvalidierung und externe Kohorte Validierung verglichen. Wir wählten die Methode der verfügbaren Fälle für die Implementierung des Online-Risiko-Tools, da sie die größte Genauigkeit in Bezug auf Kalibrierung bei der externen Validierung zeigte, wobei alle sechs Methoden ein ähnliche Fläche unter der Operationscharakteristik (AUC) zeigten. AUC und Kalibrierung im Großen über die Zehn Kohorten hinweg, die als Testdaten in der internen Lass-eine-Kohorte-weg-Kreuzvalidierung verwendet wurden, waren ebenfalls ähnlich, und die Methode der verfügbaren Fälle hatte die geringste Variabilität. Der resultierende Risikorechner wurde online auf [riskcalc.org](http://riskcalc.org) veröffentlicht, um die Verwendung in der täglichen Routine zu erleichtern.

Die Studie zu tödlichen Bergunfällen kombinierte zwei Datensätze. Der erste Datensatz umfasste 3.285 tödliche Unfälle in den österreichischen Bergen von November 2006 bis Oktober 2018. Um typische Bergsportregionen abzubilden, wurden diese Daten mit

Wetterinformationen von 43 Wetterstationen kombiniert, die über 900 Meter Seehöhe liegen. Um die beiden Datensätze zu kombinieren, wurden vier Ansätze verglichen, die die vielen fehlenden Wetterinformationen und nicht übereinstimmenden Standorte berücksichtigen. Diese Ansätze schlossen zu weit entfernte Fälle, oder Wetterstationen mit vielen Fehlwerten aus, oder imputierte Werte von der nächsten Station, wenn die Informationen fehlten. Die Ergebnisse zeigten ähnliche Effektgrößen und Signifikanzen, und für die Analysen wurde der Imputationsansatz verwendet, da er die Stichprobengrößen maximiert. Wetterinformationen wurden durch Anomalien analysiert und umfassten Temperatur, Luftdruck, relative Luftfeuchtigkeit, Strahlung, Niederschlag, Wind, Bewölkung und Schnee. Die Auswertungen erfolgten mit Daten aller Stationen gebündelt nach Saison, sowie getrennt nach Sportart oder Aktivität. Zur Ermittlung des Risikos eines tödlichen Unfalls in Abhängigkeit von Wettervariablen wurde eine multivariable logistische Regression verwendet mit dem Ergebnis, ob an einem Tag ein oder mehrere tödliche Unfälle stattfanden oder nicht. Um Multikollinearität zu vermeiden, wurde in den finalen Modellen nur die Signifikanteste ähnlicher Wettervariablen ausgewählt. Die Wettereigenschaften unterstrichen, dass wärmere, sonnigere und trockenere Tage mit geringerer Windgeschwindigkeit und höherem Luftdruck im Sommer mit tödlichen Unfällen in Verbindung gebracht wurden. Assoziationen zwischen Wettermustern und tödlichen Bergunfällen, die in dieser Beobachtungsstudie festgestellt wurden, werden möglicherweise mediiert durch den Einfluss des Wetters und seiner Wechselwirkung mit der Jahreszeit auf die Besucherzahlen. Es ist weniger wahrscheinlich, dass Skifahrer an Tagen mit wenig Schnee im Winter die Berge besuchen, was die Zahl der tödlichen Unfälle insgesamt verringert. Umgekehrt kann weniger Bergschnee für Frühlingwanderungen günstiger sein, was zu mehr Besuchern und Unfällen aufgrund schlechter Ausrüstung führen kann.

Die Forststudie kombinierte in ähnlicher Weise Wetterdaten mit Baummortalitätsdaten der neun häufigsten Baumarten in Europa (Rotbuche, Traubeneiche, Stieleiche, Silberbirke, Schwarzkiefer, Österreichische Eiche, Waldkiefer, Europäische Hainbuche und Gemeine Fichte). Insgesamt wurden 746.478 Baum-Jahr Beobachtungen aus 32 Ländern analysiert. Diese Beobachtungen stammen von 130.018 Bäumen aus 8.618 Parzellen von 2011 bis 2020. Informationen zu Bestandsalter und -ausrichtung wurden mit dem Wetter aus den ClimateEU-Daten kombiniert, die sich an die Höhe der Standorte anpassen. Bioklimatische Variablen wie Temperatur, Niederschlag und Kontinentalität wurden für verschiedene Zeiträume bis zu drei Jahre vor dem Absterben der Bäume berücksichtigt, sowie 30-Jahres-Durchschnittswerte. Da der Baumtod nur jährlich, und somit nur das kumulative Überleben über das Jahr beobachtet wird, kann die logistische Regression verwendet werden, um die intervallzensierte Überlebensanalyse anzunähern. Die Multikollinearität zwischen Risikofaktoren wurde reduziert, indem Variabelgruppen nach Ähnlichkeit gebildet wurden. Bei allen Arten mit Ausnahme der Traubeneiche waren höhere 30-Jahres-Temperaturmittelwerte mit einer höheren Wahrscheinlichkeit von Baumsterblichkeit verbunden. Die Effektgröße anderer Risikofaktoren variierte zwischen den Arten, mit ähnlichen Wetterassoziationen zwischen Österreichischer und Traubeneiche einerseits und Waldkiefer, Rotfichte und Stieleiche andererseits. Insbesondere wärmere Winter reduzierten die Sterblichkeit bei Silberbirken, Trauben- und österreichischen Eichen, während es bei den anderen Arten zu einer gegenteiligen Assoziation kam. Die Traubeneiche war am widerstandsfähigsten gegen Dürreeffekte und könnte unter Klimawandelszenarien als wichtige Baumart dienen.

# Table of Contents

<b>Summary</b> . . . . .	<b>III</b>
<b>Zusammenfassung</b> . . . . .	<b>V</b>
<b>Table of Contents</b> . . . . .	<b>VII</b>
<b>List of Figures</b> . . . . .	<b>IX</b>
<b>List of Tables</b> . . . . .	<b>XI</b>
<b>List of Acronyms</b> . . . . .	<b>XIII</b>
<b>1 Introduction</b> . . . . .	<b>1</b>
1.1 Prostate cancer . . . . .	1
1.2 International Prostate Biopsy Collaborative Group . . . . .	2
1.3 Mountain sports in Austria . . . . .	4
1.4 Meteorology in Europe . . . . .	4
1.5 Forestry in Europe . . . . .	7
1.6 Missing data . . . . .	8
1.7 Logistic regression . . . . .	11
1.8 Likelihood ratio test . . . . .	12
1.9 Outline of the thesis . . . . .	12
<b>2 Accommodating heterogeneous missing data patterns for prostate cancer risk prediction</b> . . . . .	<b>13</b>
2.1 Biopsy data . . . . .	15
2.2 Statistical analyses . . . . .	17
2.3 Results . . . . .	23
2.4 Discussion . . . . .	31
2.5 Conclusion . . . . .	35
<b>3 The influence of weather on fatal accidents in the Austrian mountains</b> <b>37</b>	
3.1 Fatal mountain accidents . . . . .	38
3.2 Weather data . . . . .	38
3.3 Statistical analyses . . . . .	43
3.4 Overview of fatalities . . . . .	45
3.5 Weather conditions on days with and without fatalities . . . . .	46
3.6 Multivariate analysis of the influence on fatalities . . . . .	48
3.7 Discussion . . . . .	50
3.8 Conclusion . . . . .	52

<b>4</b>	<b>Drought effects of temperature and precipitation on tree mortality risk</b>	<b>55</b>
4.1	European tree mortality data . . . . .	57
4.2	European weather data . . . . .	58
4.3	Statistical analyses . . . . .	59
4.4	Results . . . . .	61
4.5	Discussion . . . . .	94
4.6	Conclusion . . . . .	99
<b>5</b>	<b>Future outlook . . . . .</b>	<b>101</b>
5.1	Prostate cancer risk tool . . . . .	101
5.2	Austrian mountain sports . . . . .	102
5.3	Climate-based forest management . . . . .	104
<b>6</b>	<b>Acknowledgment . . . . .</b>	<b>109</b>
<b>7</b>	<b>References . . . . .</b>	<b>111</b>



# List of Figures

1.1	Location of the prostate in men with an example of prostate cancer. . .	1
1.2	Google Analytics usage report for the PBCG risk calculator for 2021 from <a href="https://riskcalc.org/PBCG/">https://riskcalc.org/PBCG/</a> . . . . .	3
1.3	Summary of rescued people from the Austrian mountains from 2015 to 2020 . . . . .	4
2.1	Sample sizes of eleven PBCG cohorts ranked by csPCA prevalence. . .	14
2.2	Missing risk factors. . . . .	15
2.3	World map of the eleven PBCG participating institutions collecting prostate biopsy data . . . . .	16
2.4	Comparison of imputation methods . . . . .	22
2.5	Differences between the cohorts in distributions of the risk factors (a) .	24
2.6	Differences between the cohorts in distributions of the risk factors (b) .	25
2.7	Univariate odds ratios for csPCA by variables (a) . . . . .	26
2.8	Univariate odds ratios for csPCA by variables (b) . . . . .	27
2.9	CIL and AUC performing leave-one-cohort-out cross-validation on ten PBCG cohorts. . . . .	28
2.10	Calibration plots with pointwise 95% confidence intervals (CIs) . . . .	30
2.11	Marginal and pairwise comparisons of predictions . . . . .	32
2.12	Model coefficients of available cases method . . . . .	33
2.13	Change in prostate cancer risk according to how many risk factors a patient has available . . . . .	34
2.14	Online risk calculator . . . . .	35
3.1	Locations of fatal mountain accidents . . . . .	39
3.2	Missing weather characteristics by station . . . . .	41
3.3	Data preparation and modeling process . . . . .	44
3.4	Austrian mountain fatal accidents by month . . . . .	45
3.5	Distribution of fatal accidents by discipline . . . . .	46
3.6	Distribution of fatal accident characteristics . . . . .	47
3.7	Fatal accidents by years . . . . .	48
3.8	Differences in means of meteorological variables . . . . .	49
3.9	Proportion of precipitation types . . . . .	50
3.10	Proportion of wind directions for two selected wind speeds . . . . .	51
3.11	Proportion of snow types . . . . .	52
4.1	Annual mortality by species . . . . .	62
4.2	Annual values in winter and spring weather variables and mortality . . .	63
4.3	Annual values in summer weather variables and mortality . . . . .	64
4.4	Odds ratio estimates based on stand and weather characteristics . . . .	65
4.5	Dendrogram for similar tree species . . . . .	66

4.6	Annual values of weather variables and mortality for European beech . . .	67
4.7	Spatial evaluation of modeled tree mortality for European beech . . . . .	69
4.8	Annual values of weather variables and mortality for Black pine . . . . .	70
4.9	Spatial evaluation of modeled tree mortality for Black pine . . . . .	72
4.10	Annual values of weather variables and mortality for Norway spruce . . .	73
4.11	Spatial evaluation of modeled tree mortality for Norway spruce . . . . .	75
4.12	Annual values of weather variables and mortality for Scots pine . . . . .	76
4.13	Spatial evaluation of modeled tree mortality for Scots pine . . . . .	78
4.14	Annual values of weather variables and mortality for Silver birch . . . . .	79
4.15	Spatial evaluation of modeled tree mortality for Silver birch . . . . .	81
4.16	Annual values of weather variables and mortality for Austrian oak . . . . .	82
4.17	Spatial evaluation of modeled tree mortality for Austrian oak . . . . .	84
4.18	Annual values of weather variables and mortality for European hornbeam	85
4.19	Spatial evaluation of modeled tree mortality for European hornbeam . . .	87
4.20	Annual values of weather variables and mortality for Pedunculate oak . . .	88
4.21	Spatial evaluation of modeled tree mortality for Pedunculate oak . . . . .	90
4.22	Annual values of weather variables and mortality for Sessile oak . . . . .	91
4.23	Spatial evaluation of modeled tree mortality for Sessile oak . . . . .	93
5.1	Exponential spatial basis function . . . . .	106

# List of Tables

2.1	Methods for fitting individual predictor-specific risk models. . . . .	18
2.2	Algorithms for the six risk modeling approaches. . . . .	19
2.3	External validation CIL and AUC values . . . . .	29
2.4	Odds ratios from the largest, standard, and smallest models. . . . .	30
3.1	Description of meteorological variables . . . . .	40
3.2	Sensitivity analysis for model selection. . . . .	42
3.3	Multivariable logistic regression model associations between weather variables and fatal accidents for summer and winter disciplines. . . . .	54
4.1	Tree mortality classification. . . . .	58
4.2	European tree species . . . . .	59
4.3	Weather characteristics . . . . .	60
4.4	Logistic regression model estimates for European beech . . . . .	68
4.5	Logistic regression model estimates for Black pine . . . . .	71
4.6	Logistic regression model estimates for Norway spruce . . . . .	74
4.7	Logistic regression model estimates for Scots pine . . . . .	77
4.8	Logistic regression model estimates for Silver birch . . . . .	80
4.9	Logistic regression model estimates for Austrian oak . . . . .	83
4.10	Logistic regression model estimates for European hornbeam . . . . .	86
4.11	Logistic regression model estimates for Pedunculate oak . . . . .	89
4.12	Logistic regression model estimates for Sessile oak . . . . .	92



# List of Acronyms

<b>AUC</b>	area under the receiver operating characteristic curve
<b>ARI</b>	alpha-reductase inhibitor
<b>BIC</b>	Bayesian information criterion
<b>CI</b>	confidence interval
<b>CIL</b>	calibration in the large
<b>DRE</b>	digital rectal exam
<b>csPCA</b>	clinically significant prostate cancer
<b>ICP Forests</b>	International Co-operative Programme on Assessment and Monitoring of Air Pollution Effects on Forests
<b>IRB</b>	institutional review board
<b>MAR</b>	missing at random
<b>MCAR</b>	missing completely at random
<b>MNAR</b>	missing not at random
<b>MICE</b>	multiple imputation by chained equations
<b>MRI</b>	Magnetic Resonance Imaging
<b>MSKCC</b>	Memorial Sloan Kettering Cancer Center
<b>OR</b>	odds ratio
<b>PBCG</b>	Prostate Biopsy Collaborative Group
<b>PSA</b>	prostate-specific antigen
<b>ROC</b>	receiver operating characteristic
<b>SPEI</b>	Standardized Precipitation Evapotranspiration Index
<b>TRUS</b>	transrectal ultrasound scan
<b>UCSF</b>	University of California San Francisco
<b>UT Health</b>	University of Texas Health Science Center at San Antonio
<b>VA</b>	Veterans Affairs
<b>WMO</b>	World Meteorological Organization
<b>ZAMG</b>	Central Institut for Meteorology and Geodynamics



# 1 Introduction

This thesis consists of three studies from different disciplines facing similar methodological problems. This chapter gives background to the individual topics, methodology, and an outline of the thesis.

## 1.1 Prostate cancer

Prostate cancer incidence and mortality are rapidly growing worldwide, reflecting aging, population growth, and changes in the prevalence and distribution of the main risk factors for cancer (Sung et al. 2021). Several risk factors are associated with socioeconomic development. In 2020, an estimated 19.3 million new cases and 10 million cancer deaths were experienced worldwide. Overall, prostate cancer has the fourth highest incidence, with 7.3%. Among men, with 1.4 million new cases and 375,000 deaths worldwide, prostate cancer is the second most frequent cancer and the fifth leading cause of cancer death in 2020. For age-standardized rates, Northern and Western Europe had the highest incidences, and the Caribbean had the highest mortality rates. Figure 1.1 illustrates the location of the prostate in men and shows an example of malignant tumor cells.

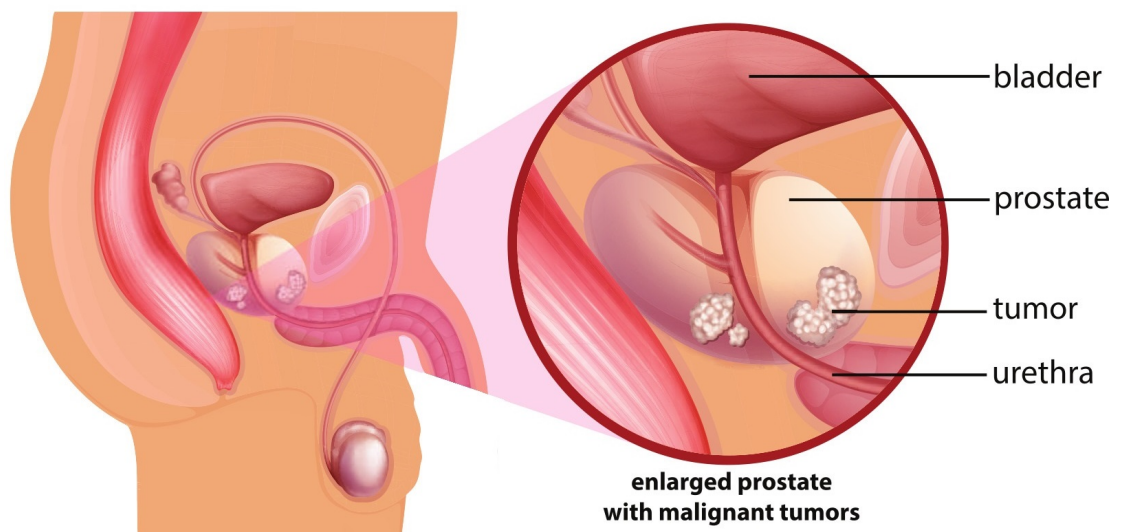


**Figure 1.1:** Location of the prostate in men with an example of prostate cancer.

The USA, Canada, and Australia experienced rapid increases in incidence rates in the late 1980s and early 1990s due to the introduction of serum prostate-specific antigen (PSA) testing, allowing the detection of preclinical cancers (Sung et al. 2021). Sharp reductions within a few years followed the dramatic increases. Mortality rates for prostate cancer have decreased in most high-income countries since the mid-1990s.

## 1.2 International Prostate Biopsy Collaborative Group

The Prostate Biopsy Collaborative Group (PBCG) was established in 2009 to improve the understanding of heterogeneity in prostate biopsy outcomes across international clinical centers (Vickers et al. 2010). To better understand the relationships between prostate biopsy outcomes and established risk factors, the PBCG collected retrospective data from ten screening and tertiary referral centers. To ensure high data quality for producing a new prostate cancer risk tool based on contemporary populations and practice, the PBCG began prospective collection from participating centers in 2014. A risk tool was modeled after the Prostate Cancer Prevention Trial risk calculator (PCPTRC; Ankerst et al. 2012), with the hypothesis that such a risk tool would have better external validation for contemporary populations. Data from eleven participating sites under local internal review board approval were prospectively collected. Cleveland Clinic, Martini Clinic (Germany), Mayo Clinic, San Raffaele (Italy), Zurich (Switzerland), Memorial Sloan Kettering Cancer Center (MSKCC), and University of California San Francisco (UCSF) were participating tertiary referral centers. Durham Veterans Affairs (VA) and VA Caribbean Center (Puerto Rico) served a lower socioeconomic status population with a high percentage of African Americans and Hispanics. Sunnybrook Health Systems in Canada and the University of Texas Health Science Center at San Antonio (UT Health) were consortia that included main hospitals, tertiary referral centers, and associated community urology providers. Four sites also provided retrospective data for prostate biopsies performed in 2006 or later. For developing the initial PBCG risk calculator, multiple methods for aggregating clinical data on a small number of variables across heterogeneous centers comprising different risk factor distributions and risk factor-outcome associations were compared. The most straightforward approach of pooling individual-level data and fitting a multiple logistic regression model proved to be the most accurate (Tolksdorf et al. 2019).

The first PBCG risk tool was published online in 2018 (Ankerst et al. 2018). The number of device users was tracked, and Figure 1.2 shows the report for the year 2021. Most usage by far can be seen in the USA, with 4,824 sessions compared to 234 in Germany for that year. Since the tool was primarily built on patients from the USA, it is the region the calculator represents best. Overall, user numbers increased by 56.5% compared to the previous year.

As with all online risk tools, the online publication continues to result in published external validation studies providing evidence for or against its generalizability to other populations, particularly in comparison to other published tools (Amaya-Fragoso and García-Pérez 2021; Carbutaru et al. 2019; Doan et al. 2021; Jalali et al. 2020; Presti et al. 2021; van Riel et al. 2022; Yildizhan et al. 2022). The PBCG tool has been primarily compared to the Prostate Cancer Prevention Trial Risk Calculator (Amaya-Fragoso and García-Pérez 2021; Carbutaru et al. 2019; Yildizhan et al. 2022), where it started from, and to the European Randomized Study of Screening for Prostate Cancer (Doan et al. 2021; Wei et al. 2021). Additionally, new risk calculators have compared their results to the PBCG risk tool, such as the Kaiser Permanente Prostate Cancer Risk Calculator (Presti et al. 2021). Studies often do not just validate multiple risk calculators. They also apply it to data from different countries to investigate the validity of the calculator for those countries. The PBCG risk calculator was, for instance, applied to Turkish



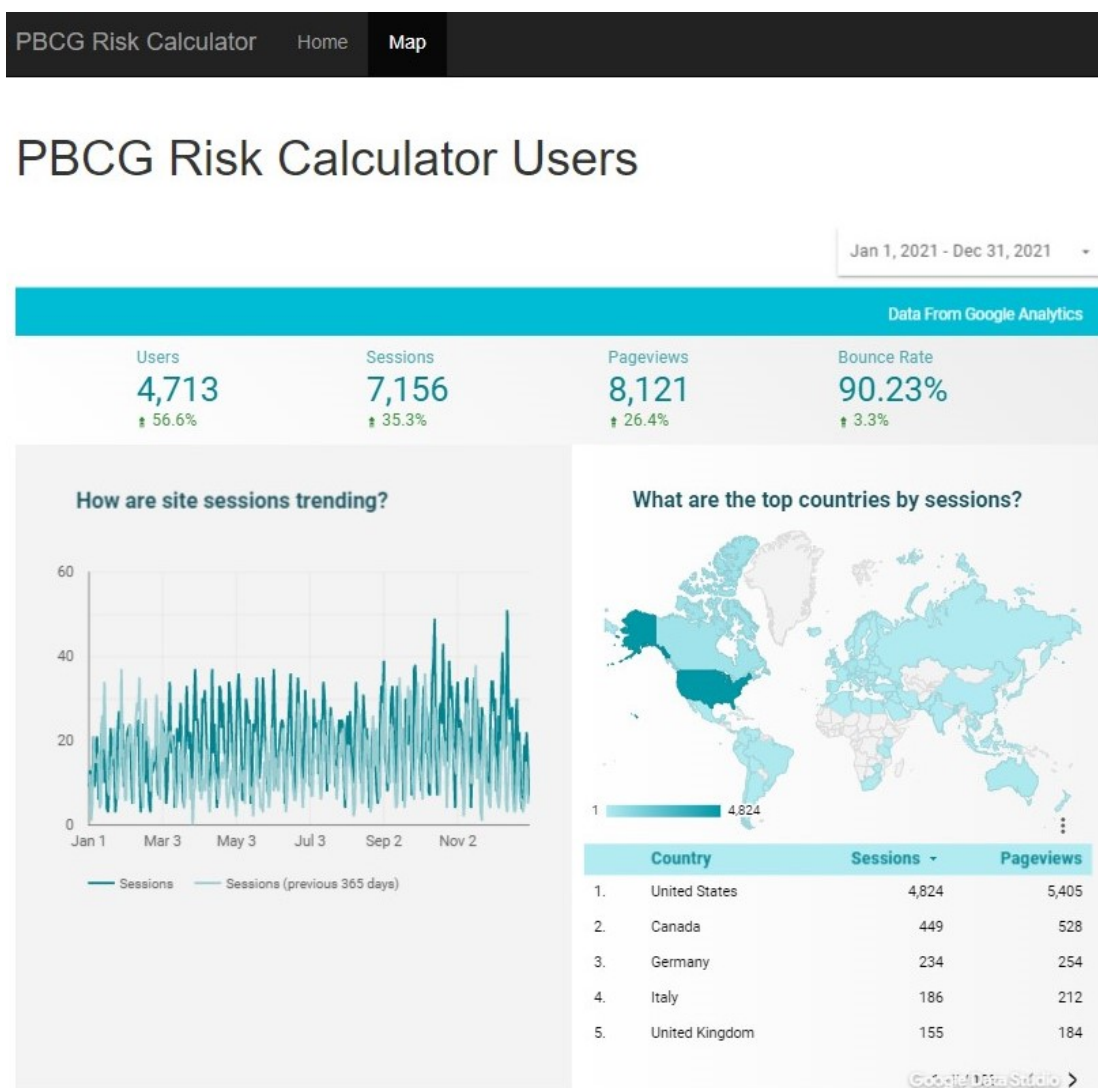


**Figure 1.2:** Google Analytics usage report for the PBCG risk calculator for 2021 from <https://riskcalc.org/PBCG/>.

(Yildizhan et al. 2022), Australian (Doan et al. 2021), Mexican (Amaya-Fragoso and García-Pérez 2021), and Irish (Jalali et al. 2020) patients.

Another group of studies suggests improvements to the PBCG risk calculator. These incorporate new methods, such as automated machine learning (Stojadinovic et al. 2020), improvement for patients with PSA less than 10 ng/ml (Stojadinovic et al. 2020), including prostate volume (Jalali et al. 2020), or usage of Magnetic Resonance Imaging (MRI) assisted biopsies (Mortezavi et al. 2021; Rubio-Briones et al. 2020; van Riel et al. 2022; Wei et al. 2021). The more recent studies include new clinical practices that are becoming more standard, suggesting the PBCG risk calculator has to be updated for contemporary clinical assistance and to remain competitive with other risk calculators. In this thesis, the PBCG data set is used to explore the impact of missing data in the development of online risk tools (Chapter 2).

### 1.3 Mountain sports in Austria

Mountains have always been of interest to humans. Early attempts to ascend mountain peaks were inspired by other than sporting motives: to build altars, seek spirits, get an overview of one's own or a neighboring countryside, or make meteorological or geological observations (Smith and Kiesinger 2020). The first time recorded for which a few men ran in the mountains intending to arrive first with common rules for all the runners was in Scotland in the year 1040, when king Malcom Canmore organized a hill race to select its postmen (Jornet 2022). Mountaineering in a contemporary sporting sense was born when a young Genevese scientist viewed Mont Blanc (at 4,807 meters, the tallest peak in Europe) in 1760 and determined that he would climb to the top of it or be responsible for its being climbed (Smith and Kiesinger 2020).

After numerous accidents in the Austrian mountains, one disaster where three men died in 1896 led to the foundation of the first alpine emergency organization in the world in Vienna. More and more locations were added, and after World War II they united (Ladenbauer 2006). Today more than 13,000 volunteers work for the Austrian mountain rescue service. In 2020, they rescued more than 8,000 people, where the largest fraction was injured alive (Figure 1.3, Bergrettung 2022a).

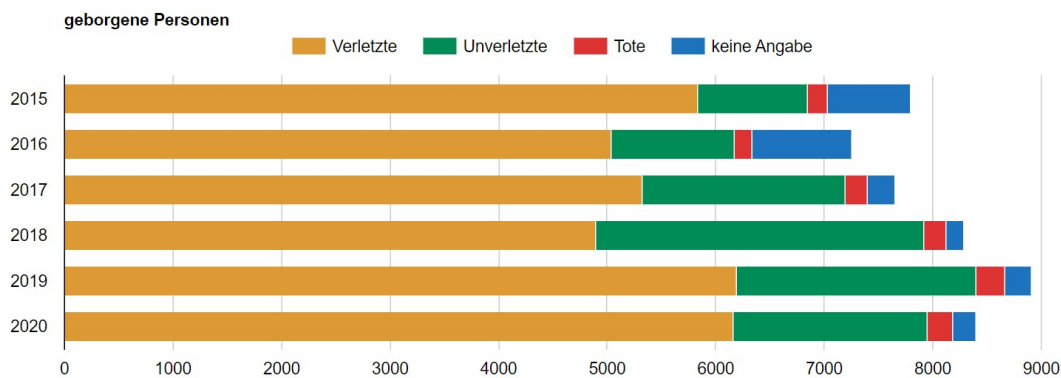


**Figure 1.3:** Summary of rescued people from the Austrian mountains from 2015 to 2020. Verletzte = injured, Unverletzte = non-injured, Tote = dead, keine Angaben = no declaration (Bergrettung 2022b).

The Austrian Alpine Safety Board was founded in 1965 after two tragic avalanche accidents. In 1967, they started to analyze mountain accidents. From 2006 onward, a contract to get accident information from the alpine police led to one of the biggest data sets for alpine accidents. An annual report is published for accident prevention for summer and winter separately, and as stated, many accidents would have been avoidable (Österreichisches Kuratorium für Alpine Sicherheit 2022).

### 1.4 Meteorology in Europe

Weather and its forecast have been interesting for humans for a long time. It has always been important for farmers to know how and when the weather changes since the

yield could vary enormously if, for example, a storm destroys the harvest. Due to the great interest in shipping worldwide, wind forecasts were essential for navigation. Since extreme events appear locally, they were regarded as punishments or warnings directed at specific communities, cities, homes, or even individuals. The oldest treatise dedicated to meteorology, *Meteorologica*, was written by Aristotle around 340 BC (Neves et al. 2017). The first three books described the formation of rain, clouds and fog, hail, winds, climate change, thunder, lightning, and hurricanes. This established system remained for around 2000 years as the standard of scientific texts. Until the early seventeenth century, almost all books on the European continent dealing with the atmosphere were essentially based on Aristotle's considerations.

The tradition of weather forecasts and the view of weather as a system ordered by physical laws built the origins of a new approach. Contributors to the emerging theory of weather have recognized that meteoric science has to be able to identify long-term changes, recurrent patterns, and predictive methods. Efforts to form an international network of weather-watchers did not succeed until the mid-eighteenth century, when the Royal Society invited all observers with training and equipment to submit their daily observations annually. Instructions were requested, including the daily reading of the thermometer, barometer, direction and force of the wind, amount of rain or snow, and the appearance of the sky. The results were published annually in the *Philosophical Transactions* journal (Neves et al. 2017).

Weather forecasts were discussed alongside religious and mystical issues in the nineteenth century. Since future predictions did not succeed significant, meteorology began to look more closely at past events, searching for repeatable patterns. This progress raised the need for organization, coordination, and centralization of scientific work associated with the first meteorological offices. In 1853, Robert Fitzroy began distributing instruments to ship officers, gathering their record books, establishing a telegraphic observation network, and publishing storm warnings and general forecasts about the weather. Synoptic maps are one of the most striking innovations of nineteenth-century meteorology, constituting a great effort to attribute form and structure to the invisible forces of the atmosphere. The visual approach brought new perspectives and reflections to meteorologists (Neves et al. 2017).

The internationalization of meteorology in the twentieth century was especially driven by the advent of the radio, which played an essential role in information communication between distant stations. In the 1950s and 1960s, numerical forecasting became possible with the invention of the first computers. The most recent significant impact was the introduction of meteorological satellites. With these satellites, it was possible to observe atmospheric circulation as a whole, thus improving the connections between processes from different locations and scales, especially in the oceans and desert regions (Neves et al. 2017).

In 1851 the Austrian emperor declared a resolution founding the central institute for meteorology and magnetic observations, which became the predecessor of the Central Institut for Meteorology and Geodynamics (ZAMG) (Zentralanstalt für Meteorologie und Geodynamik 2022). Already in 1865, they began publishing a daily weather map. In 1873 the institute organized the first international meteorology congress in Vienna, where

the International Meteorology Organization (IMO) was founded, the predecessor of the World Meteorological Organization (WMO). Nowadays, the ZAMG is a modern service company that provides, for instance, daily forecasts, earthquake and geomagnetic services, climate statistics and maps, pollutant distribution, and meteorological characteristics assisted by automated systems. From the beginning, the institute employed directors who were also recognized scientific professors, facilitating scientific research within the institute (Zentralanstalt für Meteorologie und Geodynamik 2022).

Mountains cover 25% of the earth's land surface (Chow et al. 2013). Hills and plateaus account for another 21% of the land surface. Thus, the weather in areas of complex terrain affects roughly half of the world's land surface. Although there are a variety of forecasting styles, skillful forecasting in mountainous regions typically requires a core understanding of simultaneous measurements over large scale and unique mountain processes such as airflow. Further, careful evaluation of the evolving large-scale setting and flow interaction with the terrain, knowledge of the advantages and limitations of the objective tools of forecasting over the complex landscape, and the subjective integration of these tools by the forecaster are needed (Chow et al. 2013). This thesis analyzed weather information from the ZAMG to investigate weather effects on Austrian mountain fatalities (Chapter 3).

Climate change poses a wide range of consequences for human health (IPCC 2014). Direct effects, such as more frequent and intense heatwaves, and indirect effects, such as higher allergenic pollen loads and altered vector-borne diseases, were among the first to be formally attributed to warming (Rosenzweig et al. 2008). Meanwhile, other effects on health are increasingly coming to the fore, such as injuries and mortality linked to all kinds of accidents, be it with traffic, outdoor work in agriculture or forestry, leisure activities in the mountains, as well as suicide, which is weather dependent (Deisenhammer et al. 2003). Initial studies from the USA (e.g., Leard B 2015) revealed that traffic accidents are likely to increase with the predicted warming. Equally, outdoor work-related injuries in Canada (Adam-Poupart et al. 2015), the USA (Spector et al. 2016), and Australia (McInnes et al. 2018) have been linked to heat exposure. Based on a comprehensive review of nineteen individual studies, Zacharias (2012) concluded that suicide rates have a prominent seasonal pattern with maximum temperature measures in late spring. Half of these reviewed studies reported a positive correlation between suicides and temperature or sunshine versus a negative correlation with precipitation and humidity.

Weather effects may intensify under projected climate change scenarios, where summers may experience more intense heat and winters more severe weather. This is especially important since appropriate preventive measures could reduce high economic costs and burdens on the social system. Weather data providers face more challenges on a European or even global scale. These comprise but are not limited to the available time scale, spatial resolution, amount of variables, and data update frequency.

Several publicly available climate data sets are commonly accessed for climate change impact research. The WorldClim data set of spatially interpolated monthly climate data for global land areas has a spatial resolution of approximately 1 km<sup>2</sup>. It includes monthly temperature (minimum, maximum, and average), precipitation, solar radiation, vapor pressure, and wind speed aggregated across a target temporal range of 1970 to

2000, using data from between 9,000 and 60,000 weather stations (Fick and Hijmans 2017). The original E-OBS data set presented European land-only daily 10 km-resolution gridded precipitation, as well as minimum, maximum, and mean surface temperature for the period 1950 to 2006 (Haylock et al. 2008). However, a finer resolution would be more appropriate for studying regional or local climatic effects. A continental data set with high resolution would allow research that is large in scale and still locally relevant. Moreno and Hasenauer (2016) produced a downscaled version of E-OBS, applying the delta method, which uses WorldClim climate surfaces to obtain an approximately 1 × 1 km daily climate data set covering the European Union. The downscaled data set included minimum and maximum temperature and precipitation from 1951 to 2012. ECLIPS provides 80 annual, seasonal, and monthly climate variables for two past and five future periods (Chakraborty et al. 2021). A limitation of this data set is that it is not updated regularly and is most appropriate for the past between 1961 and 2010. Even more variables are provided by Indecis (Domínguez-Castro et al. 2020); 125 climate indices mapped at a grid interval of 27 km from 1950 to 2017 were initially uploaded and are updated annually. ClimateEU provides a database of interpolated climate data for Europe that includes monthly, annual, decadal, and 30-year normal climate data starting from 1901, as well as climate change projections for the 21st century (Marchi et al. 2020). For download, 1 km grids are provided. The advantage of this data set is that it comes with software applying dynamic algorithms to generate scale-free climate variables for specific locations adjusted for altitude, thus improving the accuracy. Due to this fine-scale resolution and recent years, the ClimateEU data set is used to investigate weather and climate effects on European tree mortality (Chapter 4).

## **1.5 Forestry in Europe**

Not only humans are affected by climate change. Plants and trees also suffer from extreme weather, and species that are more heat resistant survive drought seasons better. However, adjustments are slow and take multiple generations. Chapter 4, therefore, investigates the weather and climate influence on tree mortality for the most common European tree species to guide tree managers with risk predictions.

Data for this study comes from the International Co-operative Programme on Assessment and Monitoring of Air Pollution Effects on Forests (ICP Forests), which was launched in 1985 under the Convention on Long-range Transboundary Air Pollution of the United Nations Economic Commission for Europe (ICP Forests 2022). Over the past 30 years, ICP Forests has developed into one of the world's largest biomonitoring networks, providing information on forest conditions, air pollution, climate change, and biodiversity.

The program's objectives are to provide a periodic overview of forest conditions' spatial and temporal variation concerning anthropogenic and natural stress factors (particularly air pollution) utilizing European-wide large-scale representative monitoring on a systematic network (Level I). And further, to better understand the cause-effect relationships between the condition of forest ecosystems and anthropogenic and natural stress factors using intensive monitoring on several selected permanent observation plots spread over Europe and to study the development of forest ecosystems in Europe (Level II).

Level I monitoring provides an annual overview of forest conditions based on a 16 x 16 km grid and covers around 6,000 plots in Europe and beyond. Besides annual tree crown condition assessments, it also includes assessments of soil condition, the foliar nutrient status of trees, the diversity of ground vegetation, and general information on living trees and deadwood at irregular intervals. Intensive Level II forest monitoring is critical for providing insight into cause-and-effect relationships between the condition of forest ecosystems and various stress factors, such as air pollution and drought. Around 800 plots have been established with major European forest types represented.

At present, 42 countries in Europe and beyond participate in ICP Forests. The Programme Task Force is the highest body of ICP Forests and represents all participating countries. National experts are organized in expert panels and working groups, ensuring continuous development and harmonization of the monitoring methods and contributing to data evaluations. Examples of expert panels are Ambient Air Quality, Soil and Soil Solution, Crown Condition and Damage Causes, Meteorology, Phenology, and Leaf Area Index.

### 1.6 Missing data

Unobserved and hence missing data has been a pervasive problem in data analysis since the origin of data collection (Brown and Kros 2003). Within data analysis, data preparation is the most crucial and time-consuming task that strongly influences the success of the research (Salgado et al. 2016). It is necessary to deal with missing data by deleting incomplete observations or replacing any missing values with an estimated value based on other information available, a process called imputation. Another option is going back to the data investigator to clarify missing values. This approach is very time-consuming and often not possible.

Missing data can appear for many reasons, such as non-applicable or questions of no interest to the patient, computer, automation or human error, or unrealistic values. When merging data from multiple sources, more systematic reasons for missing data arise, such as not all sources collect the same data or collect data on different scales.

All types of missing data are subject to underlying mechanisms. Salgado et al. (2016) described three missing data mechanisms distinguishable by whether the probability of response depends on the observed and missing values. Missing completely at random (MCAR) means that the probability of an observation being missing does not depend on the data. For example, imagine that a doctor forgets to record the gender of every sixth patient. There is no hidden mechanism depending on any patient characteristic. In contrast, for missing at random (MAR), the probability of a value being missing is related only to the observable data. For this mechanism, it is possible to estimate the missing values from the observed data. This case is not completely random, but it is the most general case where we can ignore the missing mechanism, as we control the information upon which the missingness depends, the observed data. Said otherwise, the probability of missing data for a particular variable does not depend on the values of that variable after adjusting for observed values. As an example for a study collecting age and prior pneumonia as variables, older people are less likely to inform the doctor that they had

pneumonia before. The response rate for prior pneumonia will depend on the variable age. Missing not at random (MNAR) refers to the case when neither MCAR nor MAR holds. The missing data depends on both missing and observed values. Determining the missing mechanism is impossible, as it depends on unseen data. From that derives the importance of performing sensitivity analyses and testing how the inferences hold under different assumptions. An example of MNAR occurs in patients with low blood pressure who are more likely to have their blood pressure measured less frequently (Salgado et al. 2016).

Methods handling missing data should be tailored to the data set of interest, the reasons for missingness, and the proportion of missing data. Generally, a method is chosen for its simplicity and ability to introduce as little bias as possible in the data set. When data are MCAR or MAR, a researcher can ignore the reasons for missing data, which simplifies the choice of the methods to apply (Salgado et al. 2016). In this case, any method can be used. Little (1988) proposed a procedure for testing the MCAR assumption. This test got further improved and implemented in statistics programs (Li 2013). As the MAR assumption is not testable, methods were suggested that test under particular assumptions (Breunig 2019; Jaeger 2006; Potthoff et al. 2006). Further, tests to distinguish MNAR and MAR were proposed (H. Wang et al. 2021). Nevertheless, it is difficult to obtain empirical evidence about whether or not the data are MCAR or MAR.

Methods exist to investigate which type of missingness persists, but classifying it into one is impossible. For example imagine a clinical survey asking about race in multiple international clinics. This question is expected in the USA but uncommon in Germany. Hence it will appear that German patients are overwhelmed with this question, so do not answer. Since there is no mechanism behind the missingness, this would be MCAR. And since this question is not common in Germany, some clinics could not ask the question at all. The missingness depends on the variable at which clinic the patient was treated and is MAR. Or, an African American can be offended by the question and choose not to answer. Since the missingness depends on the missing value, it would be MNAR. In this international study, missingness in the variable race arises due to all three types, MCAR, MAR, and MNAR, and cannot be classified into one. Since it is hard to categorize the type of missingness, sensitivity analyses across multiple methods accommodating different choices are commonly preferred.

The most widely used methods fall into three main categories, deletion (including complete-case and available-case), single imputation (including mean substitution, linear interpolation, hot and cold deck), and model-based methods (including multiple imputation, regression, and k-nearest neighbors; Salgado et al. 2016). They are explained in more detail in the following.

The simplest way to deal with missing data is to discard entire case records with missing values, which only leads to valid inferences under MCAR. In a complete case analysis, all the observations with at least one missing variable are discarded. The principal assumption is that the remaining subsample is representative of the population and will thus not bias the analysis towards a subgroup. Its main drawbacks are the reduced statistical power, waste of information, and possible analysis bias, especially if the data are not MCAR (Salgado et al. 2016).

The available-case method discards data only in the variables needed for a specific analysis. For example, if a study needs only four out of 20 variables, this method would only discard the missing observations of the four variables. The analysis is performed using all cases where the variables of interest are present. Even though this method can preserve more information, the populations of each analysis would be different and possibly non-comparable. Furthermore, the method is only unbiased under MCAR (Bennett 2001).

In single imputation, missing values are filled by some type of predicted values. Single imputation ignores uncertainty and almost always underestimates the variance. The simplest imputation method is to substitute missing values with the respective variable's mean or median. Using the median is more robust in the presence of outliers in the observed data. The main disadvantages of non-model-based imputation are that it underestimates variability and disregards relationships between variables, decreasing their correlation. While this method diminishes the bias of using a non-representative sample, it introduces other biases (Salgado et al. 2016). These methods are unbiased under MCAR (Bennett 2001).

A predictive model is created in model-based imputation to estimate values that will substitute the missing data. This can be applied in single or multiple imputation. This approach's disadvantage is that the model estimated values are usually more well-behaved than the actual values, and the models perform poorly if the observed and missing variables are independent. Multiple imputation overcomes the underestimated variance problem by considering both within- and between-imputation uncertainty. Multiple imputation is a powerful statistical technique developed by Rubin (1978), unbiased under MCAR and MAR (Bennett 2001). It is a Monte Carlo technique that requires three steps. The first is imputation, where missing values are filled in using any method of choice, leading to  $M$  completed data sets. In these  $M$  multiple-imputed data sets, all the observed values are the same, but the imputed values are different, reflecting the uncertainty about imputation. In the second analysis step, each of the  $M$  completed data sets are analyzed, for instance, by a logistic regression classifier for mortality, which gives  $M$  analyses. In the third pooling step, the  $M$  analyses are integrated into a final result, for example, by computing the mean of the  $M$  analyses.

This chapter has concerned mostly missing predictors. Similar approaches exist for missing outcomes. Since this is not relevant to this thesis, it is not further discussed. In this thesis, missing data appears in all forms. For Chapter 2, the clinics collected different variables; therefore some variables are missing completely for some cohorts. Additionally, the variables have missing values for unknown reasons. In Chapter 3, missing data occurred in both data sets. Fatal accidents lack information as well as weather data. For Chapter 4, some countries submit only mandatory variables even if they would have information about the other variables. Reasons for the general mechanism for missingness were unknown.



## 1.7 Logistic regression

In this section, we introduce a model designed for binary outcomes, the logistic regression model (Abraham and Ledolter 2006). Outcomes ( $y$ ) were coded as 1 for the event of interest and 0 for those without the event. In this thesis, the outcomes are clinically significant prostate cancer, days with a fatal mountain accident, and tree mortality. The explanatory variables ( $x$ ) can be continuous (e.g., temperature) or categorical (e.g., wind direction). This thesis's explanatory variables consist of weather characteristics, tree age and slope, and clinical risk factors.

The outcome  $y_i$  of case  $i$  with explanatory variables  $x_i = (x_{i1}, x_{i2}, \dots, x_{ip})'$  is assumed to a Bernoulli distribution with success and failure probabilities

$$P(y_i = 1|x_i) = \pi(x_i) \text{ and } P(y_i = 0|x_i) = 1 - \pi(x_i), \text{ independently for } i = 1, 2, \dots, n.$$

For  $y_i \sim Ber(\pi(x_i))$  the mean of the distribution  $E(y_i) = \pi(x_i)$  and the variance becomes  $var(y_i) = \pi(x_i)(1 - \pi(x_i))$ . In the logistic regression model, probabilities  $\pi(x_i)$  are parameterized as

$$\pi(x_i) = \frac{e^{x_i'\beta}}{1 + e^{x_i'\beta}} = \frac{1}{1 + e^{-x_i'\beta}} \text{ and } 1 - \pi(x_i) = \frac{1}{1 + e^{x_i'\beta}} = \frac{e^{-x_i'\beta}}{1 + e^{-x_i'\beta}},$$

where  $x_i'\beta = \beta_0 + \beta_1 x_{i1} + \dots + \beta_p x_{ip}$ . The probabilities are nonlinear functions of the parameters  $\beta$ . However, a simple transformation results in a linear model,

$$\frac{\pi(x)}{1 - \pi(x)} = \frac{1}{1 + e^{-x'\beta}} : \frac{e^{-x'\beta}}{1 + e^{-x'\beta}} = \frac{1}{1 + e^{-x'\beta}} \cdot \frac{1 + e^{-x'\beta}}{e^{-x'\beta}} = \frac{1}{e^{-x'\beta}} = e^{x'\beta}.$$

This ratio compares the probability of a characteristic's occurrence to its non-occurrence and is referred to as the odds of occurrence  $Odds(x)$ . Whereas probabilities are constrained to lie between zero and one, odds can take on values between zero and infinity. For  $\pi = 0.8$ , the odds for occurrence are  $0.8/0.2 = 4$ , implying that the probability of occurrence is four times as large as the probability of non-occurrence.

The logarithm of the odds is referred to as the log-odds or the logit. The logistic regression model assumes a linear model for the logit,

$$\log(Odds(x)) = \log\left(\frac{\pi(x)}{1 - \pi(x)}\right) = x'\beta = \beta_0 + \beta_1 x_1 + \dots + \beta_p x_p.$$

This representation shows that the regression coefficients represent changes in the log odds, as can be seen by the following. For a single binary explanatory variable  $x$  with values 0 and 1,

$$\begin{aligned} Odds(x = 0) &= \exp(\beta_0 + \beta_1 \cdot 0) = \exp(\beta_0), \\ Odds(x = 1) &= \exp(\beta_0 + \beta_1 \cdot 1) = \exp(\beta_0 + \beta_1), \end{aligned}$$

and for the odds ratio,

$$OR = \frac{Odds(x = 1)}{Odds(x = 0)} = \frac{\exp(\beta_0 + \beta_1)}{\exp(\beta_0)} = \frac{\exp(\beta_0) \cdot \exp(\beta_1)}{\exp(\beta_0)} = \exp(\beta_1).$$

Therefore, the regression parameters are  $\beta_1 = \log(OR)$  for the slope, and  $\beta_0 = \log(Odds(x = 0))$  for the intercept. For example, a regression coefficient  $\beta_1 = -0.2$  and  $exp(\beta_1) = 0.82$  indicates that a change from 0 to 1 reduces the odds of occurrence by the multiplicative factor 0.82. A value of  $\beta_1 = 0$  and  $exp(0) = 1$  implies that a change in the explanatory variable has no effect. Similar arguments hold for a continuous variable for an increase in  $x$  by 1. And for multiple explanatory variables for the change in odds for a unit increase in a single variable holding all others fixed. Changing an explanatory variable by  $k$  units while keeping the values of all other variables constant leads to an odds ratio  $exp(\beta \cdot k)$ .

### 1.8 Likelihood ratio test

Statistical software packages such as R evaluate the maximum value of the likelihood function  $L(\hat{\beta})$ . Likelihood ratio tests can compare the maximum likelihood under the current "full" model versus a "restricted" model, omitting one or more of the explanatory variables. The Likelihood ratio test statistic

$$2 \log \left( \frac{L(full)}{L(restricted)} \right) = 2(\log L(full) - \log L(restricted))$$

follows in large samples a chi-squared distribution with degrees of freedom given by the number of independent constraints if the constraints imposed by the restricted model are valid. Using the Likelihood ratio test, one can assess the significance of an explanatory variable with one p-value for continuous and categorical variables. Hence, one can determine the overall significance of a categorical variable independent of the number of categories.

### 1.9 Outline of the thesis

The data analysis process involves gathering the information, processing it, exploring the data, and using it to find patterns and other insights. Issues concerning data quality can appear in each step. To get a greater understanding, gathering information from multiple sources is necessary. It is a common strategy in clinical studies to reach a wider representative population by combining data from several clinics. From the clinical perspective, this increases the sample size, which is especially important for diseases with rare cases. Due to different reasons, clinics collect various amounts of patient characteristics. Patients curious about their health risk may not have results on all clinical tests. Therefore, missing predictors appear on both the model building and the prediction side. Chapter 2 compares logistic regression methods for combining data from multiple heterogeneous cohorts, with an additional focus on incorporating systematic missing data. Chapter 3 combines fatality cases in the Austrian mountains with weather information on different scales for association analyses of weather on mountain fatalities. Chapter 4 combines individual tree mortality information across Europe with plot information from two collection schemes, along with climate and weather adjusted for elevation. Missing data arise in all three applications of the thesis, demanding methods to change analyses and maximize efficiency.

## 2 Accommodating heterogeneous missing data patterns for prostate cancer risk prediction

A portion of this chapter is published in Neumair M., Kattan M.W., Freedland S.J., Haese A., Guerrios-Rivera L., De Hoedt A.M., Liss M.A., Leach R.J., Boorjian S.A., Cooperberg M.R., Poyet C., Saba K., Herkommer K., Meissner V.H., Vickers A.J., Ankerst D.P. Accommodating heterogeneous missing data patterns for prostate cancer risk prediction. *BMC Medical Research Methodology*, 2022, <https://doi.org/10.1186/s12874-022-01674-x> and Ankerst D.P., Neumair M. Active Data Science for Improving Clinical Risk Prediction. *Journal of Data Science*, 2022, <https://doi.org/10.6339/22-JDS1078>. For the first paper, Matthias Neumair developed the statistical methodology, interpreted all results, prepared the original draft, and designed and programmed the prostate cancer risk calculator. All other co-authors outside of Donna P. Ankerst were hospital clinicians and representatives who supplied data. All co-authors participated in the critical review of the manuscript for revision by Matthias Neumair. For the second paper, Matthias Neumair analyzed and visualized the data and interpreted the results. Donna P. Ankerst wrote the manuscript with contributions from Matthias Neumair.

The Prostate Biopsy Collaborative Group (PBCG) was established to improve the understanding of heterogeneity in prostate cancer biopsy outcomes across international clinical centers (Vickers et al. 2010). Figure 2.1 shows the range of the number of biopsies and prevalence of clinically significant prostate cancer (csPCA), defined as Gleason grade group  $\geq 2$ , across eleven PBCG cohorts. Prevalence is the percentage of the population affected by csPCA and calculated by  $Prev = \frac{n_{cases}}{n_{total}}$ , where  $n_{cases}$  is the number of csPCA cases, and  $n_{total}$  is the total number of patients in the corresponding group. In 2018, the PBCG developed an online risk tool based on a small set of common risk factors routinely collected in practice: prostate-specific antigen (PSA), digital rectal exam (DRE), age, African ancestry, first-degree prostate cancer family history, and history of a prior negative prostate biopsy (Ankerst et al. 2018). For developing the prior tool, multiple methods for aggregating clinical data on a small number of variables across heterogeneous centers comprising different risk factor distributions and risk factor-outcome associations were compared. The simplest approach of pooling individual-level data and fitting a multiple logistic regression model proved to be the most accurate (Tolksdorf et al. 2019). The resulting risk calculator was published online at [riskcalc.org](http://riskcalc.org) to facilitate its use in daily routine. (Carbunaru et al. 2019; Jalali et al. 2020; Mortezaei et al. 2021; Rubio-Briones et al. 2020; Stojadinovic et al. 2020).

The PBCG requested additional risk factors to those included in the current tool from its participating cohorts. However, these were not rigorously collected, with some cohorts not collecting some risk factors (Figure 2.2). In this thesis, we wanted to develop an

adaptive tool using all the information available in Figure 2.2 that would allow the user to enter as much (or as little) information as possible.

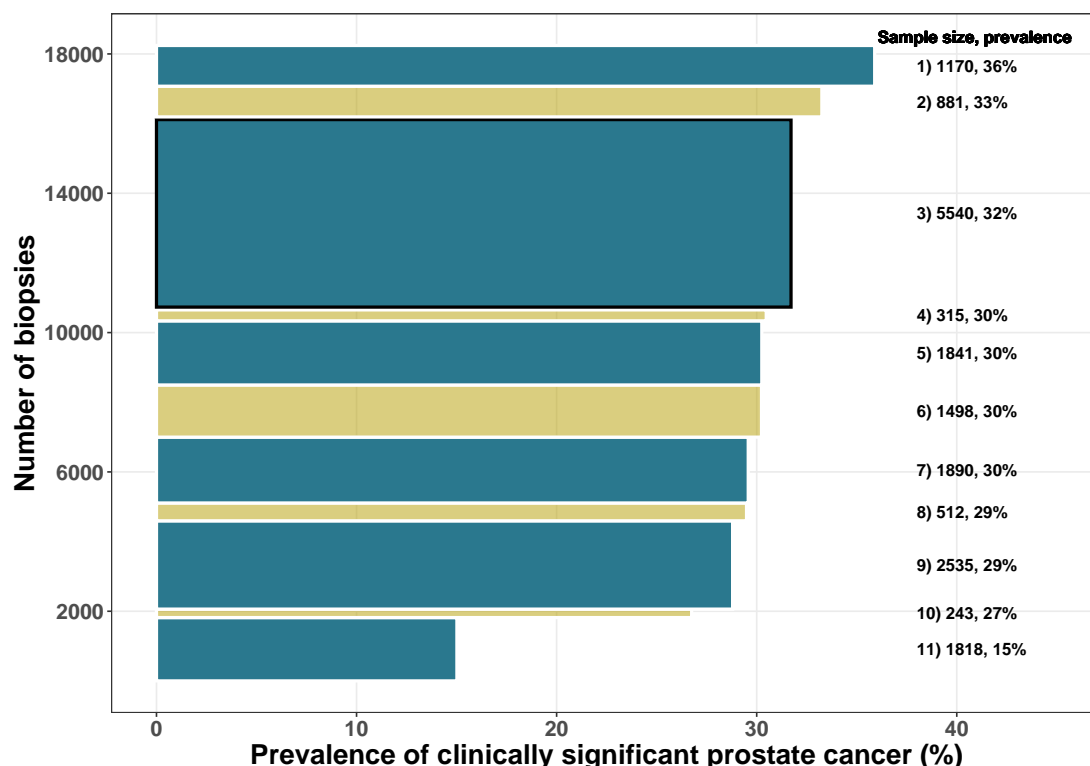


**Figure 2.1:** Sample sizes represented by the height of rectangles and prevalence of significant prostate cancer represented by the width of rectangles for the eleven PBCG cohorts used in the study. The cohorts have been numbered according to their rank of csPCA prevalence. The third cohort outlined in black was withheld to serve as an external validation cohort, with the remaining ten cohorts used for training prediction models.

Missing data in clinical research is a ubiquitous problem, and many statistical methods have been proposed to account for it (Donders et al. 2006; Janssen et al. 2010). Most procedures are applied to missing values in training data sets to develop a model. But with the emerging use of online and electronic record embedded clinical risk tools, approaches for handling missing risk factors on the user end of a risk tool requiring the predictor are coming into play. Recently, real-time imputation was proposed to extend needed cardiovascular disease management for patients with missing risk factors (Nijman et al. 2021).

This study aimed to construct a csPCA risk tool that optimizes the use of data from heterogeneous cohorts with varying missing data patterns and allows end-users of the tool predictions even when missing some risk factors. In terms of the development of a risk model on multiple cohorts with varying missing data patterns, we found four philosophically distinct approaches: available case analyses, ensembles of cohort-specific models, missing indicator methods, and imputation (Section 2.2). We compared six variations of these approaches and selected an optimal one for this application (Section 2.3). For the end-user side, we adopted an individual patient-tailored approach as we have implemented in previous tools. The user inputs the available risk factors, and a resulting

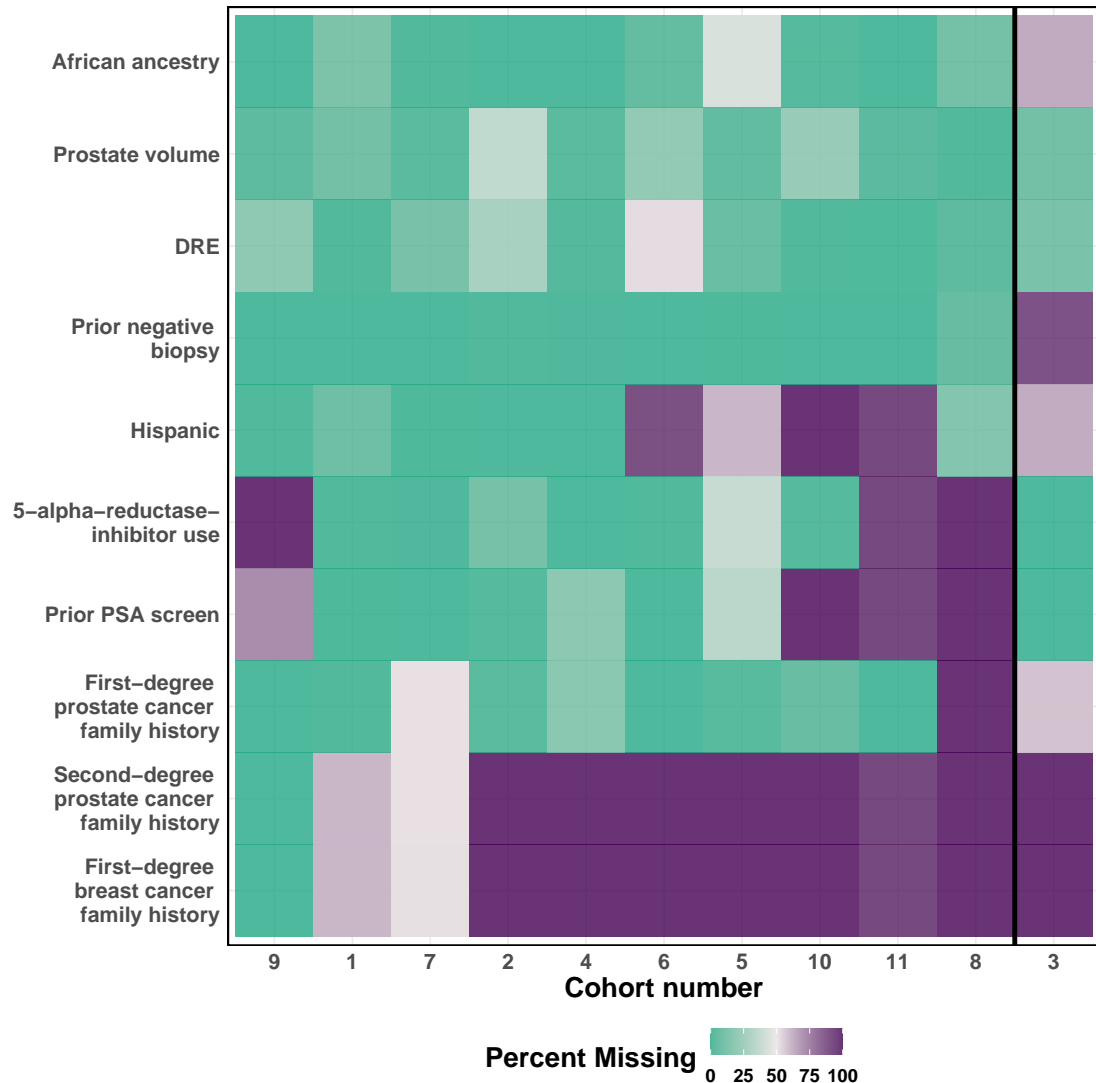


**Figure 2.2:** Missing risk factors. Amount of missing risk factor data by cohort on the x-axis; all patients were required to have PSA and age, hence 0% missing for these covariates. The 3rd cohort, separated by the black vertical line, was used as an external validation set, and leave-one-cohort-out cross-validation was applied to the other cohorts. Cohorts were sorted by missing data pattern; PSA: prostate-specific antigen, DRE: digital rectal exam.

prediction based on those risk factors is returned (Ankerst et al. 2014, 2018).

## 2.1 Biopsy data

The study was based on the risk factor and outcome data collected from January 2006 to December 2019 from trans-rectal systematic ten to twelve core biopsies. For training, ten PBCG cohorts spanning North America and Europe were used, and for validation, one PBCG European cohort was used (Figure 2.3). The risk factors collected (as shown in Figure 2.2) included the standard risk factors used in clinical practice for prostate cancer diagnosis along with other less commonly used risk factors, but with proven associations to prostate cancer (Carbunaru et al. 2019). All PBCG data were collected following local

institutional review board (IRB) approval from the University of Texas Health Science Center of San Antonio, Memorial Sloan Kettering Cancer Center (MSKCC), Mayo Clinic, University of California San Francisco, Hamburg-Eppendorf University Clinic, Cleveland Clinic, Sunnybrook Health Sciences Centre, Veterans Affairs (VA) Caribbean Healthcare System, VA Durham, San Raffaele Hospital, and University Hospital Zurich. Analyses for this retrospective study were approved by the Technical University of Munich Rechts der Isar Hospital ethics committee, with all methods performed in accordance with the guidelines and regulations of the committee. As collected data were anonymized and obtained as part of standard clinical care, consent was waived by all IRBs, except regarding second-degree prostate cancer and first-degree breast cancer family history for the VA Durham. Written consent for these variables was obtained and documented as part of a larger separate study at the VA Durham before the beginning of this study. All institutional PBCG IRB approvals are maintained by the MSKCC central data coordinating center and IRB.



**Figure 2.3:** World map of the eleven PBCG participating institutions collecting prostate biopsy data.

The ten training cohorts followed the PBCG prospective protocol in data collection, whereas the external validation cohort supplied retrospective data from a single institution that provided a high annual number of prostate biopsies for the PBCG (Ankerst et al. 2018; Tolksdorf et al. 2019). Included data came from patients who had received a prostate biopsy following a PSA test under local standard-of-care and may be seen as representative of patients in North America, including Puerto Rico and Europe. For users of the developed risk calculator, two risk factors were mandatory: PSA and age. Ten risk factors were optional: DRE, prostate volume, prior negative biopsy, 5-alpha-reductase-inhibitor use, prior PSA screen (yes/no), African ancestry, Hispanic ethnicity, first- and second-degree prostate cancer- and first-degree breast cancer-family history.

To improve data quality, we first performed data exploration and cleaning to correct or remove observations likely to be in error. We excluded patients with missing prostate biopsy cancer status and Gleason score as csPCA was the primary outcome of the analysis which was defined as Gleason grade group  $\geq 2$  on biopsy (Zhou et al. 2019). We removed patients with missing age or PSA as these are standard risk factors ubiquitously assessed for prostate cancer screening and diagnosis. Because the csPCA risk modeling was intended for patients not previously diagnosed with prostate cancer, we excluded patients with PSA values greater than 50 ng/ml. These values were likely to have a prior

positive cancer diagnosis not recorded in the supplied data set. The Hamburg Clinic, a high-volume prostate biopsy referral center and not a local urologic clinic, does not record previous prostate cancer status. Patients visiting the Hamburg clinic for prostate biopsy could be doing so under active surveillance for their prostate cancer. We excluded patients with PSA > 10 ng/ml to not eliminate the massive Hamburg population from the analysis. We only used Hamburg as a hold-out test set for validation, as in the PBCG risk tool publication by Ankerst et al. (2018). For prostate volume, we excluded values greater than 400 cc or equal to 0 cc as these are implausible values. Furthermore, we neglected patients who received Magnetic Resonance Imaging (MRI)-guided biopsy as these more accurate procedures will warrant enhanced prediction models incorporating imaging markers. To improve the model fit, we transformed PSA and prostate volume by the log-base-2. We chose this transformation because of its interpretability for the odds ratio, which becomes the change in odds for a doubling of the predictor.

The PBCG data set contains biopsy outcome information in addition to prostate cancer and Gleason grade, including the number of biopsy cores extracted and the percentage of these that are positive for prostate cancer. These allow an analysis of varying definitions of significant prostate cancer as used in the clinical literature (Matoso and Epstein 2019). In this study, we focused on csPCA as the outcome to evaluate whether the incorporation of the additional risk factors leads to an improvement in the prediction compared to the standard risk factors used in the current PBCG risk calculator.

## 2.2 Statistical analyses

Before the discussion of the multivariate analysis, we investigated the impact of variables for the prediction of csPCA one at a time using univariate logistic regressions for binary predictors. We transformed continuous predictors into binary ones by choosing relevant cutpoints to separate high versus low values.

We performed a literature search to identify the six most commonly used approaches for handling missing data in multivariable logistic regression modeling for either single or multiple cohorts, as found in this study. All of the approaches could be implemented in the R statistical package. We aimed to identify the most accurate technique for implementation in the online tool. To increase the tool's flexibility, we tailored each method to the specific list of risk factors available for one patient. For a validation set, the algorithms were applied for each individual in the validation set separately. All algorithms return logistic-regression-based expressions for the probability of csPCA; the cohort ensemble averages these for the individual cohorts. The methods are summarized in Table 2.1 and greater detail in Table 2.2.

The available cases algorithm pooled individual-level data from the training cohorts with information on the end user's variables. A main effects logistic regression model was fit for csPCA to the training data and used in a tailored prediction model for the target patient. The iterative Bayesian information criterion (BIC) selection method added stepwise BIC-based model selection to the available cases algorithm and allowed to include two-way interactions. The BIC selection started with the model that consists of

**Table 2.1:** Methods for fitting individual predictor-specific risk models for members of a test set by combining data from multiple cohorts. All individuals in the training and test cohorts have two predictors, PSA and age, and then any subset, including none, of ten additional predictors for a total of twelve predictors, denoted by  $X$ . The set of predictors available for the new individual is denoted by  $X^*$ . All models use logistic regression to predict csPCA. MICE=Multiple imputation by chained equations; BIC = Bayesian Information Criterion defined as the log-likelihood – (number of covariates)  $\times$  log(sample size).

Method	Definition
Available cases	Pool individual-level data with $X^*$ measured across all cohorts and fit a model including $X^*$ as main effects.
Iterative BIC selection	Same as available cases, but with an iterative stepwise BIC-based model selection to determine the optimal subset of $X^*$ and interactions.
Cohort ensemble	Separate models are built for each cohort using the coinciding variables of the cohort and the patient.
Categorization	All individuals in all cohorts are used. Predictors are categorized with missing as one of the categories so that the complete list of predictors $X$ is used.
Missing indicator	Include an indicator for missing a continuous predictor value and the interaction with the predictor as additional variables in the analysis. Mostly similar to categorization.
Imputation	Impute missing covariates in the training set following the MICE method. Mean imputation for missing values in prediction.

all variables as main effects and was hence based on a small sample size since it requires complete records. Due to the chosen starting variables, interactions were considered from the beginning. If a risk factor was not selected in the optimal model by the selection process, the procedure was re-started, excluding the risk factor, allowing more individuals from the training set to be included in model development. A patient provides a certain amount of covariates as input to the algorithm. Since this input varies on the patient, each combination of input variables developed its own model.

For the BIC, we follow the definition of Schwarz (1978). We consider a set of models  $\mathcal{M}_m$  for  $m = 1, \dots, M$ , which differ in their included covariates. We consider the inclusion of twelve risk factors and all possible two-way interactions. Including an intercept for every model, the number of parameters to be estimated,  $k_m$  for model  $\mathcal{M}_m$ , ranges between 1 and  $1 + 12 + \binom{12}{2} = 79$ . To choose a suitable model among all candidates, given the observed outcomes of csPCA = (csPCA<sub>1</sub>, ..., csPCA<sub>n</sub>) for  $n$  patients, the following equation is maximized:  $BIC(\mathcal{M}_m) = -\log(f(\text{csPCA}|\hat{\theta}_m)) + k_m \log(n)$ , where  $\theta_m \in \mathbb{R}^{p_m}$  is the vector of parameters in the model  $\mathcal{M}_m$ ,  $f(\text{csPCA}|\theta_m)$  the density function of the data given parameters  $\theta_m$ , also called likelihood function.  $\hat{\theta}_m$  is the parameter set that maximizes this function. For logistic regression and assuming independence of the individual records, this is given explicitly:  $\log(f(\text{csPCA}|\theta_m)) = \sum_{i=1}^n \text{csPCA}_i x_i' \theta_m - \sum_{i=1}^n \log(1 + \exp(x_i' \theta_m))$ , where  $x_i$  is the covariate vector of individual  $i$ .



Rather than pooling data across cohorts, the cohort ensemble method constructed separate models for each cohort, restricting to risk factors available by the end-user and collected by the training cohort. A risk factor was considered available in a training cohort if it was measured in 40% or more participants. Otherwise, it was not included to not prohibitively reduce the sample size for constructing a cohort-specific model. Because models were fit to single cohorts and some of the cohorts had small sample sizes, information from individual cohorts could be low or inadequate for robust multivariable model construction. For example, cohort 10 had only 243 biopsies. Such cohorts were not excluded because even though they may lack power for obtaining statistical significance of individual coefficients, the goal was to optimize out-of-sample prediction. Cohort-specific risks were averaged over the cohorts for the end user's result.

**Table 2.2:** Algorithms for the six risk modeling approaches. Starting variables are available risk factors from the user. Used and cohort variables are subsets or all of the starting variables corresponding to those used by the model and those with less than 40% missing rates in the cohort.

---

Algorithm: Available cases

---

- 1 Subset the PBCG data set by records without missing values for *starting variables*
- 2 Fit main effects logistic regression model with *starting variables* to the PBCG subset pooled for all cohorts

---

Algorithm: Iterative BIC selection

---

- 1 *used variables* = *starting variables*
- 2 while the number of used variables reduces do
- 3 Subset the PBCG data set (pooled for all cohorts) by *used variables*
- 4 Use only complete records
- 5 Perform logistic regression BIC selection starting with main effects up to two-way interactions
- 6 *used variables* = variables in the selected model (either as main effect or as interaction)
- 7 *risk* = Predict csPCA risk with information in *starting variables*
- 8 end while

---

Algorithm: Cohort ensemble

---

- 1 *cohort variables* = variables of each cohort with less than 40% missing records
- 2 for all cohorts do
- 3 *used variables* = variables of *starting variables* that are in *cohort variables*
- 4 Subset the PBCG data set by cohort and *used variables*
- 5 Use only complete records
- 6 Perform logistic regression BIC selection starting with main effects up to two-way interactions
- 7 *used variables[cohort]* = variables in the selected model (either as main effect or as interaction)

```
8   risk[cohort] = Predict csPCA risk with information in starting  
   variables  
9   end for  
10  overall risk = mean(risk)
```

---

Algorithm: Categorization

---

```
1   Categorize all predictor variables with the additional factor not available (NA).  
   Continuous variables with missing values are categorized.  
2   Fit main effects logistic regression model with all variables to the PBCG data  
   set pooled for all cohorts
```

---

Algorithm: Missing indicator

---

```
1   Categorize all categorical predictor variables with the additional factor missing.  
   Add for continuous variables with missing values an indicator variable, whether  
   the variable was missing or not  
2   Fit main effects logistic regression model with all variables and include the  
   interactions of the indicator with the corresponding variable in the model to  
   the PBCG data set pooled for all cohorts
```

---

Algorithm: Imputation

---

```
1   Run 30 imputations by chained equations (mice) on the training PBCG data  
   set  
2   for all imputed data sets do  
3     Fit main effects logistic regression model with all variables in the  
     model to the imputed PBCG data set pooled for all cohorts  
4   end for  
5   Impute missing values in the test case with means of the training set  
6   Average the coefficients from mice for use in the prediction models
```

---

The categorization algorithm returned to pooling data across all training cohorts and additionally transformed all continuous risk factors to categorical. Missing data could hence be added as an extra category. For inherently categorical risk factors, such as DRE, categories were coded as normal, abnormal, and missing. Prostate volume was stratified to  $< 30$ ,  $30$  to  $50$ , and  $> 50$  cc, as previously suggested, such that it could be obtained by pre-biopsy DRE or transrectal ultrasound scan (TRUS) before adding the additional category of missing (Roobol et al. 2012). The advantage of this approach was that only one model is fit and needed by the end-user. The missing indicator algorithm was similar to the categorization algorithm but did not require the categorization of continuous variables (Groenwold et al. 2012). Instead, it introduced an indicator equal to 1 if the corresponding risk factor was missing versus 0 if not missing. The model included the indicator and the interaction with the risk factor. Since prostate volume was the only continuous risk factor that was sometimes missing, the missing indicator algorithm differed from the categorization algorithm in only one variable. Second-degree prostate cancer- and first-degree breast cancer family history were either both collected or not at all by the individual cohorts. Adding a missing category to them would therefore induce multicollinearity. To avoid this, they were combined into a single new 5-category risk factor with second-degree prostate cancer family history only, first-degree breast cancer family history only, both present, none present or missing.

Multiple imputation has been recommended for fitting statistical models to training data to handle either outcomes or risk factors missing at random (MAR) (van Buuren and Groothuis-Oudshoorn 2011). In the case here, the outcome of csPCA was not missing for any individuals, so imputation was applied only for missing risk factors. Data were pooled across all ten cohorts to form the training set, and imputation was applied using the pooled set and not by cohort. For a patient in the training set with multiple missing risk factors, multiple imputation by chained equations (MICE) sequentially imputes missing data according to full conditional models appropriate to the risk factor data type. Therefore, it uses all other risk factors available as covariates along with the outcomes that have been fit to complete cases in the training set (van Buuren and Groothuis-Oudshoorn 2011; I. R. White et al. 2011). The R mice package uses five imputations as default, and the literature also recommended ten iterations (Bodner 2008; van Buuren and Groothuis-Oudshoorn 2011). We implemented 30 imputations as the average percentage of missing values across all risk factors in the training set. We averaged models built on the 30 imputed data sets for the final training set risk model. For the end-user or member of the validation set who is missing a risk factor, the algorithm imputed its value using mean values from the training set only and not from other members of a validation set, as the latter would not be available in practice (I. R. White et al. 2011).

We used internal cross-validation to compare the mean imputation approach with median imputation and MICE applied to the test case added to the validation set. Further, we tried two different approaches to combine the 30 imputed data sets. On each of the imputed data sets, a model was fit. The first approach combines the 30 models by building the average of each coefficient (pooled). The final model is used for the prediction of the test case. The second approach uses all 30 models to predict the test case and takes the mean of the predictions as the final prediction (average). Figure 2.4 shows no difference between averaging coefficients before prediction and averaging predictions. Median imputation performed slightly worse than the other two approaches in calibration in the large (CIL) but better in terms of area under the receiver operating characteristic curve (AUC) for some cohorts. The measures are described after the next paragraph. The other two approaches were comparable. Therefore, we choose pooled mean prediction as it is computationally the fastest and easiest in implementation.

External validation on the European cohort, which was not used for training, was measured by discrimination using the AUC along with its 95% confidence interval (CI), CIL, which evaluates the average difference between the predicted risk and binary csPCA outcome for each patient in the validation set, and calibration-in-the-small by calibration curves of observed versus predicted risk according to deciles of predicted risk. Internal leave-one-cohort-out cross-validation using the same metrics was performed by alternatively holding out one of the ten PBCG cohorts as a test set and training the models on the remaining nine cohorts. Distributions of AUCs and CILs from the ten test validations were visualized by violin plots showing smoothed histograms and boxplots showing medians and interquartile ranges. All analyses were performed in the R statistical package (R Core Team 2021).

Validation was evaluated by discrimination measured by the AUC (Hanley and McNeil 1982), accuracy measured by calibration curves and CIL (van Calster et al. 2019). The AUC consists of sensitivity and specificity, which depend on a threshold  $c$  that classifies

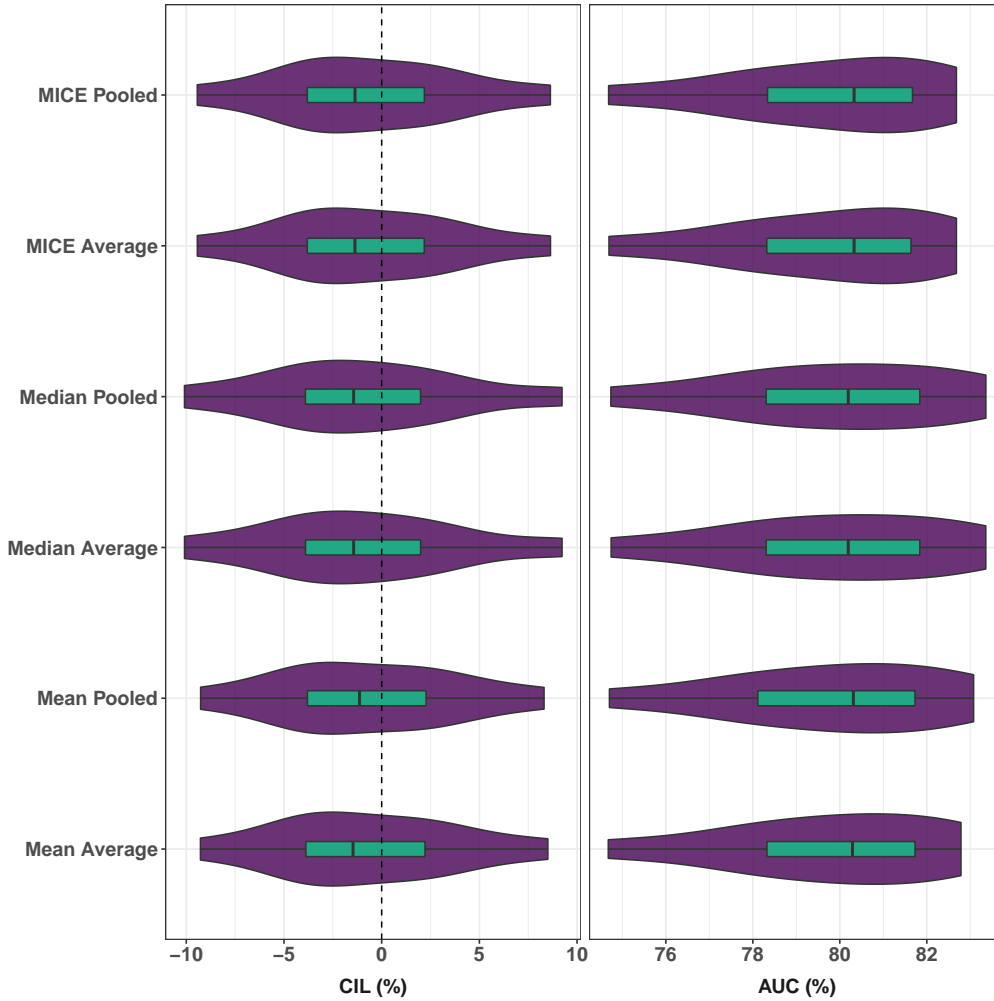


**Figure 2.4:** Comparison of imputation methods for prediction by internal cross-validation of the ten PBCG cohorts. The test patient's missing values are imputed by mean, median, and MICE. Pooling the model coefficients is compared to averaged predictions.

the patients with predicted risks  $> c$  as cases and  $\leq c$  as controls in the validation set:

$$Sens(c) = \frac{n_{\text{cases, predicted risk} > c}}{n_{\text{cases}}}, \quad Spec(c) = \frac{n_{\text{controls, predicted risk} \leq c}}{n_{\text{controls}}},$$

where  $n_{\text{cases}}$  is the number of patients with csPCA and  $n_{\text{cases, predicted risk} > c}$  is the number with csPCA and predicted risk greater than  $c$ . Higher sensitivity and specificity indicate a better model prediction. Similarly, the numbers for the controls are defined. The receiver operating characteristic (ROC) curve plots sensitivity versus 1-specificity for all possible thresholds  $c \in [0, 1]$ , and the AUC is the area underneath the resulting graph. Therefore, the higher the AUC, the better.

Calibration curves and the  $CIL = mean(\text{predicted risks}) - mean(\text{observed outcome})$  are used for accuracy, and they compare how well observed and predicted risks agree. For calibration curves, individual risks are plotted on the x-axis. Since the outcomes to be plotted on the y-axis are either zero or one, locally weighted regression was used to get a smooth line through the binary results. To assess CIL, the average predicted risk is compared with the overall event rate. The algorithm generally overestimates

risk when the average predicted risk is higher than the overall event rate. Conversely, underestimation occurs when the observed event rate is higher than the average predicted risk.

## 2.3 Results

Among 12,703 biopsies from ten PBCG cohorts used for training, 3,597 (28%) had csPCA, compared to 1,757 out of 5,540 (32%) csPCA cases in the external validation cohort (Figure 2.1). In terms of prevalence, the cohorts seem to be almost homogeneous around 30%, and only cohort 11 has a lower one at 15%. The sample size ranges from 243 in cohort 10 to 5,543 in cohort 3. All cohorts collected PSA and age but varied in the collection of the other ten risk factors, with some cohorts not collecting some risk factors at all (Figure 2.2). Differences between the cohorts in terms of distributions of the twelve risk factors and their associations with csPCA are shown in Figures 2.5 and 2.6. PSA greater than ten showed a higher prevalence of csPCA for all cohorts. For cohort 2, the high cases got excluded as described in Section 2.1. Cohort 11 has a lower overall prevalence, but the trend is the same. For age, we see similar patterns for men older than 65 years. Cohort 7 had the highest fraction of older men. For abnormal DRE ("Yes"), all cohorts showed higher prevalences besides cohort 7, with the highest prevalence in the missing group ("NA"). For smaller prostate volumes, higher csPCA prevalence could be found. For the other variables, trends could be seen less strongly.

Figures 2.7 and 2.8 show each variable's univariate odds ratios (ORs). We dichotomized continuous variables with an integer close to the median as a cutpoint. The x-axis shows the proportion of the dichotomized risk factor.

In Figure 2.7, we see that the overall OR estimate, which pools data from all eleven cohorts, lies in the middle of the cohort-specific ORs for PSA, age, prostate volume, and prior negative biopsy, and that almost all of them were significant. For DRE, ORs from cohorts 7 and 10 pull overall OR downwards. These two were the only ones not significant. For African ancestry, the situation was more interesting since the cohorts disagreed whether csPCA risk increases for African ancestry or not (ORs greater as well as smaller 1). The overall OR estimate was driven downwards from the non-significant cohort-specific ORs. Additionally, Overall included also values of cohorts that had only non-African patients.

For prior PSA measurement, cohort 3 was outside of the cluster in terms of prevalence (Figure 2.8). Furthermore, the cohorts were not agreeing about the influence since they appeared both above and under an OR of one, while almost all of them were not significant. We got a similar behavior for the first-degree prostate cancer family history. Second-degree prostate cancer and breast cancer family history were only collected by some cohorts. Additionally, all single cohort ORs showed no significant effect. For Hispanic ethnicity, cohort 7, which had mostly Hispanic patients, pulls the overall OR estimate upwards. Most of the cohort-specific ORs were insignificant, but the overall OR was. The reason was that pooling leads to a larger sample size of Hispanic and non-Hispanic individuals, thereby increasing the power to detect differences. This was

## 2 Accommodating heterogeneous missing data patterns for prostate cancer risk prediction

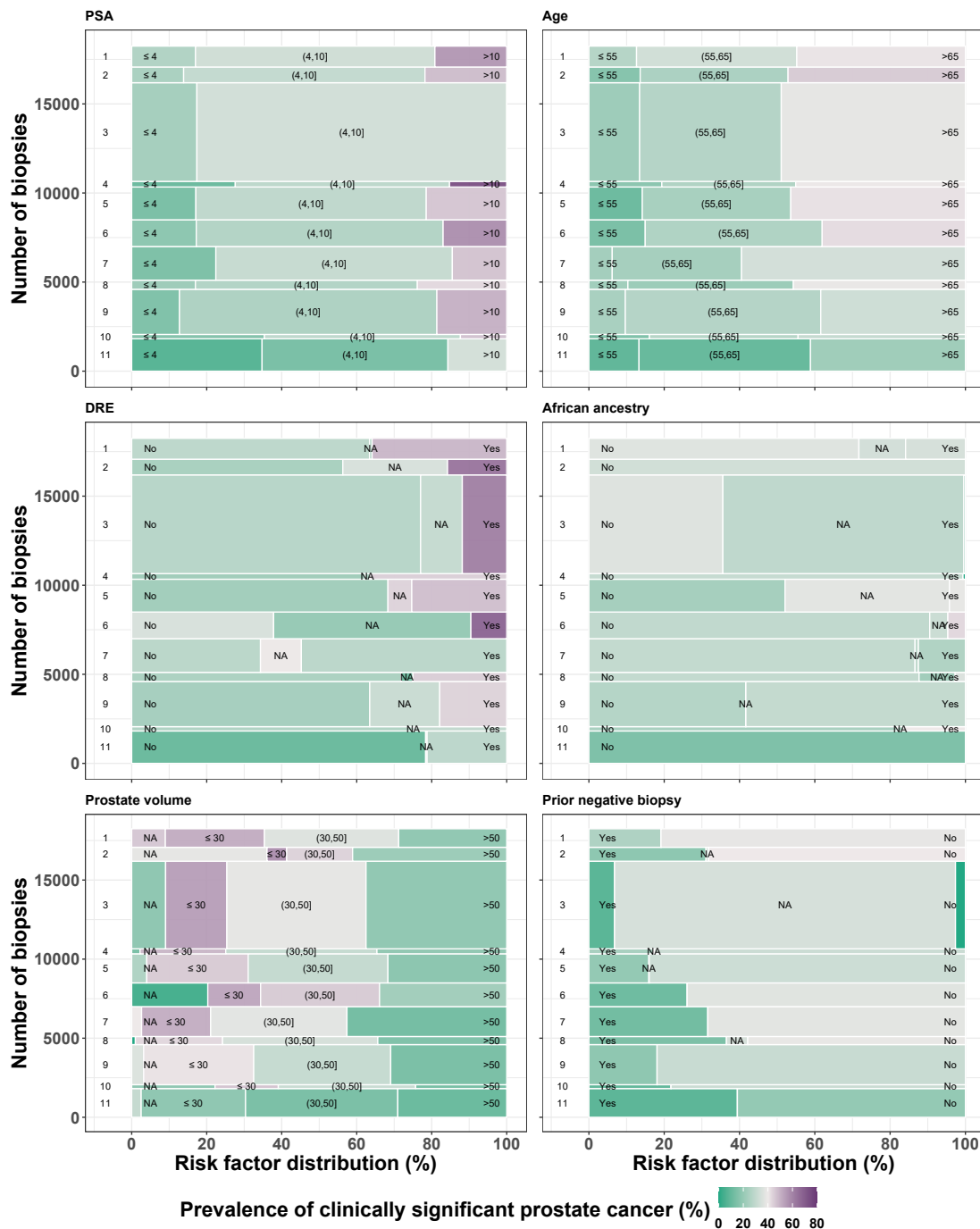


**Figure 2.5:** Differences between the cohorts in distributions of the twelve risk factors and their associations with csPCA (a). Continuous risk factors were split into three groups low, medium, and high, additionally to the group missing indicated by NA. The x-axis shows the percentage of the group within the cohorts. The y-axis shows the number of biopsies consistent between the different subfigures. NA = missing.

why the cohort 7 OR, higher than the overall OR, was not significant. For 5-alpha-reductase inhibitor (ARI) treatment, neither the cohort-specific ORs nor overall OR were significant. Most cohorts cluster underneath one but cohort 4 was far above one. Since 5-ARI was a prevention measure for prostate cancer, this made the estimate from cohort 4 suspect and warranted investigation of the patients included in the 5-ARI group.

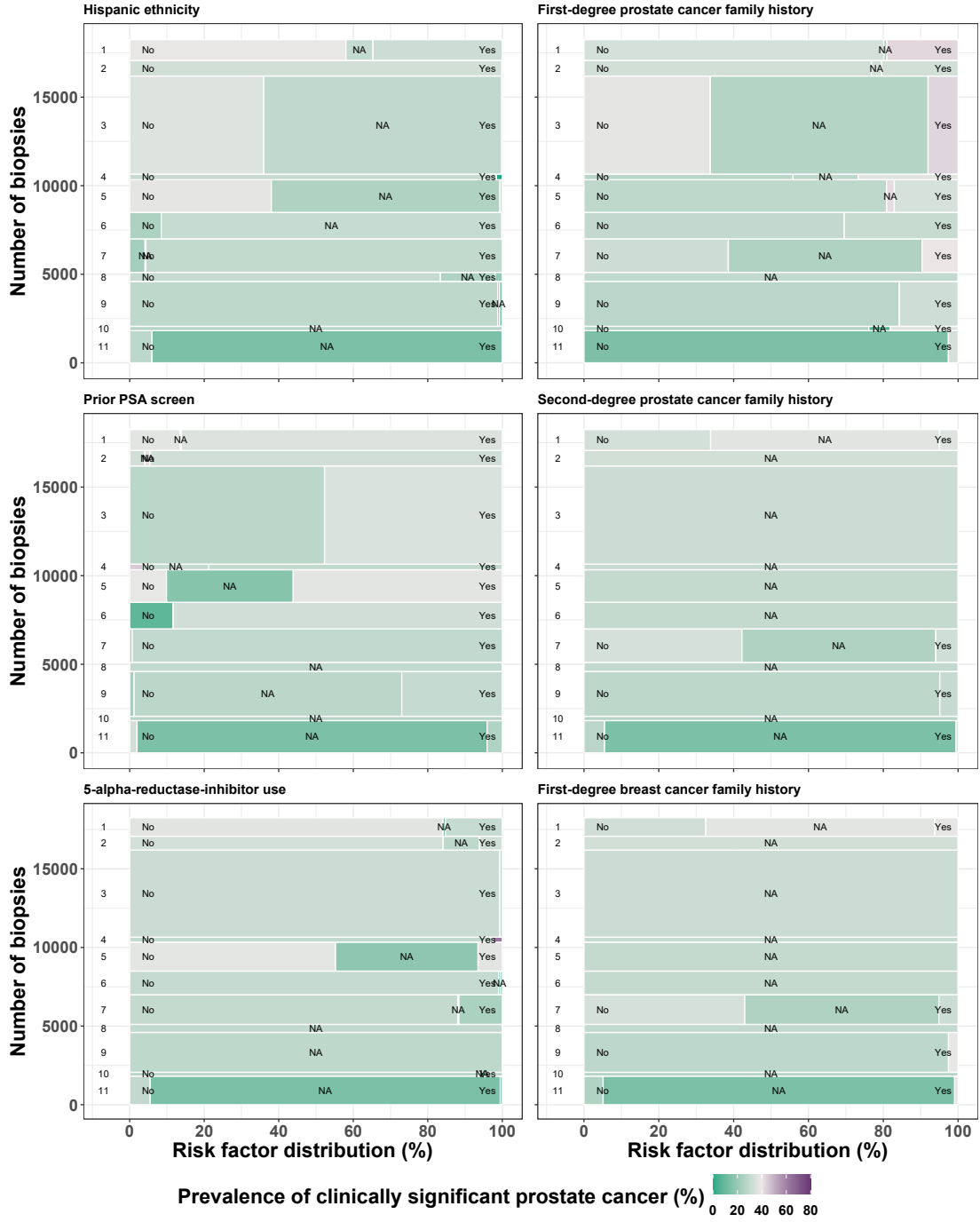


**Figure 2.6:** Differences between the cohorts in distributions of the twelve risk factors and their associations with csPCA (b). Continuous risk factors were split into three groups low, medium, and high, additionally to the group missing indicated by NA. The x-axis shows the percentage of the group within the cohorts. The y-axis shows the number of biopsies consistent between the different subfigures.

Pooling seems appropriate for most of the variables, but it might be misleading for some variables. So the pooling approach should be compared to other approaches that accommodate the missing values and related sample size problems.

## 2 Accommodating heterogeneous missing data patterns for prostate cancer risk prediction

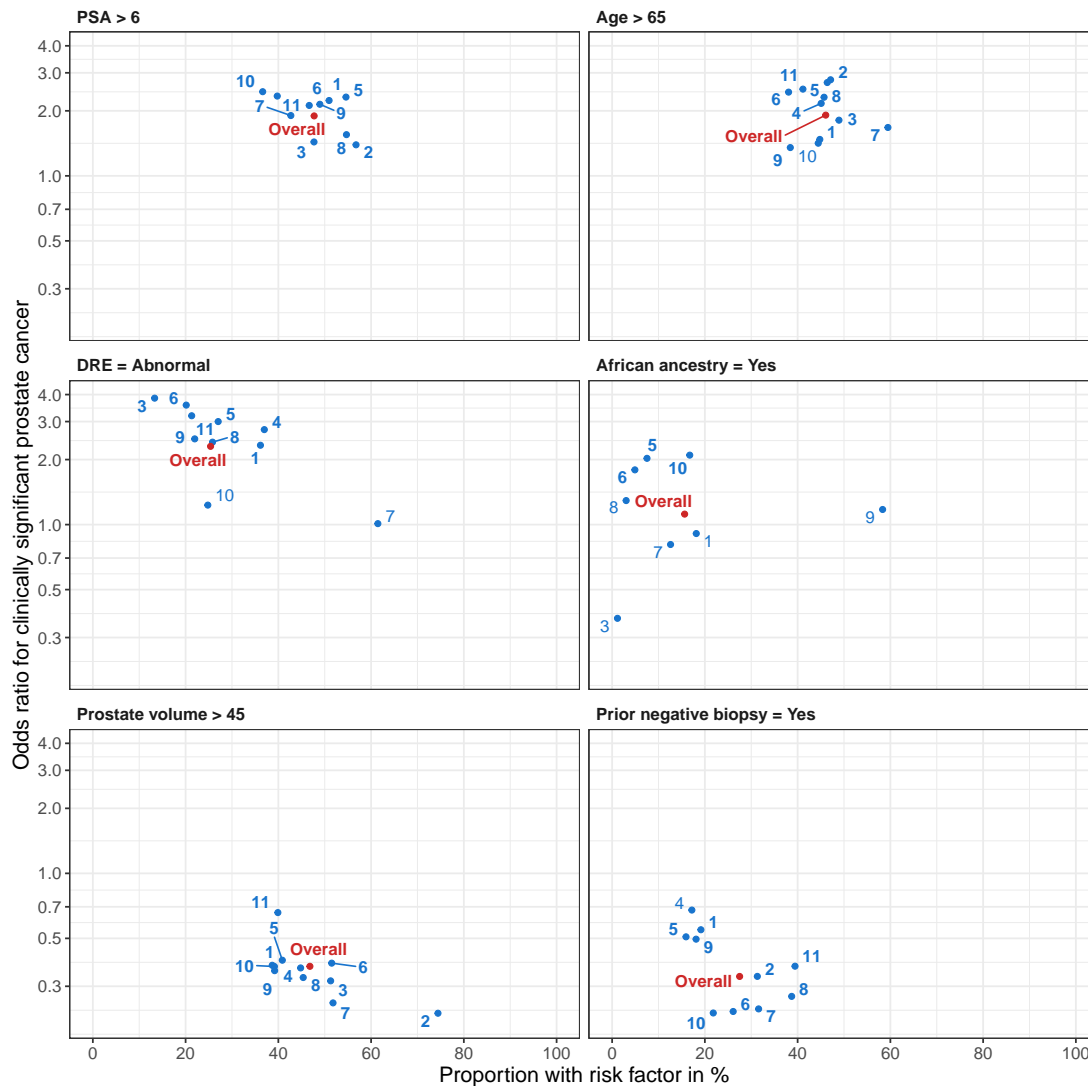


**Figure 2.7:** Baseline demographics and univariate odds ratios for the association between risk factors and csPCA by cohort. Overall indicates pooled data from all cohorts. Bold indicates significance at the 0.05 level. Data was not shown for PSA for cohort 4 (Proportion with risk factor (PRF) in %: 39.4, OR: 6.1, significant) and DRE for cohort 2 (PRF: 21.9, OR: 5.0, significant) because numbers were out of the range of the plot. Not shown cohorts for African ancestry: 2, 4, 11; for prior negative biopsy: 3, because either did not measure the variable, had only one outcome or unstable predictions; PSA: prostate-specific antigen, DRE: digital rectal exam.

In leave-one-cohort-out internal cross-validation across the ten PBCG cohorts to ultimately be used for training the online model, the iterative BIC selection method had the lowest median CIL (-0.2%), while the available cases method had the highest (2.6%, Figure 2.9). All of them were minor in magnitude. CIL values ranged from -11 to 11% across the ten cohorts used as test sets. All six methods had nearly the same median AUC at 80%, and values ranged from 74 to 84% across the ten test sets. The categorization and missing indicator methods had larger variations in CIL and AUC than the other methods.

In external validation, all six methods either under or over-predicted observed risks since



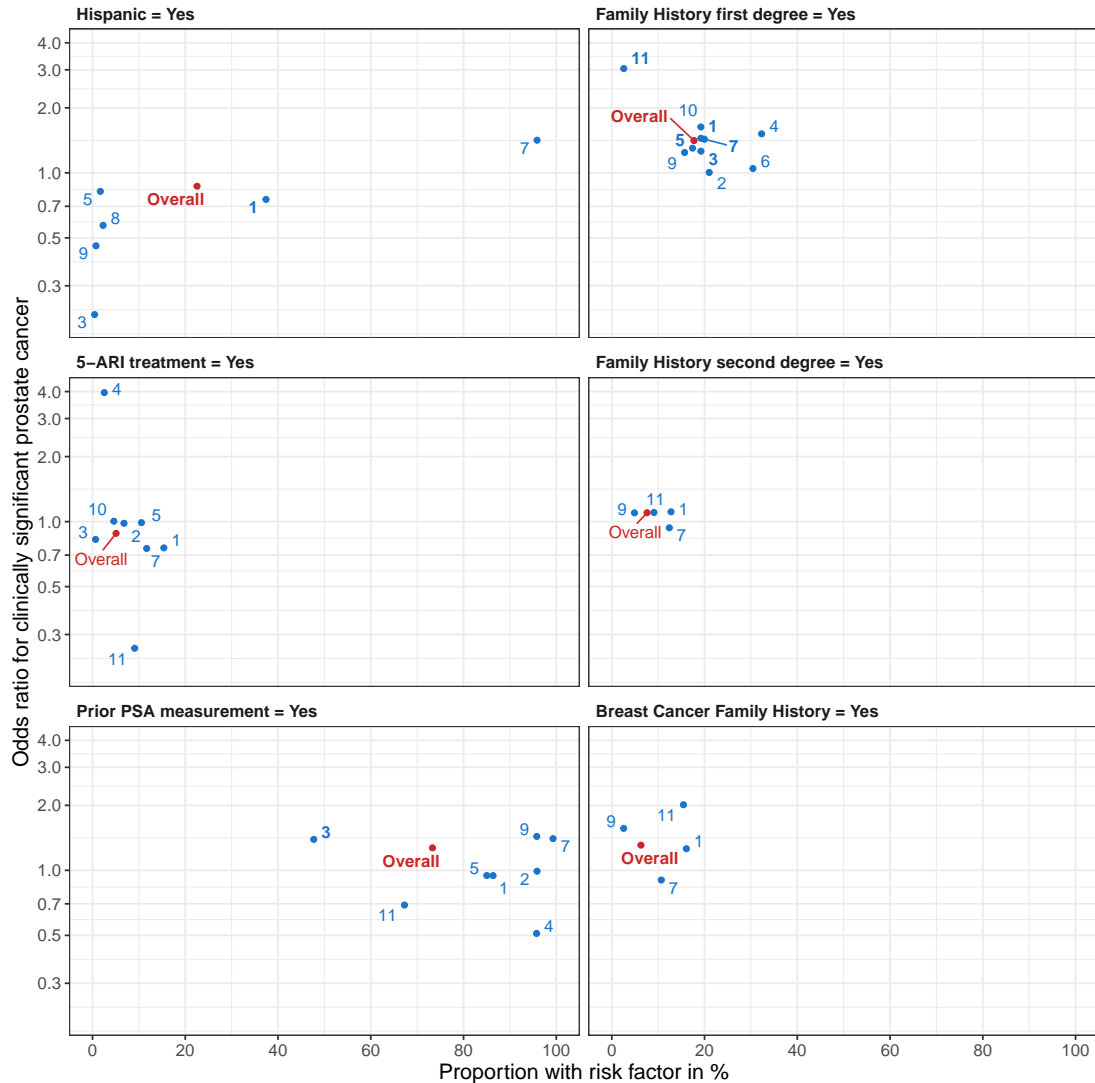


**Figure 2.8:** Baseline demographics and univariate odds ratios for the association between risk factors and csPCA by cohort. Overall indicates pooled data from all cohorts. Bold indicates significance at the 0.05 level. Data was not shown for prior PSA for cohort 6 (Proportion with risk factor in %: 88.3, OR: 5, significant) because numbers were out of the range of the plot. Not shown cohorts for prior PSA: 8,10; for 5-ARI treatment: 6, 8, 9; for Hispanic ethnicity: 10, 4, 6, 2, 11; for first-degree family history: 8; for second-degree and breast cancer family history: 10, 3, 4, 6, 2, 5, 8, because either did not measured the variable, had only one outcome or unstable predictions; PSA: prostate-specific antigen.

none of the 95% CIs for CIL, computed as the average predicted risk minus the disease prevalence in the external validation cohort (32%), contained the value 0 (Table 2.3). The available cases method was the most accurate, under-predicting risk on average by 2.9%. The categorization and missing indicator methods over-predicted risks by 3.5% and 4.2%, respectively, while all other methods under-predicted risks, with imputation the worst by 12.4%. Similar results can be seen in the important prediction range between 0 and 50% predicted risk, where available cases performed best with the closest line to the bisector (Figure 2.10). Additionally, we can see that imputation is consistently under-predicting and worse for higher risks. The AUCs ranged from 75.4% for the iterative BIC selection method to 77.4% for the missing indicator method, but all 95%

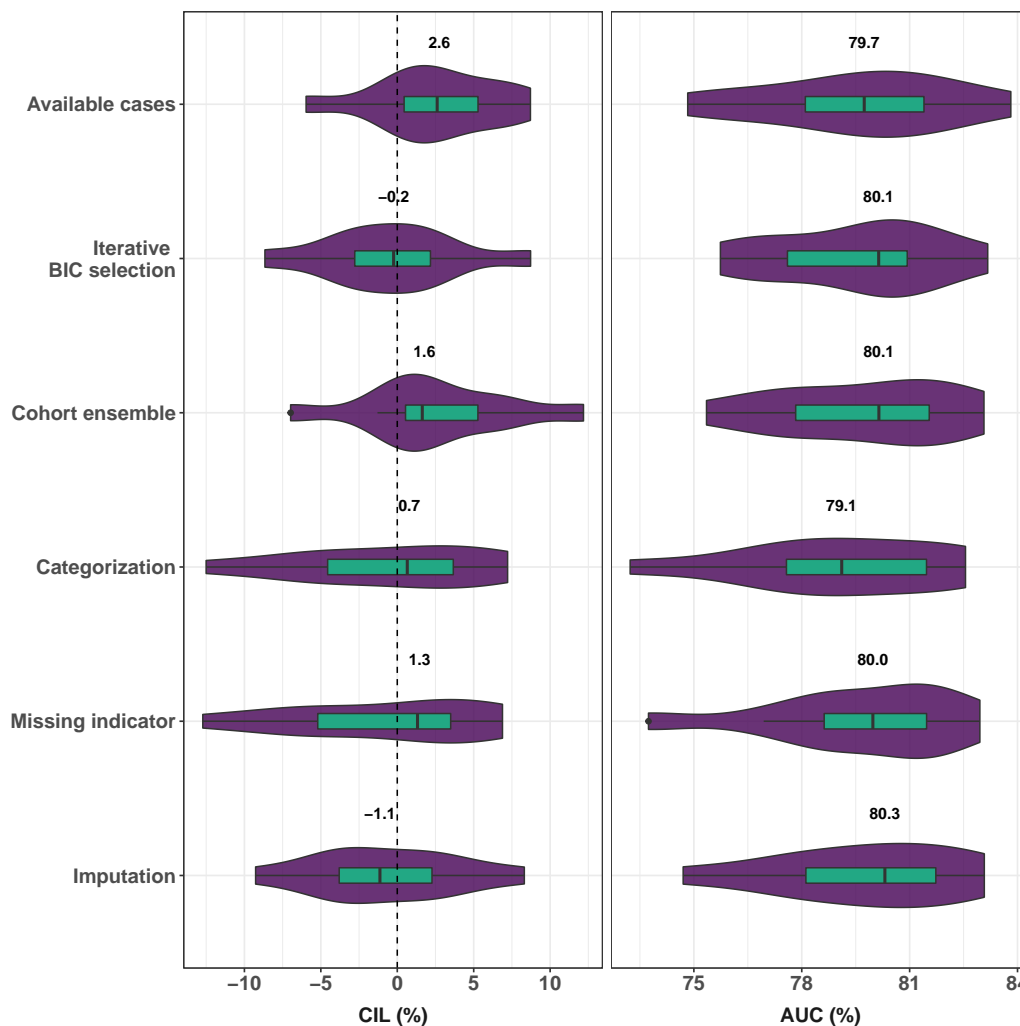


**Figure 2.9:** CIL and AUC performing leave-one-cohort-out cross-validation on ten PBCG cohorts. Median values are indicated with numbers and as vertical lines in the boxes.

CIs overlapped (Table 2.3).

Comparisons of individual predictions from the six different methods for the 5,540 members of the external validation cohort are shown in Figure 2.11. As seen on the diagonal, for all methods, the distribution of predicted risks for csPCA cases was higher than for non-csPCA individuals, but considerable overlap remained. Correlations of predictions by the six methods were high, all exceeding 0.8. The iterative BIC selection, cohort ensemble, and available case methods were similar methods. All use only complete cases for a specified individual’s risk factor profile and hence were highly correlated. The remaining three methods adjusted for missing data in some manner and were less correlated with these methods, with categorization the least correlated, though still very highly correlated.

We chose the available cases method for implementation of the risk tool online since it showed the highest accuracy in calibration in external validation (Figure 2.10), where all six methods showed equivalent AUCs (Table 2.3). AUCs and CILs across the ten cohorts used as test sets in the internal leave-one-cohort-out cross-validation were also similar, and the available cases method had the lowest variability (Figure 2.9). The

**Table 2.3:** External validation CIL and AUC values with risks as percentages along with 95% confidence intervals.

Method	CIL	(95% CI)	AUC	(95% CI)
Available cases	-2.9	(-4.0, -1.8)	75.7	(74.4, 77.1)
Iterative BIC selection	-8.6	(-9.7, -7.5)	75.4	(74.0, 76.8)
Cohort ensemble	-7.1	(-8.2, -6.0)	76.4	(75.1, 77.7)
Categorization	3.5	(2.4, 4.6)	76.6	(75.2, 77.9)
Missing indicator	4.2	(3.1, 5.3)	77.4	(76.1, 78.7)
Imputation	-13.3	(-14.4, -12.2)	75.9	(74.5, 77.2)

available cases method is less computationally intensive than multiple imputation and is valid under MAR assumptions based on unobserved risk factors and outcomes. This untestable assumption may be assumed as approximately holding when all established risk factors for outcomes are assumed to have been collected (Mealli and Rubin 2015).

To implement the prediction tool online, we fit 1,024 models to allow for all possible missing risk factor patterns among ten risk factors in order to use the maximum prostate biopsies possible from the ten PBCG cohorts. The smallest model only contains PSA and age, utilizing all 12,703 biopsies from the ten PBCG cohorts since these two risk factors were measured for all individuals. The largest model includes all 12 risk factors and was constructed from only 1,334 biopsies from three PBCG cohorts, as these were the only complete cases. These two risk models are shown in Table 2.4, with all possible models accessible online at [riskcalc.org](http://riskcalc.org). Figure 2.12 shows boxplots of all coefficients of the 1,024 models. The intercept had a wide range which is ok since it depends on how many and which variables were included in the model. Age, PSA, prostate volume, DRE, and all family history variables had consistent effects in terms of increasing or decreasing csPCA odds. Other characteristic effects depend on the remaining variables in the model. Hispanic ethnicity turns out to have often no effect (median OR close 1), but its OR ranges up to around 2. The comparison of risk predictions for a high and low-risk patient depending on the combination of available risk factors is shown in Figure 2.13. The more risk factors, the more accurate the prediction becomes. As more predictors were missing, the risk prediction was more moderate, which means for the high-risk patient a risk of 30% instead of 80%, and for the low-risk patient a predicted risk of up to 10% instead of close to 0%. Further, one could observe a high prediction variability depending on the available risk factors. Evaluated on the same validation set of 5,540 biopsies as used for Table 2.3, the original PBCG risk tool published in 2018 (Ankerst et al. 2018) based on only six of the twelve risk factors used here obtained a CIL of -5.9 (95% CI -7.1, -4.7), and an AUC of 66.9 (95% CI 65.4, 68.5), which is 10 points lower than any of the methods incorporating the additional risk factors. Adding just prostate volume to these six risk factors and evaluating on the validation set yielded a CIL of -10.1 (95% CI -11.2, -9.0) and an AUC of 75.6 (95% CI 74.2, 76.9; p-value < 0.0001 for test of equality of this AUC to that from the standard model). Assessment of prostate volume, however, requires an invasive procedure that is not routinely performed in advance of the prostate biopsy.

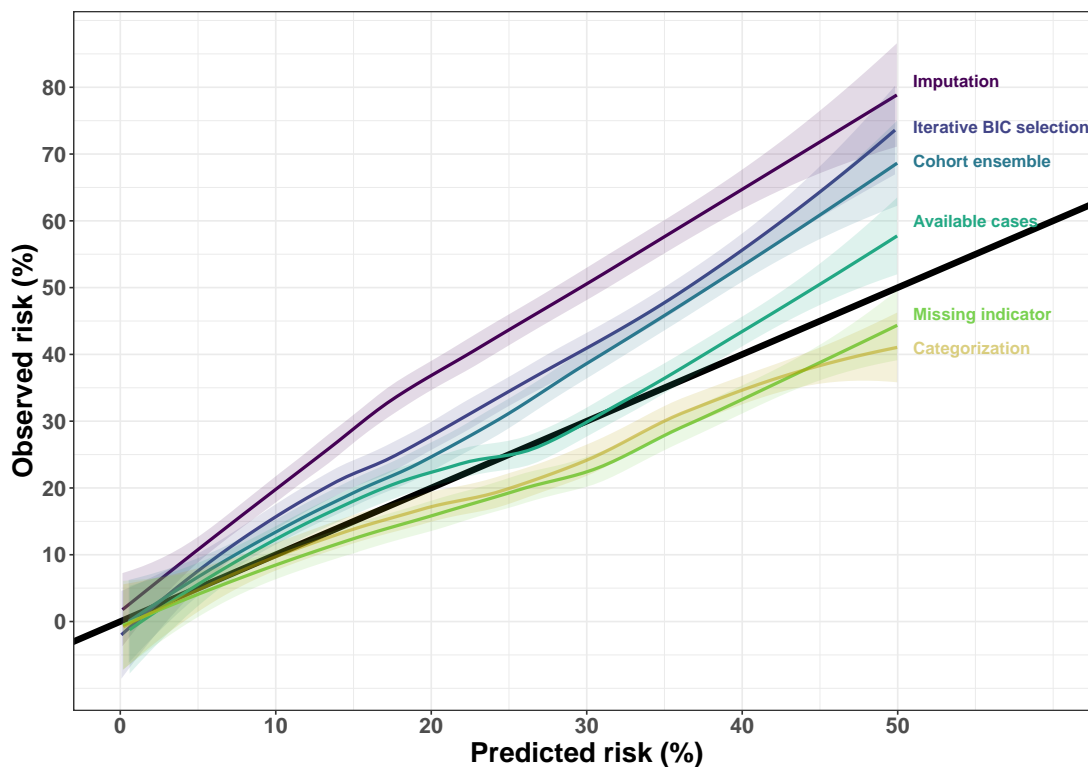


**Figure 2.10:** Calibration plots with shaded pointwise 95% CIs for the six modeling methods applied to ten PBCG training cohorts and validated on the external cohort. The diagonal black line is where predicted risks equal observed risks. Lines below the diagonal indicate over-prediction, and lines above under-prediction on the validation set.

**Table 2.4:** Odds ratios from the largest, standard, and smallest models in terms of the number of 12 risk factors available from an end-user. Sample sizes were the number of individuals in the training set with all risk factors available (complete cases) and the number of cohorts contributing to the complete cases. In total, 1,024 models were available based on the option of including ten risk factors, all except PSA and age. R code for all 1,024 models is available at the Cleveland Clinic Risk Calculator library, <https://riskcalc.org/ExtendedPBCG/>.

Odds ratios for the full model containing twelve risk factors based on a fit to 1,334 prostate biopsies from three cohorts.

Risk factor	Odds ratio	95% CI	p-value
Age	1.07	(1.05, 1.09)	< 0.0001
PSA (log2)	2.38	(1.98, 2.89)	< 0.0001
African ancestry			
No	Ref	–	–
Yes	0.68	(0.45, 1.03)	0.08
Prostate volume (log2)	0.25	(0.20, 0.32)	< 0.0001
DRE			
Normal	Ref	–	–
Abnormal	1.95	(1.46, 2.60)	< 0.0001
Prior negative biopsy			
No	Ref	–	–
Yes	0.32	(0.22, 0.45)	< 0.0001

Hispanic ethnicity			
No	Ref	–	–
Yes	1.08	(0.78, 1.50)	0.6
5-alpha-reductase-inhibitor use			
No	Ref	–	–
Yes	0.96	(0.63, 1.44)	0.8
Prior PSA screen			
No	Ref	–	–
Yes	0.71	(0.38, 1.34)	0.3
First-degree prostate cancer family history			
No	Ref	–	–
Yes	1.93	(1.38, 2.69)	0.0001
Second-degree prostate cancer family history			
No	Ref	–	–
Yes	1.30	(0.86, 1.96)	0.2
First-degree breast cancer family history			
No	Ref	–	–
Yes	1.15	(0.77, 1.70)	0.5
Odds ratios for the model containing the six standard risk factors based on a fit to 8,432 prostate biopsies from 9 cohorts.			
Age	1.05	(1.04, 1.06)	< 0.0001
PSA (log2)	1.99	(1.86, 2.12)	< 0.0001
African ancestry			
No	Ref	–	–
Yes	1.26	(1.11, 1.44)	0.0005
DRE			
Normal	Ref	–	–
Abnormal	2.57	(2.29, 2.88)	< 0.0001
Prior negative biopsy			
No	Ref	–	–
Yes	0.28	(0.24, 0.32)	< 0.0001
First-degree prostate cancer family history			
No	Ref	–	–
Yes	1.94	(1.70, 2.22)	< 0.0001
Odds ratios for the smallest model containing two risk factors based on a fit to 12,703 prostate biopsies from 10 cohorts.			
Age	1.05	(1.05, 1.06)	< 0.0001
PSA (log2)	1.72	(1.64, 1.80)	< 0.0001

## 2.4 Discussion

Systematic missing clinical data across heterogeneous cohorts pose challenges for both model developers and end-users. We compared six methods that have been proposed for handling missing data with the objective to find the method most likely to perform well in multiple external validation studies of a globally accessible online risk tool. As with

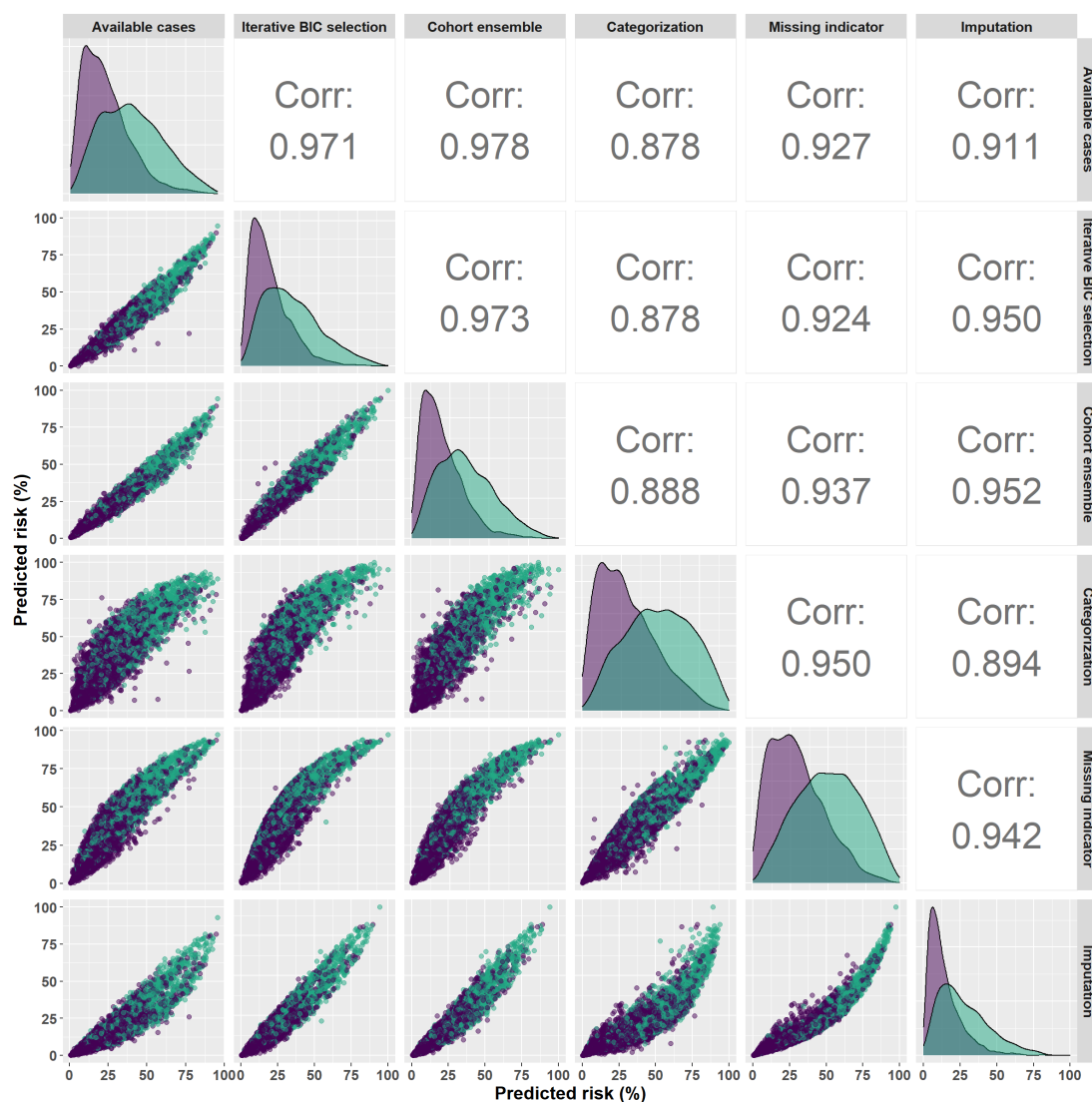


**Figure 2.11:** Marginal and pairwise comparisons of predictions from the six methods for the 5543 biopsies of the external validation set, pooled and stratified by csPCA status (31.7% with csPCA). Corr indicates Pearson correlation. Turquoise displays individuals with csPCA and purple without.

all online risk tools, an online publication of the original PBCG continues to result in published external validation studies providing evidence for or against its generalizability to other populations, particularly in comparison to other published tools (Amaya-Fragoso and García-Pérez 2021; Carbuñaru et al. 2019; Doan et al. 2021; Jalali et al. 2020; Presti et al. 2021; van Riel et al. 2022; Yildizhan et al. 2022). To date, by the exclusion of prostate volume, the original PBCG tool has competed less favorably with the other tools incorporating this information. Publication of the expanded risk tool incorporating prostate volume (Figure 2.14) will hopefully increase its accuracy for doctors and patients as to be evinced by forthcoming external validation studies.

Statisticians have recommended the available case method as it is valid even when data are MAR. This means that whether or not a risk factor is missing is independent of the unknown value of the risk factor, conditional on the known outcome and other available risk factors for the patient (Donders et al. 2006; Hughes et al. 2019; Mealli and

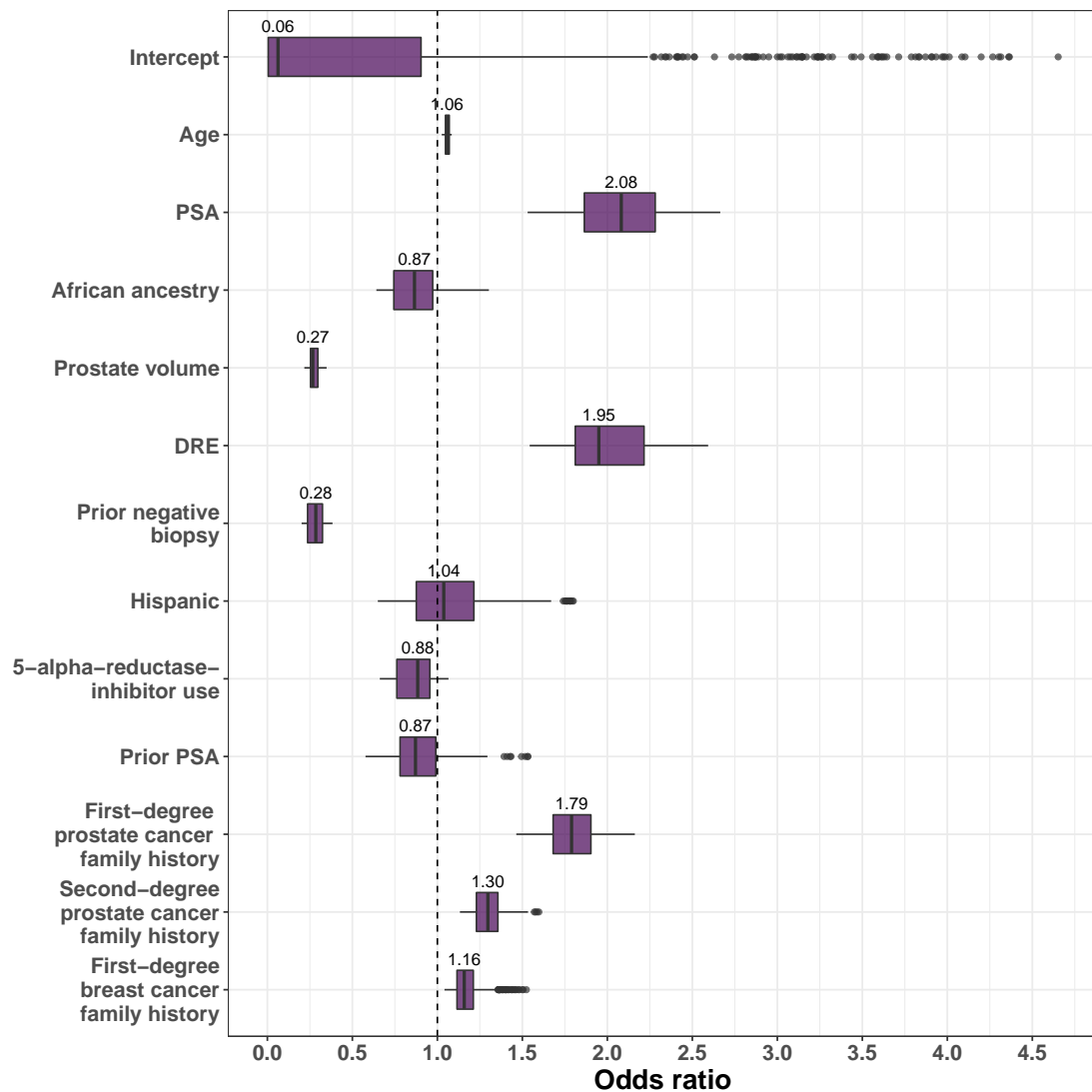


**Figure 2.12:** Model coefficients of available cases method. In total, 1,024 models were available based on the option of including ten risk factors, all except PSA and age.

Rubin 2015). The majority of risk factors collected across the PBCG are those typically collected in urological clinics from men presenting for PSA screening or follow-up. The most ubiquitous and predictive risk factors, PSA and age, have been collected for all PBCG participants and are exempt from missing data assumptions. Men typically receive multiple PSA screening tests. The PBCG used the PSA most recent but prior to the prostate biopsy. In some cases, the assumption of MAR for the remaining risk factors may be questionable. For example, the prostate volume may not have been reported when the value was assessed to be too low, or csPCA was not discovered on biopsy. There is no statistical test for MAR. Hence we relied on external and internal cohort-based validations to compare the available case to competing methods for selecting the method that produces optimal performance across a range of scenarios that would be encountered in practice. The available cases method was driven by the user and has been referred to as the  $2^k$  model approach (Hoogland et al. 2020) and Multiple Models for Missing values at Time Of Prediction approach (Ma et al. 2020) in the literature.

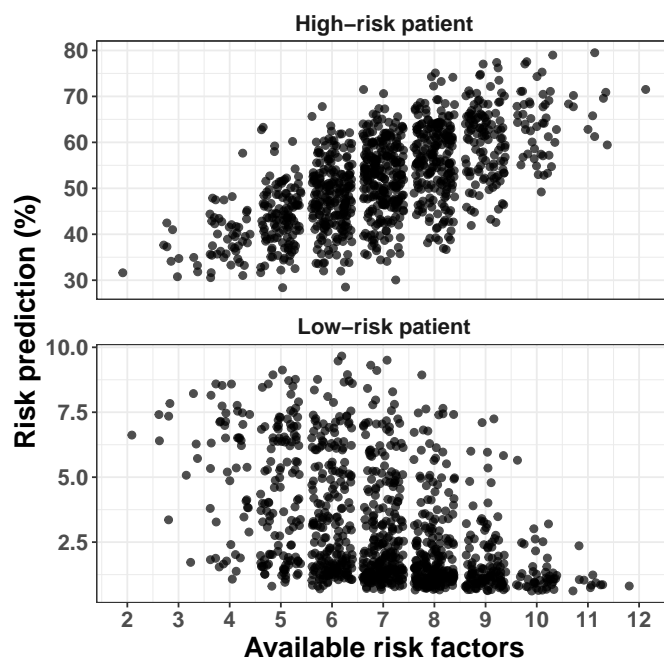


**Figure 2.13:** Change in prostate cancer risk according to how many risk factors a patient has available based on the 1,024 potential models. The low risk patient is 60 years old, has PSA of 1 ng/mL, non African ancestry, has prior biopsy performed, normal DRE, no first-degree family history, no second-degree family history, no first-degree breast cancer family history, prostate volume of 44 cm<sup>3</sup>, had 5-ARI treatment, is non-Hispanic, and had a prior PSA measurement. The high risk patient is 75 years old, has PSA of 4 ng/mL, has African ancestry, has not performed prior biopsy, has abnormal DRE, first-degree family history, second-degree family history, first-degree breast cancer family history, has prostate volume of 44 cm<sup>3</sup>, had no 5-ARI treatment, is Hispanic, and had no prior PSA measurement.

The missing indicator method has been shown to potentially result in biased odds ratios, even when data are missing completely at random. This means no relation, conditional or not, between whether a risk factor is missing and all other variables. This leads to strong recommendations against its use for causal or explanatory inference (Donders et al. 2006; Mealli and Rubin 2015; van der Heijden et al. 2006). The categorization method suffers from the same potential biases since it changes all continuous predictors to categorical ones before applying the missing indicator method. A recent study affirmed that such methods could be used for randomized trials as the missingness of protocol-specified variables would be randomized by the random treatment assignment, thus eliminating systematic bias (Groenwold et al. 2012).

The emergence of clinical risk prediction tools embedded in electronic health records, where missing data are large and systematic, has led to support for the missing indicator method. It is used in model development to match the method used when the model is deployed, and that if informative presence is potentially informative with respect to prediction, it should be leveraged (Sisk et al. 2021; Sperrin et al. 2020). Machine learning and other supervised learning methods follow the principle of developing prediction models to optimize accuracy on internal and external validation, often with uninterpretable models. The renowned James-Stein result shows that an estimator with effects shrunk towards zero can be preferable to the unbiased estimator. These concepts



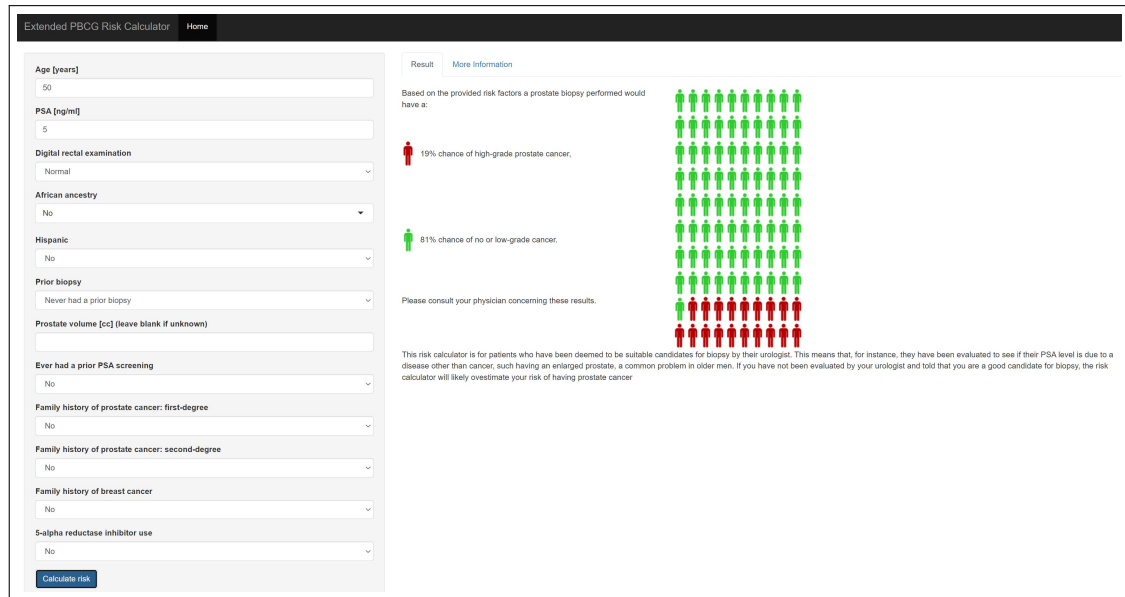


**Figure 2.14:** Online risk calculator using all 1,024 models is available at the Cleveland Clinic Risk Calculator library, <https://riskcalc.org/ExtendedPBCG/>.

are often applied in regularized regression approaches for situations with high numbers of predictors (Stein 1956). Across the validations performed in the PBCG, the potentially biased missing indicator and categorization methods did not perform substantially worse than the available cases methods. We agree that caution should be exercised towards their use when data are combined across cohorts, where some cohorts do not collect some risk factors at all, as this was the case with extended family history in this study. In this case, the effect of the missing category was confounded with that of the cohort. The coefficient for missing prostate volume following the missing indicator method fit to the ten PBCG cohort data was close to zero. Meaning a patient with missing prostate volume had nearly 0 odds of csPCA compared to a person not missing prostate volume, which can only be a cohort effect.

## 2.5 Conclusion

In addition to contributing to model development techniques for systematic missing data across heterogeneous cohorts, we have provided helpful methods for the end-user of online risk tools, namely the fit of multiple models for different risk factor missing data patterns. Such work enables more users to access online risk tools. Each model was fit to all complete cases that contained the risk factors, thus optimizing information and accuracy for the user. Our online tool requires PSA and age for use and any collection of up to ten additional risk factors. As consortia and available data grow in size, so does the amount of missing data as well. A flexible modeling strategy accommodating missing data on both the development- and user-end maximizes information by utilizing multiple data sources and increases accessibility to a broader band of patients by including those limited in risk factor assessment.



### 3 The influence of weather on fatal accidents in the Austrian mountains

A portion of this chapter is published in Neumair M., Estrella N., Menzel A., Ankerst D.P. The influence of weather on fatal accidents in Austrian mountains. *Weather, Climate, and Society*, 2021, <https://doi.org/10.1175/WCAS-D-21-0082.1>. Matthias Neumair analyzed the data, performed all statistical association analyses and interpreted the results. Nicole Estrella provided the data. Matthias Neumair wrote the manuscript with contributions from Donna P. Ankerst and Annette Menzel.

Recent studies have established the detrimental effects of non-optimal temperatures on mortality (Martínez-Solanas et al. 2021; Urban et al. 2021) and cause-specific mortality (Burkart et al. 2021), including COVID-19 outbreaks (Quilodrán et al. 2021), acute cardiovascular events (Saucy et al. 2021), respiratory and renal disorders (Kollanus et al. 2021), and suicide (Deisenhammer et al. 2003; Heo et al. 2021). Identification of temperature effects on mortality risks, whether due to small elevations above or below normal or extreme events such as heat waves, promotes the development of health warning systems that can mitigate risks (Issa et al. 2021).

Since hiking and climbing in summer and snow-related sports in winter have become increasingly popular, mountain accidents and fatalities have been increasingly subject to periodic monitoring to ensure the safety of tourists and sports enthusiasts (Faulhaber et al. 2020; Lischke et al. 2001; McIntosh et al. 2008; Rugg et al. 2020). Links between temperature, weather conditions, and outdoor accidents were established, leading to a hypothesis of potentially similar influences on fatal mountain accidents (Unguryanu et al. 2020). George (1993) identified climatic factors leading to mountain weather hazards and highlighted the need for accurate weather forecasts. Pascual and Callado (2010) reported the association between mountain accidents in the Pyrenees and winter storms for twelve selected accidents with defined accident patterns. They concluded that the described weather conditions should be communicated to visitors by suitable forecasts. Ruedl et al. (2012) showed the influence of low ambient temperatures and snowfall on knee injuries in female skiers at five Austrian ski areas. The German Alpine Association concluded that the extremely hot summer of 2003 increased physical problems and worsened unfavorable terrain conditions, ultimately leading to increased mountain emergencies (DAV 2015). Hiking routes in the Mont Blanc massif had to be changed in response to warming during recent decades (Mourey et al. 2019).

Weather effects may intensify under projected climate change scenarios, where summers may experience more intense heat and winters colder temperatures in mid-latitudes, resulting in new extremes in precipitation and climate events (IPCC 2018). The objective

of this study was to first comprehensively describe the mountain fatal accident patterns observed in Austria during a 12-year period (Section 3.4) and then quantify the influence of weather on these patterns (Sections 3.5 and 3.6). As one of the top tourist and outdoor sports destinations in Europe, Austria serves as an ideal model for preventative measures to reduce the health burden from mountain accidents imposed by projected increases in non-optimal temperatures (Burkart et al. 2021).

## 3.1 Fatal mountain accidents

The Austrian Alpine Safety Board (Österreichisches Kuratorium für Alpine Sicherheit) documents all fatal accidents in mountainous terrain across Austria, excluding the flat regions of Burgenland and Vienna. Austria lies in the center of Europe, spanning 46 to 49 degrees N in latitude and 9 to 17 degrees E in longitude. It is a worldwide destination for mountain sports (its highest mountain is 3,797 meters) due to its natural and accessible landscape. This study was based on data from November 2006 to October 2018, comprising 12 years and 3,466 fatal accidents related to mountain sports disciplines. Following local traditions, the winter sports period comprised November to April, and the summer comprised May to October. Information provided for each accident were the date, number of fatalities, discipline, municipality, state, and geographical coordinates of the nearest station. Text information on light and weather conditions at accident sites was also provided but missing in 15% and 6% of records in the winter and summer seasons, respectively. They were hence only described without formal analysis. Geographical coordinates that were missing or erroneously fell outside of Austria were imputed using coordinates of the respective municipality center. Since fatal accidents were combined with the closest weather station for analysis, the small number of potential inaccuracies did not impact the analysis. Starting with a data set of 3,466 fatal accidents, records with missing location (41), flight (102), cave (6), and lift accidents (11), as well as winter sports occurring during the summer season (17) and summer sports in the winter season (4), were excluded, yielding 3,285 fatal accidents, 1,817 in summer and 1,468 in winter, for analysis (Figure 3.1).

## 3.2 Weather data

Daily weather information on 36 variables from 43 climate stations with an elevation greater than or equal to 900 meters above sea level from November 1, 2006 to October 31, 2018 was provided by the Central Institut for Meteorology and Geodynamics (ZAMG) in Vienna. The locations are shown in Figure 3.1, and the variables are described in Table 3.1. The threshold of 900 meters was chosen to mirror regions typical for mountain activities as covered by the safety board.

To exclude annual and location dependencies of continuous weather variables, the World Meteorological Organization (WMO) recommends the calculation of anomalies, which measure differences from averages or normalized values (World Meteorological Organization 2017). Anomalies for each continuous weather variable were computed by subtracting the station-specific median of that variable across all days of the study

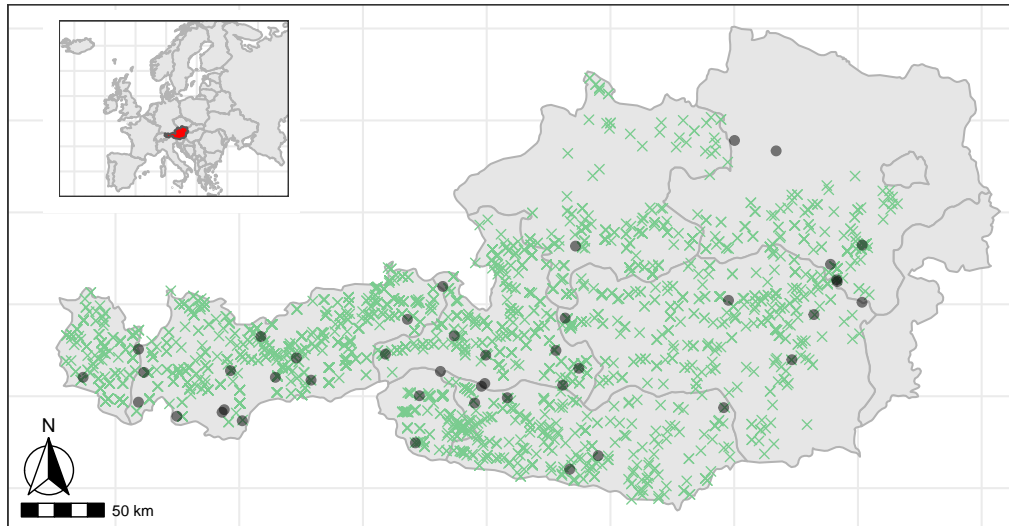


**Figure 3.1:** Locations of 3,285 fatal mountain accidents from November 2006 to October 2018 in Austria. Black dots show the locations of 43 climate stations, and green crosses the fatal accidents.

period, November 1, 2006 to October 31, 2018.

**Table 3.1:** Description of meteorological variables collected at 43 climate stations of the ZAMG.

Meteorological variable	Measure / Time	Unit/categories
Air temperature	Max, min, avg, 7 am, 2 pm, and 7 pm	°C
Air Pressure	Avg, 7 am, 2 pm, and 7 pm	hPa
Relative humidity	Avg, 7 am, 2 pm, and 7 pm	%
Global radiation	Total	kWh m <sup>-2</sup>
Precipitation	7 am, 7 pm, and total (7 am on measurement day – 7 am on following day)	mm
Precipitation type	7 am, 7 pm, and total (7 am on measurement day – 7 am on following day)	e.g. rain, snow, hail
Wind speed	7 am, 2 pm, and 7 pm	Beaufort; m s <sup>-1</sup>
Wind direction	7 am, 2 pm, and 7 pm	1-32, 32 = north, 16 = south
Maximum wind speed	12 am – 11:59 pm	m s <sup>-1</sup>
Time maximum wind speed	12 am – 11:59 pm	hh:mm
Cloudiness/coverage	Avg, 7 am, 2 pm, and 7 pm	1/10ths of cover
Snow height	7 am	cm
Snow type	7 am	No snow cover, spots, perforated snow cover, and full snow cover
Fresh snow height	Total (7 am previous day – 7 am measurement day)	cm

Max, min, and avg indicate the daily maximum, minimum, and average; total indicates the daily sum. All times are in local time.

For instance, the average temperature anomaly of station 1 on 17th August 2011 is calculated by:

$$\text{Anomaly } temp_{\text{avg}}(2011-08-17) = temp_{\text{avg}}(2011-08-17) - \text{median}(temp_{\text{avg}}(2007-08-17), temp_{\text{avg}}(2008-08-17), \dots, temp_{\text{avg}}(2018-08-17))$$

The Haversine formula (Robusto 1957) was used to map latitude and longitude coordinates of the locations where fatal accidents occurred to the closest of the 43 climate stations to match weather variables and anomalies to dates of fatal accidents. The Haversine distance measure  $d$  for two longitude-latitude coordinates in degrees with the average earth radius (6,371 km) and the identity  $\sin^2(\frac{\phi}{2}) = \frac{1-\cos(\phi)}{2}$  applied, summarizes to

$$d = 2 \cdot 6371 \cdot \arcsin\left(\sqrt{\frac{1}{2} - \frac{1}{2} \cos\left(\frac{(lat_2 - lat_1) \cdot \pi}{180}\right) + \frac{1}{2} \cos\left(\frac{lat_1 \cdot \pi}{180}\right) \cdot \cos\left(\frac{lat_2 \cdot \pi}{180}\right) \cdot \left(1 - \cos\left(\frac{(lon_2 - lon_1) \cdot \pi}{180}\right)\right)}\right)}\right)$$

Some stations did not consistently collect all weather variables, particularly cloudiness, radiation, precipitation amount and type, and snow height and type (Figure 3.2). When a variable was not measured at the closest station, values from the nearest station with the variable available were used. As a sensitivity analysis, models were fit under four different approaches for the corresponding overall model for summer and winter. The first method incorporated all stations and only complete cases not further than 50 km apart from the next weather station. The second approach excluded stations with high missingness (stations 1 to 17), and only complete cases not further than 50 km from the next weather station were concerned. The third method excluded stations with high missingness (stations 1 to 17) and used all cases. The fourth method included all cases by using the weather of the nearest station to measure the missing variable.

All results were similar in magnitude and statistical significance, as shown in Table 3.2. The last approach was used for all analyses as it maximizes the sample size and hence the power.

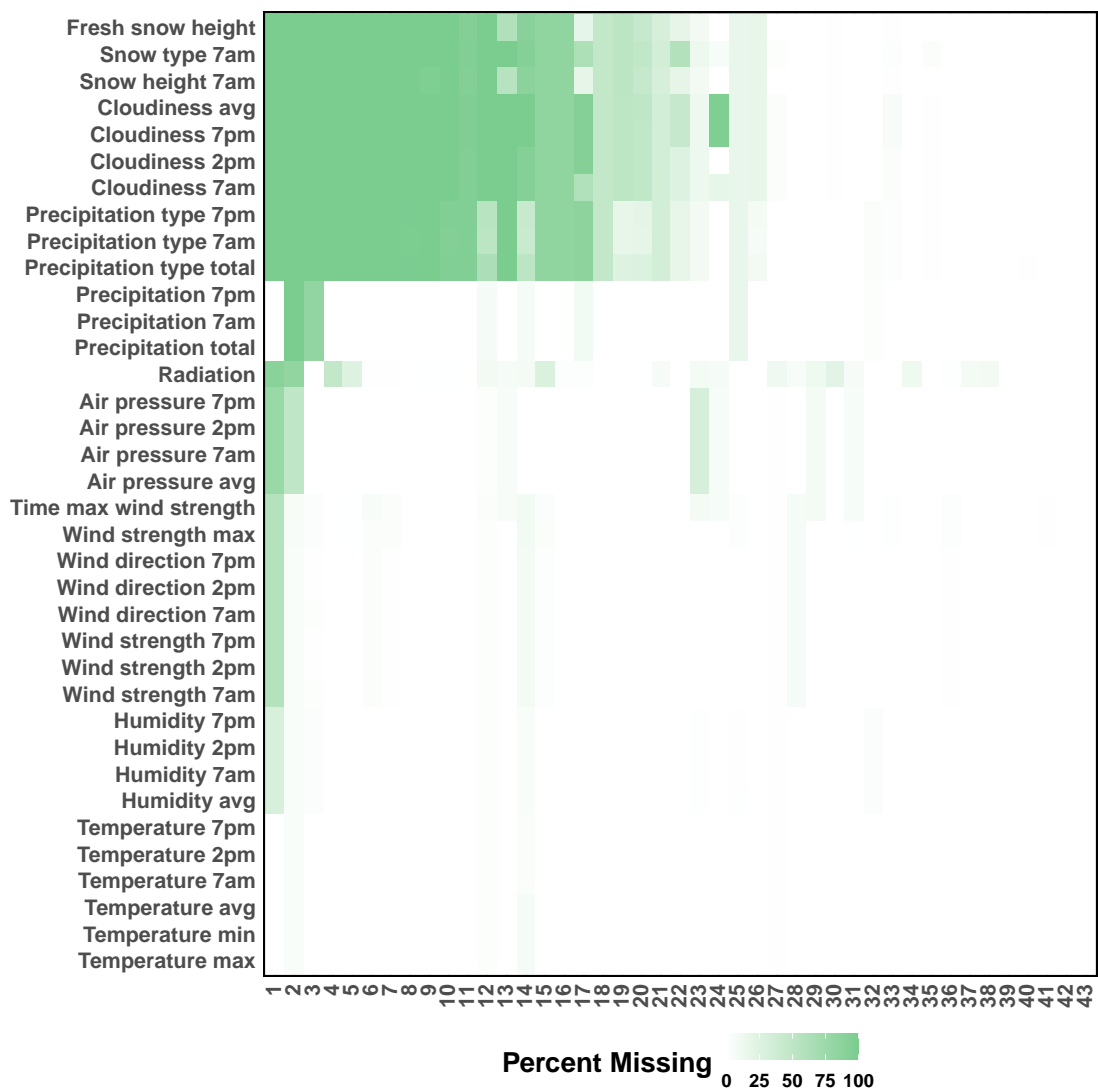


**Figure 3.2:** Missing characteristics for the 43 Austrian weather stations from November 1, 2006 to October 31, 2018

**Table 3.2:** Sensitivity analysis for model selection. Odds ratios and p-values for four approaches are listed along with the corresponding sample size by season.

Meteorological variable	Odds Ratio	p-value
Days with fatalities included:		
All stations, $\leq 50$ km, no imputation: summer 818, winter 728		
Excluded station 1-17, $\leq 50$ km, no imp: summer 1,353, winter 1,109		
Excluded station 1-17, no imputation: summer 1,460, winter 1,189		
Nearest station imputation: summer 1,770, winter 1,441		
<b>Summer</b>		
Temperature 2 pm (by 1 °C)	1.03	0.001
	1.04	<0.0001
	1.03	<0.0001
	1.03	<0.0001
Cloudiness (average)	0.94	<0.0001
	0.94	<0.0001
	0.94	<0.0001
	0.95	<0.0001
Snow type, reference = none		
- Spots	0.85	0.5
	0.71	0.07
	0.70	0.06
	0.67	0.03
- Perforated snow cover	0.35	0.002
	0.47	0.0004
	0.43	0.0002
	0.39	0.0001
- Full snow cover	0.24	<0.0001
	0.35	<0.0001
	0.35	<0.0001
	0.27	<0.0001
Weekend	1.32	0.0002
	1.32	<0.0001
	1.34	<0.0001
	1.35	<0.0001
<b>Winter</b>		
Humidity 2 pm	1.00	0.07
	1.00	0.05
	1.00	0.01
	0.99	<0.0001
Cloudiness (average)	0.94	<0.0001
	0.94	<0.0001
	0.95	<0.0001
	0.97	0.0004
Snow type, reference = none		
- Spots	1.18	0.4
	1.05	0.7



---

	1.06	0.7
	1.17	0.2
- Perforated snow cover	1.65	0.001
	1.66	<0.0001
	1.60	<0.0001
	1.22	0.07
- Full snow cover	1.72	<0.0001
	1.60	<0.0001
	1.51	<0.0001
	1.49	<0.0001
Weekend	1.45	<0.0001
	1.49	<0.0001
	1.50	<0.0001
	1.40	<0.0001

---

### 3.3 Statistical analyses

Analyses were performed with data of all stations pooled by season (summer May to October, winter November to April) as well as separately by discipline or activity. Before moving to multivariate analyses, linear regressions were performed to evaluate trends in activity-specific fatalities by year. Additionally, two-sample t-tests and Pearson chi-square tests were calculated as appropriate to assess differences in weather phenomena between days with versus without fatalities, analyzing one weather variable at a time as preprocessing step without controlling for the concomitant effects of other variables. Multivariate models were analyzed to assess independent effects of weather factors, adjusting for all variables.

Effects of weather and climate variables on daily time series of mortality or morbidity counts are typically modeled by Poisson distributed lag models as state of the art (Rodrigues et al. 2020). Rare events such as those occurring in this study can lead to parameter instability, requiring modifications or simplifications to reach efficient effects (Krawczyk 2016). During the study period, a fatal accident was recorded for less than 2% of all days, and only 2.2% of days with fatal accidents had more than one fatal accident at the same station. Applications of time series models with outcomes that were 0 counts for over 98% of all days led to estimates of dependence equal to 0. Treating days as independent and using the Poisson distribution as applicable for independent count data similarly led to instability for the same reason that most counts were zero. Among those that were not zero, most were one. Multivariable logistic regression with the outcome of whether one or more fatal accidents occurred on a day (day with fatal accident) versus not (day without fatal accident) was used to obtain stable estimates for detecting the risk of a fatal accident as a function of weather variables. Likelihood ratio tests were performed to obtain statistical significance. For these analyses, the wind speed was transformed from the Beaufort scale to wind speed in meters per second. To account for potential dependence among fatal accidents associated with the same weather station, we ran additional analyses incorporating a random effect assumed to be normally distributed for the 43 weather stations. This model assumes that all fatal accidents that occurred in the vicinity of the same weather station were correlated.

Covariate effect sizes and statistical significance were nearly identical to those here, and hence this model was not pursued further.

To avoid overfitting due to multicollinearity, the selection of which weather variables to include in the logistic regression models was performed in two steps. In the first step, Akaike's information criterion was used to select the most predictive univariate characteristic of each group of weather variables (e.g., temperature as daily mean, minimum, maximum, or measurements at 7 am, 2 pm, and 7 pm). In the second step, a more stringent Bayesian information criterion selection process on selected variables from the first step, along with an indicator variable for weekend effects, was performed (Figure 3.3).

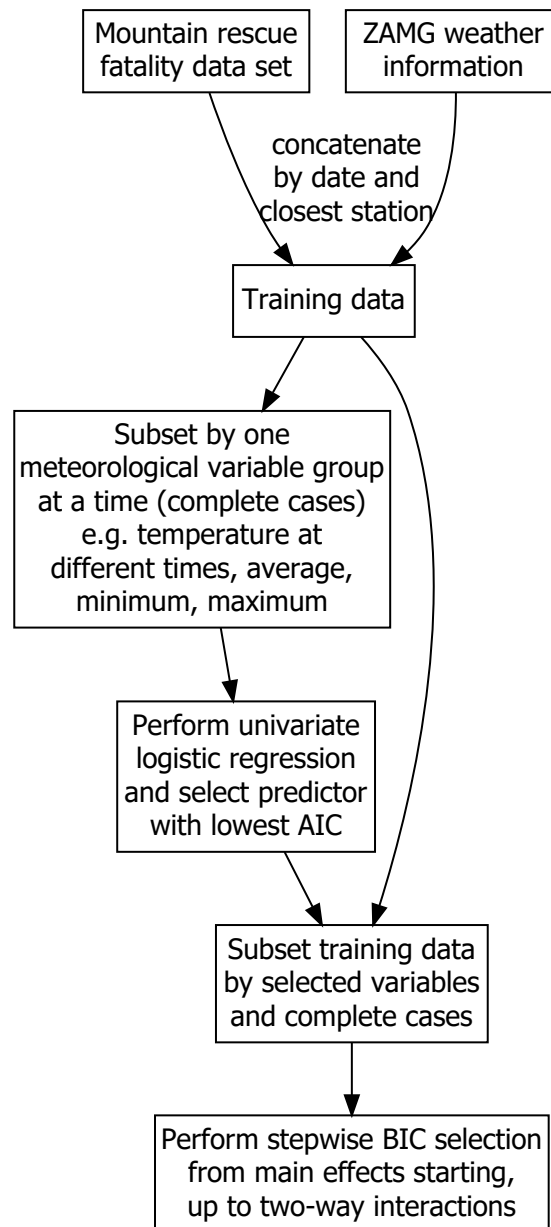


**Figure 3.3:** Data preparation and modeling process.

All statistical tests were performed at the two-sided 0.05 level of statistical significance, and along with all analyses, in the R statistical software version 4.1.1 (R Core Team 2021).

### 3.4 Overview of fatalities

Characteristics of the 3,285 Austrian alpine fatal accidents reported from November 2006 to October 2018 are summarized in Figures 3.5 and 3.6. Figure 3.4 justifies the choice of seasons with minima between April and Mai, and November. More fatal accidents occurred in summers (55.3% of 3,285) compared to winters (44.7%). Mountaineering, comprising hiking and trekking, had the most fatal accidents in summer (54.4% of 1817), and skiing the most in winter (29.4% of 1,468). Two causes of fatal accidents consistently high in summer and winter were suicides, comprising 9.4% and 8.3% of all fatal accidents during the respective season, and forestry work accidents at 7.8% and 9.1%, respectively. There were no significant annual trends in the total number of fatalities or fatalities due to the six most common reasons over the decade 2007 to 2017 (Figure 3.7, all p-values > 0.05). As seen in Figure 3.6, most fatal accidents occurred on weekends, with the highest share on Saturdays in summer and winter (18.2% and 18.3%, respectively). In most accidents, only one fatality occurred (summer 98.3%, winter 97.7%), and the highest number of fatalities per accident was six, resulting from an alpine tour accident in 2017 in the state Salzburg. The high-tourism region of Tyrol experienced the most fatalities, contributing 36.1% of all fatal accidents in summer and 37.3% in winter. According to text reports, 80.5% of fatal accidents occurred in daylight and 5.9% in darkness in summer, while for winter, these percentages changed to 67.8% and 7.6%, respectively. The majority of fatalities occurred with sunshine reported (summer 61.9%, winter 51.8%), followed by clouds (summer 16.3%, winter 22.1%), rain (2.3%) in summer, and the combination of snowfall and cloudiness (2.2%) in winter.

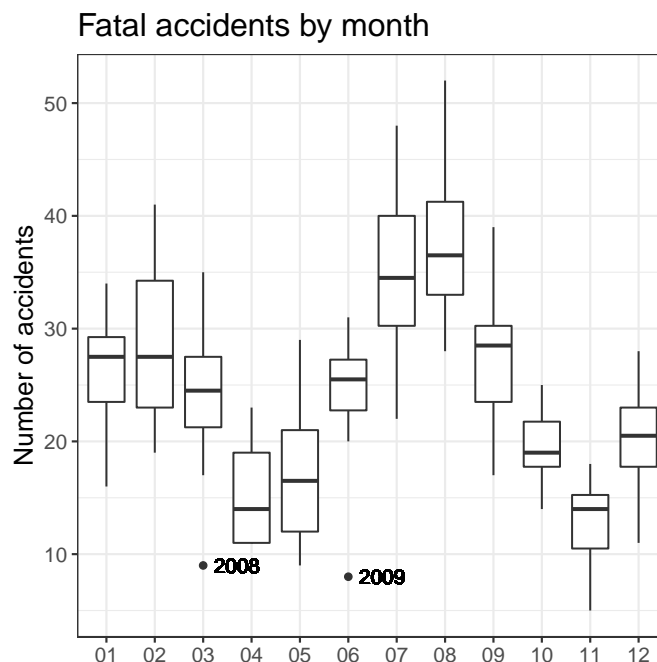


**Figure 3.4:** Austrian mountain fatal accidents by month. Years classified as outliers are indicated by individual points labeled with the corresponding year.

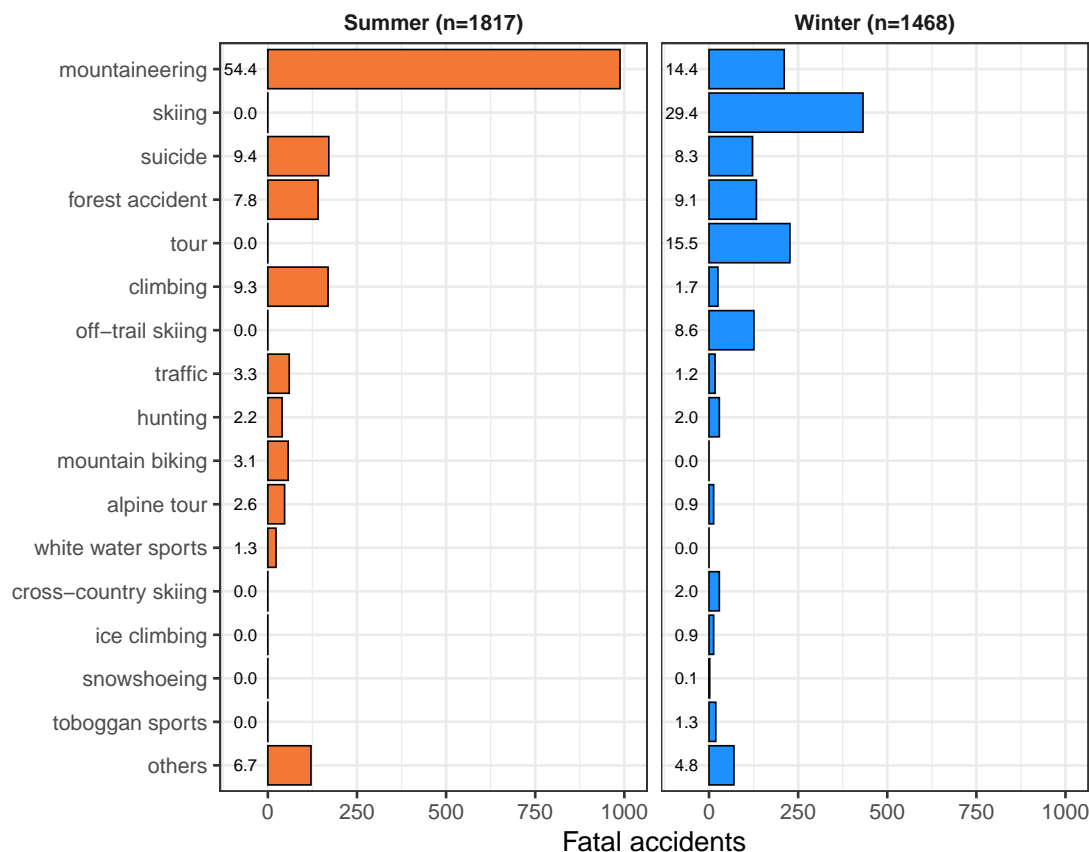


**Figure 3.5:** Distribution of fatal accidents by discipline and season between 1 November 2006 and 31 October 2018.

### 3.5 Weather conditions on days with and without fatalities

For summer, all meteorological variables reported by the ZAMG were significantly different between days with and without fatalities (all  $p$ -values  $<0.001$ ), except for wind speed at 2 pm ( $p$ -value 0.3), as shown in Figure 3.8. The greatest difference for temperature measures occurred at 2 pm with 1.28 °C warmer temperatures for days with fatalities compared to days with no fatalities, for air pressure at 7 am with 0.92 hPa higher, for humidity at 2 pm with 3.77 percentage points lower, for global radiation with 0.42 kWh/m<sup>2</sup> higher, for total precipitation with 0.96 mm lower for days with fatalities compared to days without fatalities. Days with fatalities were 8.8 percentage points less cloudy at 7 am compared to days without fatalities. These characteristics underlined that warmer, sunnier, and dryer days with reduced wind speed and higher air pressure were associated more with fatal accidents in summer.

Figure 3.9 shows significant ( $p$ -values  $<0.0001$ ) differences between precipitation conditions on days with and without fatalities. For summer days when fatalities occurred, more often no precipitation occurred (54.2% versus 44.1%), and hence on days with any kind of precipitation there was a lower risk for fatalities. More northern and north-western wind occurred at 2 pm on days with fatalities. For most of the proportions, wind directions were very similar (Figure 3.10). In summer, more fatalities occurred on days with no

### 3.5 Weather conditions on days with and without fatalities

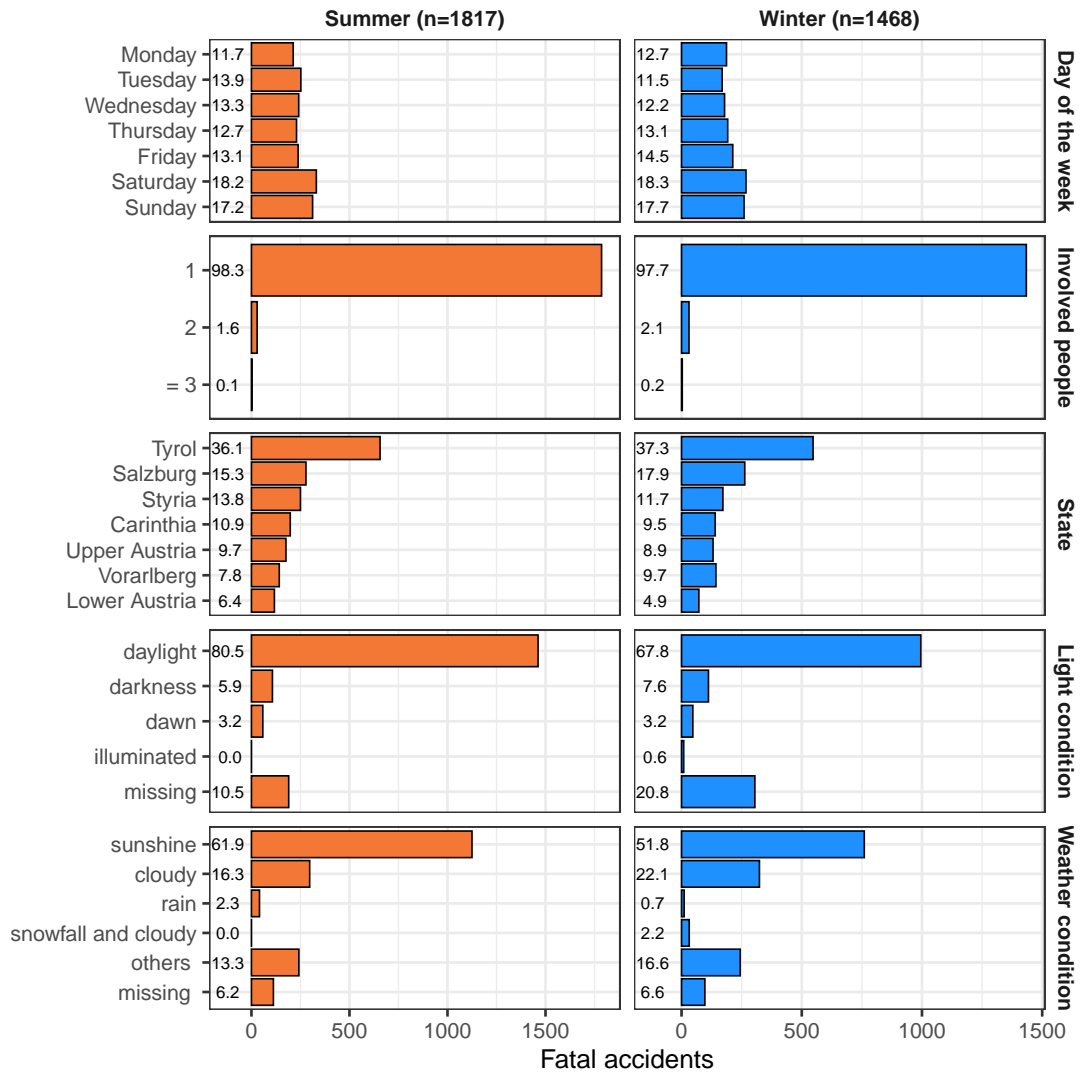


**Figure 3.6:** Distribution of fatal accident characteristics by season between 1 November 2006 and 31 October 2018.

snow cover (95.8% versus 89.1%; Figure 3.11). All characteristics showed significant differences with p-values less than 0.0001.

For winter seasons, several characteristics failed to be significantly different between days with and without fatalities, such as the minimum, average, and morning temperature measurement, wind speed, and fresh snow height (p-values 0.05 to 0.8). The greatest respective significant differences were observed for the temperature at 2 pm (0.57 °C warmer for days with fatalities), for air pressure at 7 am (0.79 hPa higher), for humidity at 2 pm (3.91 percentage points lower), for global radiation (0.15 kWh/m<sup>2</sup> higher), for total precipitation (0.48 mm lower for days with fatalities compared to days without fatalities). Days with fatalities were 6.08 percentage points less cloudy at 7 pm compared to days without fatalities. Overall, the climate effects in winter were more moderate than in summer (Figure 3.8).

Figure 3.9 shows significant (p-values <0.0001) differences between precipitation on

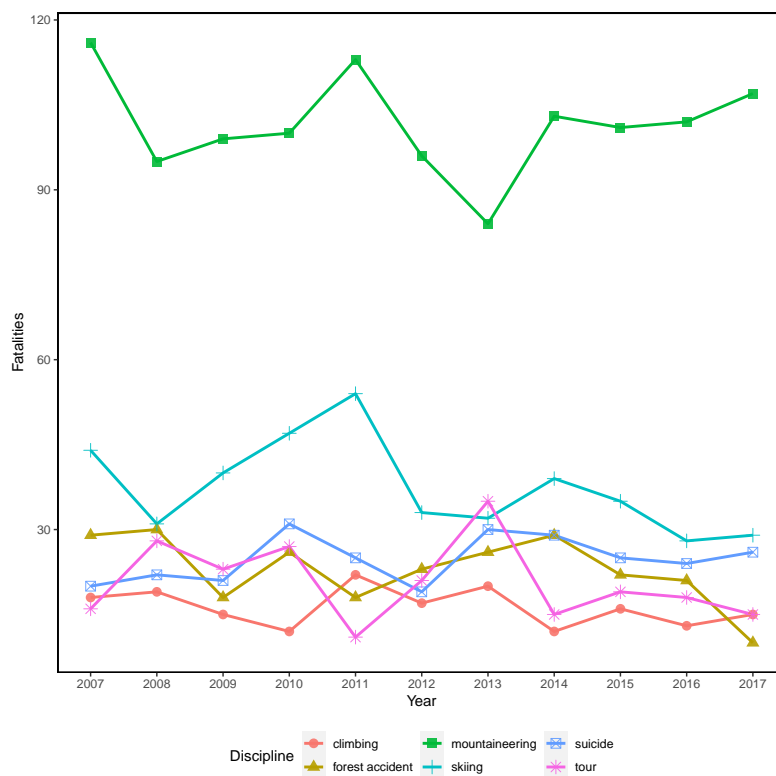


**Figure 3.7:** Annual numbers of fatal accidents in Austrian mountains for the six most common disciplines (2,459 fatalities in total).

days with and without fatalities in winter. For days where fatalities occurred, more often no precipitation occurred (57.5% versus 49.2%). On days with any kind of precipitation, there was a lower risk for fatalities (42.5% versus 50.8%). On days with fatalities, more south-eastern wind occurred at 2 pm. For most of the proportions, wind directions were very similar (Figure 3.10). On winter days with normal snow cover (64.1% versus 57.5%; p-value <0.0001) more fatalities occurred (Figure 3.11).

### 3.6 Multivariate analysis of the influence on fatalities

Multivariable analyses revealed the influence of key weather variables influencing fatal accidents, including cloudiness, snow type, global radiation, precipitation, temperature, and humidity (Table 3.3). Statistically significant weekend effects, increasing the odds of fatal accidents, were detected for many of the specific disciplines. It was adjusted for this effect in the calculation of the magnitudes of impacts of the particular weather variables, which are now discussed in turn.

The impact of the cloudiness was to reduce the odds of fatal accidents both in the winter and summer. Specifically, a 10% increase in cloudiness reduced the odds of fatal accidents by 5% for mountaineering, 10% for climbing, 9% for other summer sports, and 7% for skiing in the winter.

While snowfall reduced the odds of fatal accidents in the summer, it more pronouncedly

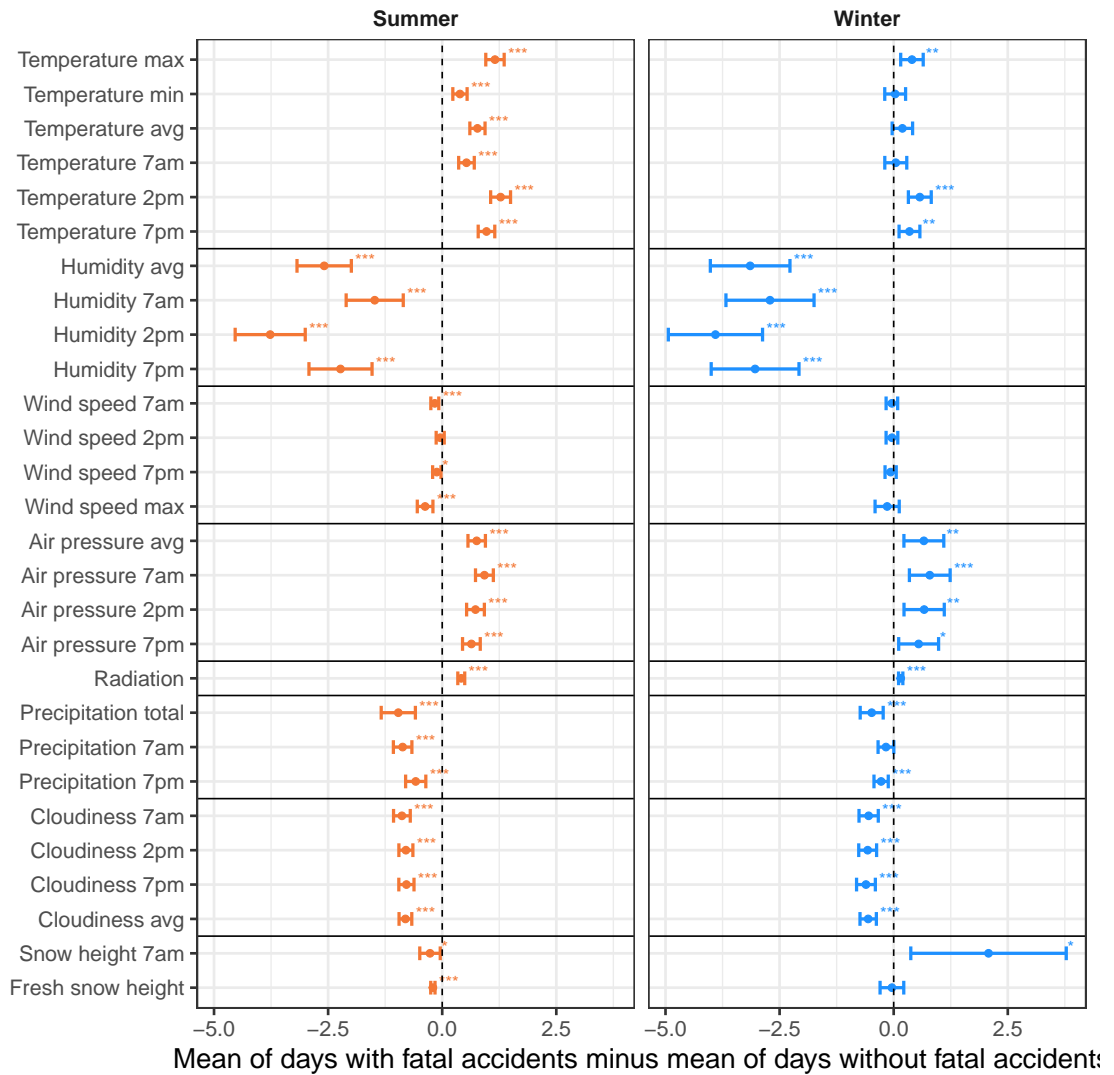


**Figure 3.8:** Differences in means of meteorological variables between days with and without fatalities along with 95% confidence intervals. Horizontal lines separate meteorological groups; days with missing data are not included; significant differences are indicated by \*\*\* for p-value <0.001, \*\* <0.01, and \* <0.05.

increased the odds of fatal accidents in the winter. Specifically, for mountaineering in the summer, the odds ratios for fatal accidents for the snow types spots, perforated and full, compared to the reference of no snow, were 0.45, 0.36, and 0.20, respectively. In other words, full snow reduced the odds of a fatal accident by 80%. In contrast, the respective odds ratios for skiing in the winter were 1.88, 2.52, and 3.69, meaning that full snow increased the odds of a fatal accident nearly 4-fold. For off-trail skiing in the winter, the odds ratios for fatal accidents for the respective snow types compared to no snow were 2.42, 2.33, and 7.39.

Global radiation increased the odds of fatal mountaineering accidents in the summer and tours in the winter, with odds ratios of 1.11 and 1.28, respectively, per kWh/m<sup>2</sup> increase. Precipitation was only associated with fatal accidents in the summer due to climbing, with an odds ratio of 0.85 per 1mm increase. The temperature influenced fatal accidents both in summer and winter, with odds ratios due to mountain biking and suicide of 1.13

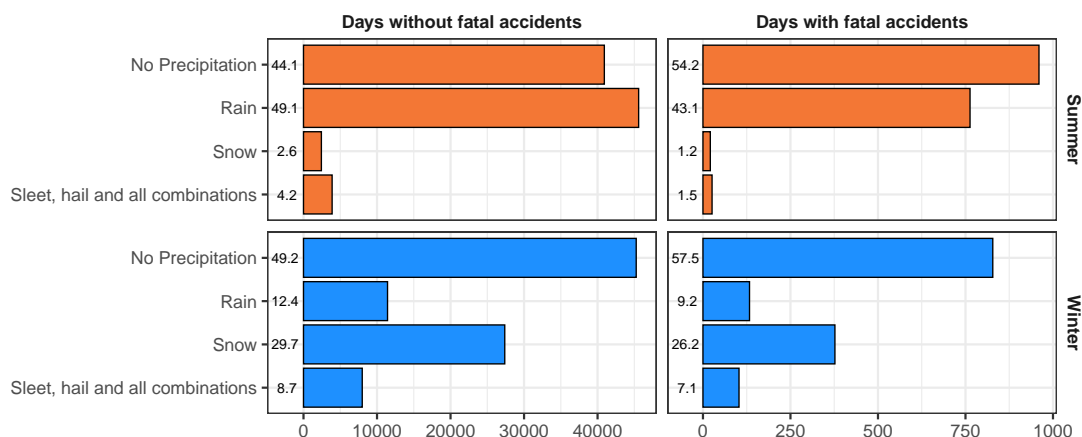


**Figure 3.9:** Proportion of precipitation types between days with and without fatalities by season.

and 1.08, respectively, per 1°C increase. Finally, relative humidity only slightly reduced winter mountaineering fatal accidents, with an odds ratio of 0.98 for an increase of 1%.

### 3.7 Discussion

Adverse impacts of climate change on human health, especially through an increase in extreme weather incidents, may be alleviated by clear adaptation strategies and preventive measures. Recently, effects on fatal mountain accidents have come into focus, also due to novel popularity in mountaineering activities. Although descriptions of the effects of the Central European heatwave of summer 2003 suggested strong impacts in the Alps (DAV 2015), a comprehensive analysis of weather effects on mortality in the mountains has been lacking so far. This study quantified for the first time the impact of weather on fatal mountain accidents in the highly visited region of Austria in Central Europe. The findings here confirm similar results from previous studies on selected disciplines and regions.

Aschauer et al. (2007) analyzed skiing accidents in winter and compared the information with randomly selected skiers in a ski resort in Austria. They reported a smaller number of injuries during poor weather conditions, for example during increased clouds, which is supported by this study. Aschauer et al. (2007) claimed further that the risk was reduced during cloudy weather as fewer people went skiing.

Suicide represents a not uncommon reason for mountain fatalities, as validated in this study. Sim et al. (2020) showed a link between suicide, higher temperatures, and other weather patterns. Koszewska et al. (2019) associated a special warm mountain wind with suicide and showed an effect by season. The present study detected an association between suicides and warmer temperatures in winter, supporting Ajdacic-Gross et al. (2007). They found the effect was more a factor of lack of cold rather than heat. Deisenhammer et al. (2003) showed an association between suicide and high temperature, low relative humidity, thunderstorms, and days following thunderstorms in the state of Tyrol. However, in this study across Austria, most suicides were committed when it was



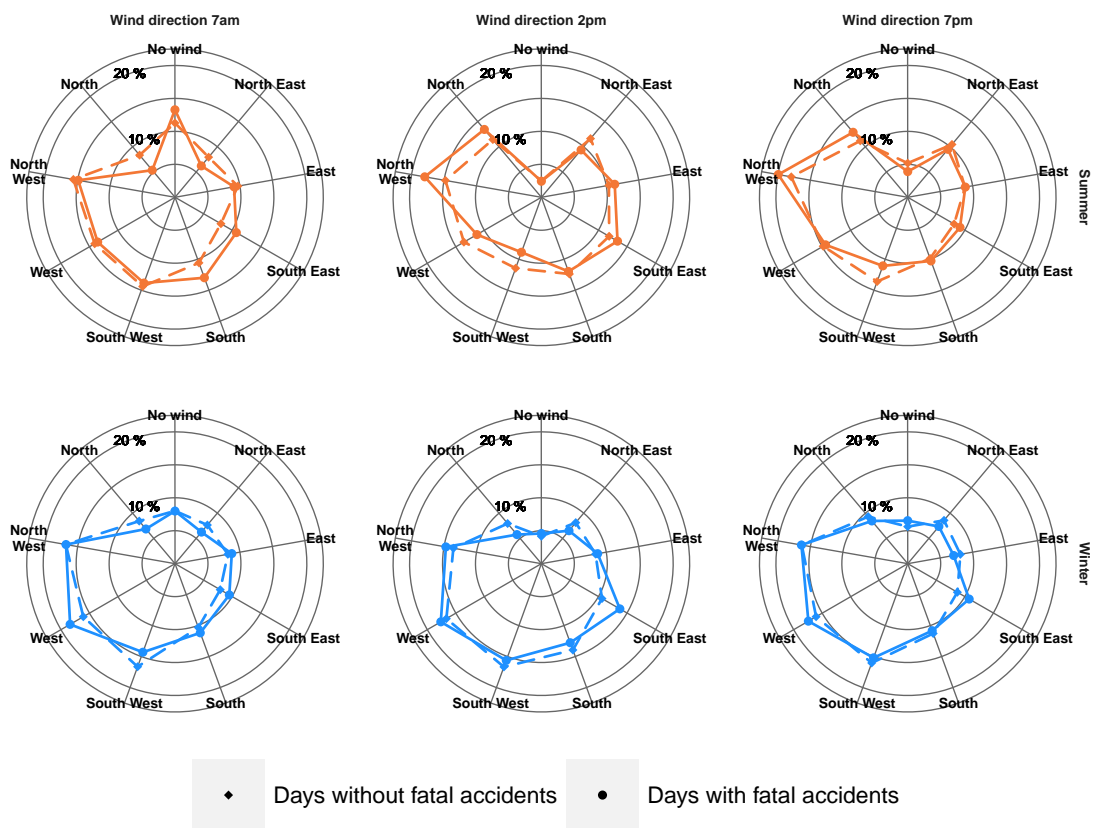


**Figure 3.10:** Proportion of wind directions between days with and without fatalities by season.

sunny (48.2%) or cloudy (30.7%), with only one fatality occurring during a thunderstorm.

T. Mueller et al. (2019) prospectively analyzed injuries on ski touring. They concluded that poor weather was one of the leading causes of injuries, though a precise definition of poor weather was not provided. In this study, increased odds of fatal accidents for tours in the winter were only associated with higher global radiation, which could be due to higher numbers of visitors attracted by more favorable weather forecasts, worse snow conditions, or more exhaustion. Soulé et al. (2017) reported ski tours as the third-highest reason for fatal accidents in French mountain areas. They concluded that their results do not necessarily imply that ski tours are the most dangerous due to a lack of participant numbers.

Climate change is presumed to (directly) alter the mountain experience encompassing all tourism and recreation activities via impacts on the mountain cryosphere, ecosystems, infrastructure, and hazards (Hock et al. 2019). But also (indirectly) via climate-change-induced altered economic growth, including reductions to the available household income for tourism; see Pretis et al. (2018). Shorter seasons of snow cover and declining glaciers reduce skiing options and the attractiveness of trekking. Thawing permafrost threatens the safety of hikers and mountaineers, for example leading to changes in iconic routes to the Mont Blanc (Mourey et al. 2019). If the climate changes as projected under several scenarios (IPCC 2018), summer sports periods will become longer, potentially increasing

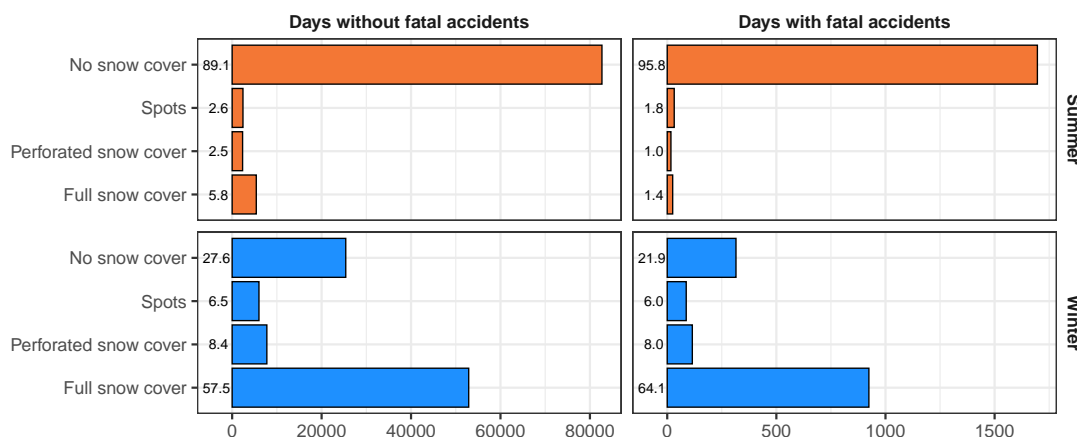


Figure 3.11: Proportion of snow types between days with and without fatalities by season.

fatal accidents, as the link to weather patterns has shown here.

A limitation of the analyses is that individual characteristics, including gender or potential human risk factors, are not included in the provided database of the Austrian Board of Trustees for Alpine Safety but require additional surveys and case-control studies as described, e.g., by Faulhaber et al. (2020). However, the analysis here focused on all fatal accidents as well as by discipline, and the proportion of age-gender subgroups by discipline can be vaguely inferred. Specific weather conditions at the accident site were recorded in text form and were often missing. Here, more detail and comprehensive reporting might help identify more precise patterns associated with fatal accidents, as would more exact coordinates of the accident site. Therefore, analyses of particular types of accidents, which depend on hazards at a certain location, such as avalanches and lighting accidents, could then be performed (Ströhle et al. 2018; Techel et al. 2016). In general, (direct) climatic influences on human mobility have to be taken into account. There is some debate on the multi-causal nature of mobility as reported, e.g., by Thalheimer et al. (2021) for the case of herders in East Africa; however, the time period of this study would not anticipate changing social norms or economic opportunities to be of short-term influence on a traditional tourism area in Central Europe. Nevertheless, since the numbers of visitors to the Austrian mountains were not recorded, analyses could not adjust for effects due to increased visitor numbers. However, weekend effects served as a surrogate that was adjusted for in the analyses.

### 3.8 Conclusion

Associations between weather patterns and fatal mountain accidents detected in this observational study may be mediated by the influence of weather and its interaction with the season on visitor numbers. Skiers are less likely to visit mountains on low-snow days in the winter, which would reduce overall fatal accidents. Conversely, less mountain snow may be more favorable for spring hikes, leading to more visitors and accidents due to improper equipment. Alpine safety councils, such as the Alpine Skiing Safety Council in Norway (Ekeland et al. 1989) or the Austrian Board of Trustees for Alpine

Safety (Austrian Board of Trustees for Alpine Safety 2021), focus on recommendations and standards for construction, equipment, and behavior in the mountains, as checking the weather forecast to prevent injuries and fatal accidents. Furthermore, the Austrian Board of Trustees for Alpine Safety and cooperators established an emergency app in 2019 for parts of Austria, Italy, and Germany to improve the rescue speed. Weather forecasts with associated increased accident risks could be directly incorporated into the app, advising recreational visitors in the mountains to behave cautiously when weather patterns interact with the season to increase the risk of fatal accidents.

**Table 3.3:** Multivariable logistic regression model associations between weather variables and fatal accidents for summer and winter disciplines.

Meteorological variable	Odds Ratio	95% confidence interval	p-value
<b>Summer</b>			
<b>Mountaineering (n=965)</b>			
Cloudiness average (by 1/10)	0.95	0.92 – 0.97	<0.0001
Snow type, reference = none			<0.0001
- Spots	0.45	0.24 – 0.76	
- Perforated snow cover	0.36	0.17 – 0.65	
- Full snow cover	0.20	0.10 – 0.34	
Global radiation (by 1 kWh/m <sup>2</sup> )	1.11	1.06 – 1.16	<0.0001
Weekend	1.45	1.27 – 1.65	<0.0001
<b>Climbing (n=169)</b>			
Precipitation 7 am (by 1 mm)	0.85	0.78 – 0.93	<0.0001
Cloudiness 7 am (by 1/10)	0.90	0.86 – 0.94	<0.0001
<b>Mountain biking (n=57)</b>			
Temperature 7 pm (by 1°C)	1.13	1.05 – 1.21	0.0005
<b>Alpine tour (n=47)</b>			
Weekend	2.85	1.60 – 5.09	0.0004
<b>White water sports (n=23)</b>			
Weekend	4.70	2.04 – 11.67	0.0002
<b>Others (n=121)</b>			
Cloudiness 2 pm (by 1/10)	0.91	0.86 – 0.96	0.0003
<b>Winter</b>			
<b>Mountaineering (n=210)</b>			
Relative humidity 2 pm (by 1%)	0.98	0.98 – 0.99	<0.0001
Weekend	1.69	1.28 – 2.23	0.0002
<b>Skiing (n=428)</b>			
Cloudiness 2 pm (by 1/10)	0.93	0.90 – 0.95	<0.0001
Snow type, reference = none			<0.0001
- Spots	1.88	1.09 – 3.13	
- Perforated snow cover	2.52	1.60 – 3.92	
- Full snow cover	3.69	2.74 – 5.10	
Weekend	1.45	1.19 – 1.77	0.0002
<b>Suicide (n=121)</b>			
Temperature 7 am (by 1°C)	1.08	1.04 – 1.13	<0.0001
<b>Tour (n=225)</b>			
Global radiation (by 1 kWh/m <sup>2</sup> )	1.28	1.12 – 1.46	0.0004
Weekend	2.08	1.60 – 2.70	<0.0001
<b>Off-trail skiing (n=124)</b>			
Snow type, reference = none			<0.0001
- Spots	2.42	0.63 – 8.01	
- Perforated snow cover	2.33	0.69 – 7.31	
- Full snow cover	7.39	3.71 – 17.50	

no significance:

forest accident, traffic, hunting, cross-country skiing, ice climbing, snowshoeing, toboggan sports

The number of days with fatal accidents the model is based on is given by n.

## 4 Drought effects of annual and long-term temperature and precipitation on mortality risk for nine common European tree species

A portion of this chapter is published in Neumair M., Ankerst D.P., Potocic N., Timmermann V., Ognjenovic M., Brandl S., Falk W. Warmer climate and weather patterns increase the risk of mortality for common European tree species. *bioRxiv*, 2022, <https://doi.org/10.1101/2022.11.10.515913>. Matthias Neumair performed all statistical analyses, visualization and interpretation of results. Matthias Neumair wrote the manuscript with contributions from all other co-authors.

Mortality as premature tree death is a ubiquitous phenomenon in ecosystems in space and time that can manifest as a diffuse background process, as self-thinning in stands, or due to pulse events that include phenomena such as heat waves, droughts, fires, floods, windstorms, ice storms, snow, and pest outbreaks. The frequency and magnitude of the latter are expected to change because of human behaviors interacting with climate and land-use change, as well as species invasions (Jentsch and P. White 2019). In addition, background tree mortality is likely to be affected by gradual climate changes, such as increasing temperature and decreasing water availability (Taccoen et al. 2019). Forest management with a tendency towards even-aged monocultures on sites outside the natural range of species, as in the case of Norway spruce in Europe (Caudullo et al. 2016), is another factor that increases mortality risk (Brandl et al. 2020). Mortality of dominant trees in stands results in an economic loss (Hanewinkel et al. 2013) and reduces ecosystem services to various degrees (R. C. Mueller et al. 2005; Thom and Seidl 2016).

Mortality events can either happen fast (as a result of storms, fire, and bark beetle outbreaks) or rather slow through various decline processes (most often interactions including climate, insects, or pathogens like root rot or blue stain fungi). Previous studies have found associations between tree mortality and climate (Brandl et al. 2020), weather (Neumann et al. 2017), soil (Maringer et al. 2021), stand parameters (Maringer et al. 2021; Taccoen et al. 2021), and insects and diseases (Anderegg et al. 2015). However, tree mortality is a complex process (Anderegg et al. 2015; Manion 1991) and difficult to decipher due to competing and largely unobserved mechanisms operating over large climatic gradients. For example, the weather has both direct and indirect effects on tree vitality, e.g., via its impact on insect populations (Anderegg et al. 2015).

Climate change influences many processes related to disturbances and tree mortality (Machado Nunes Romeiro et al. 2022). Warmer winters affect growth in temperature-limited regions, but in boreal or temperate forests also increase risks for frost damage (missing snow cover), insect attacks (reproduction and survival), wildfire, and root rot (Machado Nunes Romeiro et al. 2022). Rising temperatures have major impacts on drought severity due to vapor pressure deficit leading to climate change-type drought (Carnicer et al. 2011), hot or hotter drought (Allen et al. 2015). Although drought has historically shaped European forests (e.g., Przybylak et al. 2020), steep temperature rises are likely to increase the frequency and magnitude of record events (Allen et al. 2015; Forzieri et al. 2021; Park Williams et al. 2013; Senf and Seidl 2021b). These phenomena strike managed forests that differ from natural forests in many ways and tend to lower resilience and robustness due to low complexity (species, genetics, structure, thinning regime).

Two interrelated physiological mechanisms are associated with drought-induced tree mortality. The first is a hydraulic failure through partial or complete loss of xylem function from embolism that inhibits water transport, leading to tissue desiccation. The second is carbon starvation as a consequence of stomatal closure. Reduced carbon uptake leads to an imbalance between carbohydrate demand and supply, resulting in difficulties in meeting osmotic, metabolic, and defensive carbon requirements, which weaken trees and makes them more vulnerable to biotic and abiotic stresses. In extreme cases, this can lead to mortality by carbon starvation (Adams et al. 2017; McDowell and Allen 2015).

Tree species (and regionally adapted ecotypes) differ in their tolerance to environmental stress and, therefore, their ability to withstand changes in climate and climate-induced disturbances (W. Wang et al. 2012). Choat et al. (2018) state that “plants have limited physiological potential to respond to rapid changes in the environment” due to the fine balance of carbon gain and the risk of hydraulic failure. So, despite a general adaptation to environmental conditions, e.g., in life expectancy, growth rates, root to shoot allocation patterns, leaf area index, and leaf phenology, stomatal control or water use efficiency that reflect their differing distribution, strong changes in climate have the potential to harm trees. Whereas xylem hydraulic failure seems to be ubiquitous across multiple tree taxa at drought-induced mortality, evidence supporting carbon starvation is not universal and more common for gymnosperms than angiosperms (Adams et al. 2017). Species differ in their degree to adapt wood anatomical traits (Vander Mijnsbrugge et al. 2020) or, e.g., the degree to which they can compensate for leaf damage caused by insects during the spring (e.g., summer shoots of *Q. petraea* and *Q. robur*). Furthermore, tree species suffer from specialized insects or pests. For example, Norway spruce is strongly affected by the bark beetle *Ips typographus* (McDowell and Allen 2015). The shallow root system of spruce intensifies drought risk (Caudullo et al. 2016; Netherer et al. 2019). Another example of differences is the consequence of premature leaf shedding, which in the case of beech, with its thin bark, can lead to bark damage and a spiral of decline (Schuldt et al. 2020).

Managed forests in Europe accumulated substantial amounts of biomass in the 20th century. The changes in forest structure in combination with climate change and other human impacts led to an episode of increasing forest disturbances in recent decades (Senf and Seidl 2021a). To fulfill ecosystem services in the future, it is essential to increase

the resilience of managed stands and, to do that, understand the causes and patterns of mortality. Long-term climate values, such as 30-year temperature or precipitation averages, constitute predisposing factors that may lead to a slow decline and a gradual increase in background mortality. However, an effect on mortality might become only apparent in combination with inciting factors, i.e., current or very recent annual climate anomalies. To capture these effects, this study investigated data series until 2020, as the 2018 drought and heat wave in central and eastern Europe were described to be accompanied by large-scale mortality and lag effects (Brun et al. 2020; Schuldt et al. 2020; Senf and Seidl 2021b). Revealing the links between long-term climate data, short-term weather anomalies and mortality could help improve management. This study focuses on long-term 30-year average climate (temperature, precipitation) and yearly weather anomaly-induced mortality patterns in Europe as these are expected to increase dramatically (Forzieri et al. 2021; Senf and Seidl 2021b).

Because mortality is a rare event in forests, short-term or small-scale studies lack power to identify key management and climatic indicators. The pan-European International Co-operative Programme on Assessment and Monitoring of Air Pollution Effects on Forests (ICP Forests) crown condition data set covers a large climatic gradient and therefore provides a rich information source for mortality modeling studies (Brandl et al. 2020; Neumann et al. 2017). Therefore, this data set was used in this study despite a limited information depth on stand characteristics and soil information, related to mortality (Maringer et al. 2021; Taccoen et al. 2021). The time series was limited to 2011 to 2020 due to the introduction of the removal code in the data in 2011 and to control for common long-term average effects in the analysis of the most recent and relevant data for contemporary forests.

The three hypotheses of this study were, first, individual tree mortality is driven by both annual anomalies and long-term 30-year average temperature and precipitation effects, interacting with stand variables and species. Second, the effects of drought in Europe can be witnessed via temperature and precipitation on tree mortality in the drought year and the following years. Third, although heterogeneous by species, risk mortality profiles among species that grow at similar sites may exhibit similarities.

## 4.1 European tree mortality data

The ICP Forests provided tree mortality data across Europe for the decade spanning 2011 to 2020. Level I data on systematic 16x16 km grids were pooled with Level II intensive monitoring plots (Michel et al. 2018). Although these monitoring levels used different plot designs, they shared the same assessment method, and data were pooled to tree-year observations. Individual tree crown condition has been assessed annually by the ICP Forests since the 1980s, depending on the country. Since 2011 Level I trees were reported with an additional removal or mortality code, enabling distinction between trees that died and trees that were removed through management operations. Even though this removal code was established for Level II plots earlier, tree observations starting from 2011 were used for both data sets to have a consistent time range. The mortality events were classified as those due to biotic and abiotic causes, as well as standing

dead trees where the cause of death was unknown (Table 4.1). Planned utilization (forest management) and fallen trees were excluded. The status of fallen trees is often unknown due to an ambiguity in the ICP Forests coding system. Overall, 746,478 tree-year observations from 32 countries were analyzed. These observations came from 130,018 trees from 8,618 plots over the ten years studied.

**Table 4.1:** Tree mortality classification.

Description	Category	Mortality
Utilization for biotic reasons, e.g. insect damage	Tree has been cut and removed, only its stump has been left	Yes
Utilization for abiotic reasons, e.g. windthrow	Tree has been cut and removed, only its stump has been left	Yes
Biotic reasons, e.g. bark beetle attack	Standing dead tree	Yes
Abiotic reasons, e.g. drought, lightning	Standing dead tree	Yes
Unknown cause of death	Standing dead tree	Yes
Tree alive and measurable (new, note this is different than a missing value)	Tree alive	No
Tree alive, in current and previous inventory	Tree alive	No
New alive tree (ingrowth)	Tree alive	No
Alive tree (present but not assessed in previous inventory, incl. replacement trees)	Tree alive	No

For all plots, the plot information aspect (Flat, South, West, . . . ) and stand mean age were used. Since individual tree age was not recorded, mean stand age was used as a proxy, provided in 20-year classes, with one category for irregular stands. The irregular mean stand age class refers to uneven-aged stands containing two or more distinct age classes. For inclusion analyses, only codominant and dominant trees older than 40 years were considered to focus on climatic drought and neglect competition effects. Only the most common European tree species were included in the analysis. Specifically, only the nine species with more than 10,000 tree-year observations and at least 100 dead trees in the sample were included in the analysis, as shown in Table 4.2.

## 4.2 European weather data

Tree mortality data were combined with weather data at plot location from ClimatEU (Marchi et al. 2020), which mapped climate indices at a 2.5 arcmin grid (approximately 5 km) over Europe. An advantage was that the data software applied partial differential equations to adjust the weather for the provided elevation. Bioclimatic variables such as temperature, precipitation, and continentality were considered for different periods. A complete list of all variables can be found in Table 4.3. Annual and seasonal weather characteristics of the year of reported tree death and the three previous years were used. Winter was defined as December of the previous year to February, spring as March to May, summer as June to August, and the vegetation period



as May to September. To account for the general environment a tree grew in, anomalies of the weather variables were calculated at the plot level by subtracting the 30-year mean of the years 1981 to 2010 of the seasonal value. The climate normal for these 30 years was selected because all tree stands experienced it. Annual, summer, and vegetation period variables from the year before tree death were used as risk factors since crown condition assessments were performed in summer. As further predictors, the cumulative means of the previous three years were calculated, starting from the first concerned year, depending on summer or winter variables. Climate normals were used as predictors for the general environment, with additionally the difference of mean warmest and mean coldest temperature, resulting in 50 weather characteristics of interest.

**Table 4.2:** European tree species present in the study with data on tree-year observations from 2011 to 2020.

Scientific name	Common name	Alive (n)	Dead (n)
<i>Fagus sylvatica</i>	European beech	147,930	419
<i>Pinus nigra</i>	black pine	45,102	132
<i>Picea abies</i>	Norway spruce	156,740	1,399
<i>Pinus sylvestris</i>	Scots pine	225,722	953
<i>Betula pendula</i>	silver birch	21,549	145
<i>Quercus cerris</i>	Austrian oak	28,536	101
<i>Carpinus betulus</i>	European hornbeam	17,550	103
<i>Quercus robur</i>	pedunculate oak	47,945	277
<i>Quercus petraea</i>	sessile oak	51,643	232
	Total	742,717	3,761

### 4.3 Statistical analyses

To investigate yearly trends and corresponding weather effects, mortality was reported as the number of observed dead trees in one year divided by all observed trees for that year and compared with the annual weather variables averaged for all available trees for one year. All annual measures were standardized to mean 0 and standard deviation 1 over the ten years. Mortality was shown for all tree species together and combined with the weather trends described in an exploratory fashion. Associations in annual trends do not necessarily imply significant associations in the aggregated logistic regression models, which pool all annual observations and adjust for all potential confounding variables, such as age. Individual annual trend analyses do not have sufficient sample sizes to adjust for confounding variables and would lead to high amounts of multiple comparisons and spurious statistical associations. Pooling annual data into a single logistic regression for investigating the multiple conflicting effects on tree mortality obtains sufficient sample size and power for detecting significant effects of weather and climate factors regardless of the year(s) in which they occurred. Because tree death is only observed yearly, meaning that the specific date of the death is not observed and only the cumulative survival over the year, ordinary survival models that do not account for interval censoring, such as the Cox proportional hazards model, are not

**Table 4.3:** Weather characteristics. Variables of the first three groups were available for each year from 2010 to 2020; 30-year averages were calculated from 1981 to 2010 and kept fixed for each year.

Variable	Group
Average temperature of the coldest month (°C)	Winter temperature
Average temperature in winter (Dec.(previous year) - Feb.) (°C)	Winter temperature
Average temperature of the warmest month (°C)	Vegetation period temperature
Average temperature in spring (Mar. - May) (°C)	Vegetation period temperature
Average temperature in summer (Jun. - Aug.) (°C)	Vegetation period temperature
Average temperature in vegetation period (Mai - Sep.) (°C)	Vegetation period temperature
Total precipitation in winter (mm)	Precipitation
Total precipitation in spring (mm)	Precipitation
Total precipitation in summer (mm)	Precipitation
Annual total precipitation (mm)	Precipitation
Total precipitation in vegetation period (mm)	Precipitation
30-year normal of average temperature of the coldest month (°C)	Normal temperature
30-year normal of average temperature of the warmest month (°C)	Normal temperature
30-year normal of average temperature in winter (°C)	Normal temperature
30-year normal of average temperature in spring (°C)	Normal temperature
30-year normal of average temperature in summer (°C)	Normal temperature
30-year normal of average temperature in vegetation period (°C)	Normal temperature
30-year normal of temperature difference between average temperature of the warmest and coldest month, or continentality (°C)	Normal temperature
30-year normal of total precipitation in winter (mm)	Normal precipitation
30-year normal of total precipitation in spring (mm)	Normal precipitation
30-year normal of total precipitation in summer (mm)	Normal precipitation
30-year normal of annual total precipitation (mm)	Normal precipitation
30-year normal of total precipitation in vegetation period (mm)	Normal precipitation

appropriate. Abbott (1985) showed that logistic regression could be used to approximate interval-censored survival data analysis. Following Boeck et al. (2014), this approach was adopted to analyze yearly tree mortality in this thesis. Age and aspect were only considered as a predictor in the final model for a tree species if tree-year observations were observed for all categories. The interpretation of the coefficients from logistic regression is as follows: the exponential of the coefficient for a particular covariate in the model is the odds ratio (OR) for experiencing tree mortality for a unit increase in the covariate according to its unit of measurement, for example for an increase in one degree Celsius (°C) temperature or its anomaly. For categorical variables, the interpretation is the

change in OR for each category compared to a reference category. As the unit increase, we chose one °C for temperature and 50 mm for precipitation variables as a reasonable difference over the large gradient of Europe. We calculated the area under the receiver operating characteristic curve (AUC) for model evaluation as an accuracy measure. An AUC greater than 50% indicates the ability to detect tree mortality (Mandrekar 2010).

Risk factor significance was assessed via likelihood ratio tests, with all tests performed at the 0.05 level of significance. For selecting the optimal model, forward selection starting with an intercept-only model was performed as follows. Conditioned on the current model, adding a variable with the smallest p-value among all variables not in the model was considered and included if the p-value fell below 0.05. Multicollinearity among risk factors was reduced by building variable groups according to similarity following approaches in species distribution modeling by Mellert et al. (2011) and Thurm et al. (2018). Therefore, variable groups were formed, as shown in Table 4.3. For each group of qualitatively similar variables, such as multiple measures of precipitation, only the best single variable significantly improving the model in terms of the lowest p-value was included in the model. The disadvantage of incorporating both long-term average (climate normal) and immediate anomaly (weather data) climate signals in models is their correlation, which leads to interference within the regression models and, sometimes, contradictory effects. Interaction terms were included in the models when statistically significant. These were used to gain insight into the interfering effects of the correlated risk factors. This procedure led to models with a maximum of five main effects from climate or weather variables plus potential interaction terms among them. For each species, the final model was evaluated at each location in the data set with the corresponding weather factors and visualized via prediction maps alongside areas of observed dead trees. Similar reacting tree species were identified by hierarchical cluster analysis on the transformed model coefficients, whether they were increasing or decreasing the odds of mortality. All computations and figures were made with the statistical package R version 4.1.1 (R Core Team 2021).

## 4.4 Results

In total, 746,478 tree-year observations were recorded among nine species from 2011 to 2020 (Table 4.2).

Annual rates of mortality for the nine species, shown in Figure 4.1, vary from near 0% to above 2.5% and show peaks after the 2013, 2015, and 2018 drought periods in Central Europe. Norway spruce and silver birch exhibited the highest mortality values, exceeding 1.5% in 2019 and 2020. Figures 4.2 and 4.3 overlay the trends in mortality along with annual average temperature and precipitation variables, showing how increases in temperature or decreases in precipitation could induce increases in mortality for all species. Here we can also see effects that were unrelated to mortality. Therefore, Figures 4.6, 4.8, 4.10, 4.12, 4.14, 4.16, 4.18, 4.20 and 4.22 show the corresponding plots by individual species only for significant effects. For instance, for European beech, only the average temperature of the warmest month is selected for the final model from Figure 4.3. Significant associations between mortality and weather characteristics are summarized in Figure 4.4 and show heterogeneity of effects across the nine species.

#### 4 Drought effects of temperature and precipitation on tree mortality risk

Multivariate risk models across species performed relatively well for predicting mortality, with all AUCs exceeding 67%.

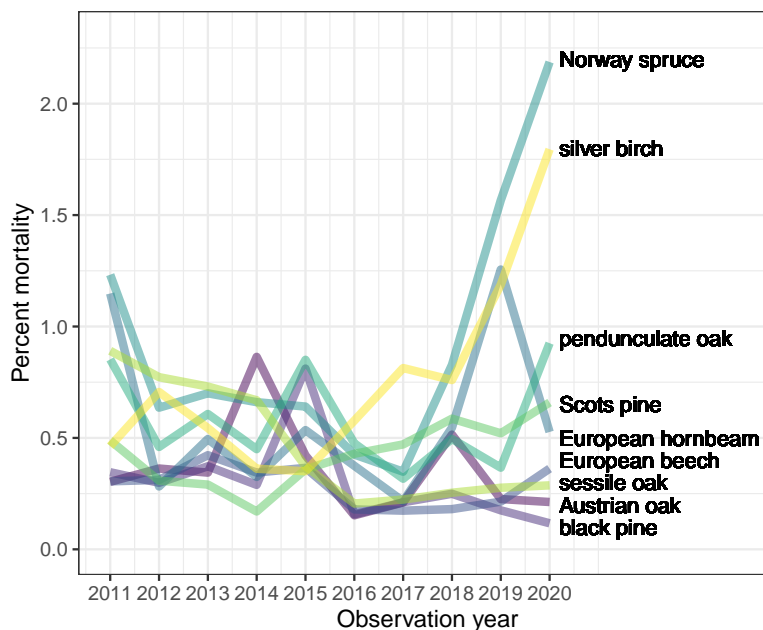


**Figure 4.1:** Annual mortality by species from 2011 to 2020.

Tree species in Figure 4.4 were grouped according to clustering of effects (Figure 4.5). Sessile oak is mostly different from the other species but slightly grouped with European beech and black pine as they all showed decreasing mortality with increased vegetation period temperature. Scots pine and Norway spruce were the only two species with decreasing effect of the interaction of precipitation and vegetation period temperature. Together with pedunculate oak, these three species had all individual effects with increasing mortality. Austrian oak and silver birch had a decreasing effect with higher winter temperatures. European hornbeam and Austrian oak showed decreasing mortalities with more normal precipitation. For clustering, the individual variable of the variable group was neglected, and they are discussed in the following paragraphs.

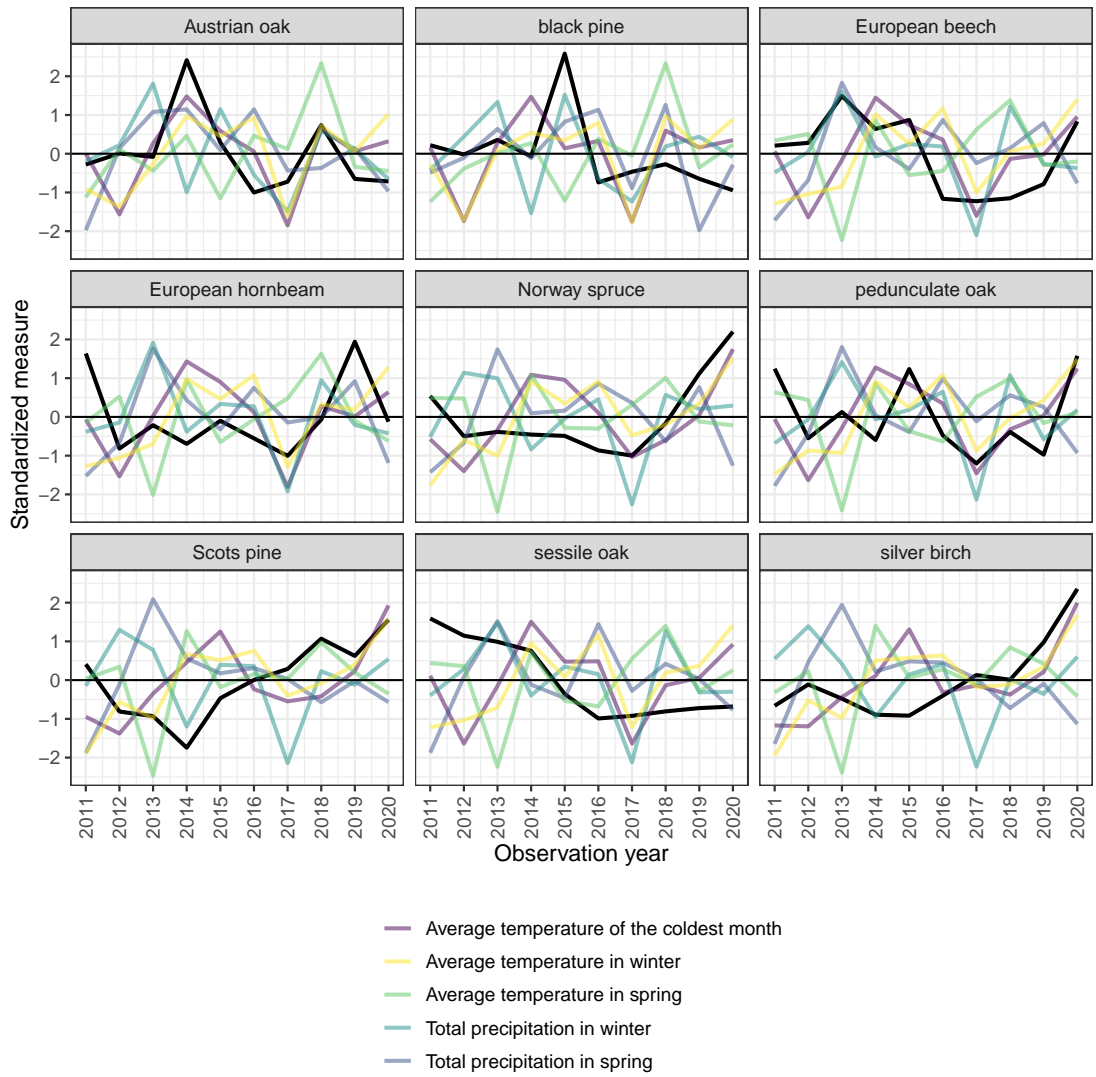


**Figure 4.2:** Annual values in winter and spring weather variables and mortality (black line) for the individual species. All variables have been standardized by subtraction of their means and divided by their standard deviations.

#### 4 Drought effects of temperature and precipitation on tree mortality risk

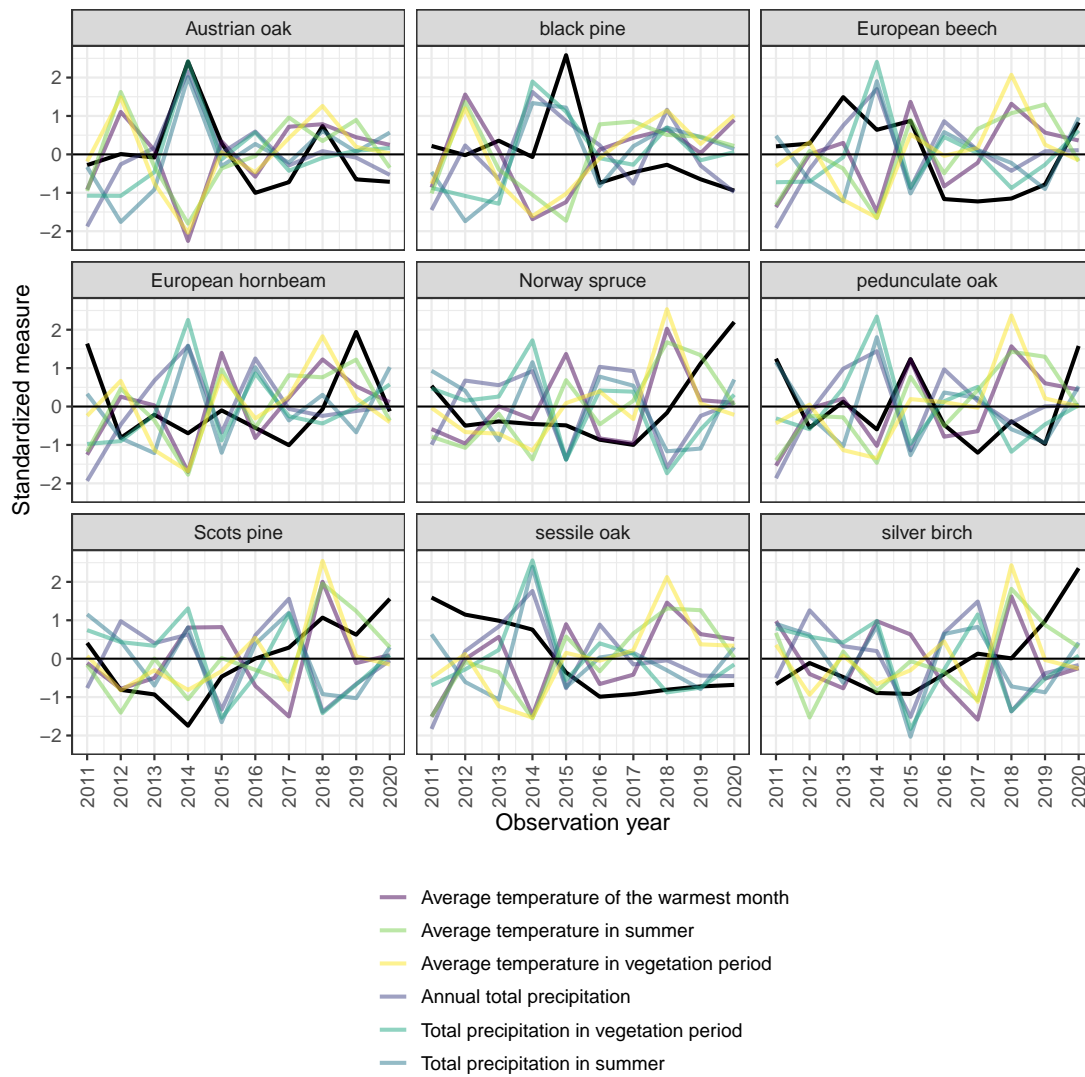


**Figure 4.3:** Annual values in summer weather variables and mortality (black line) for the individual species. All variables have been standardized by subtraction of their means and divided by their standard deviations.

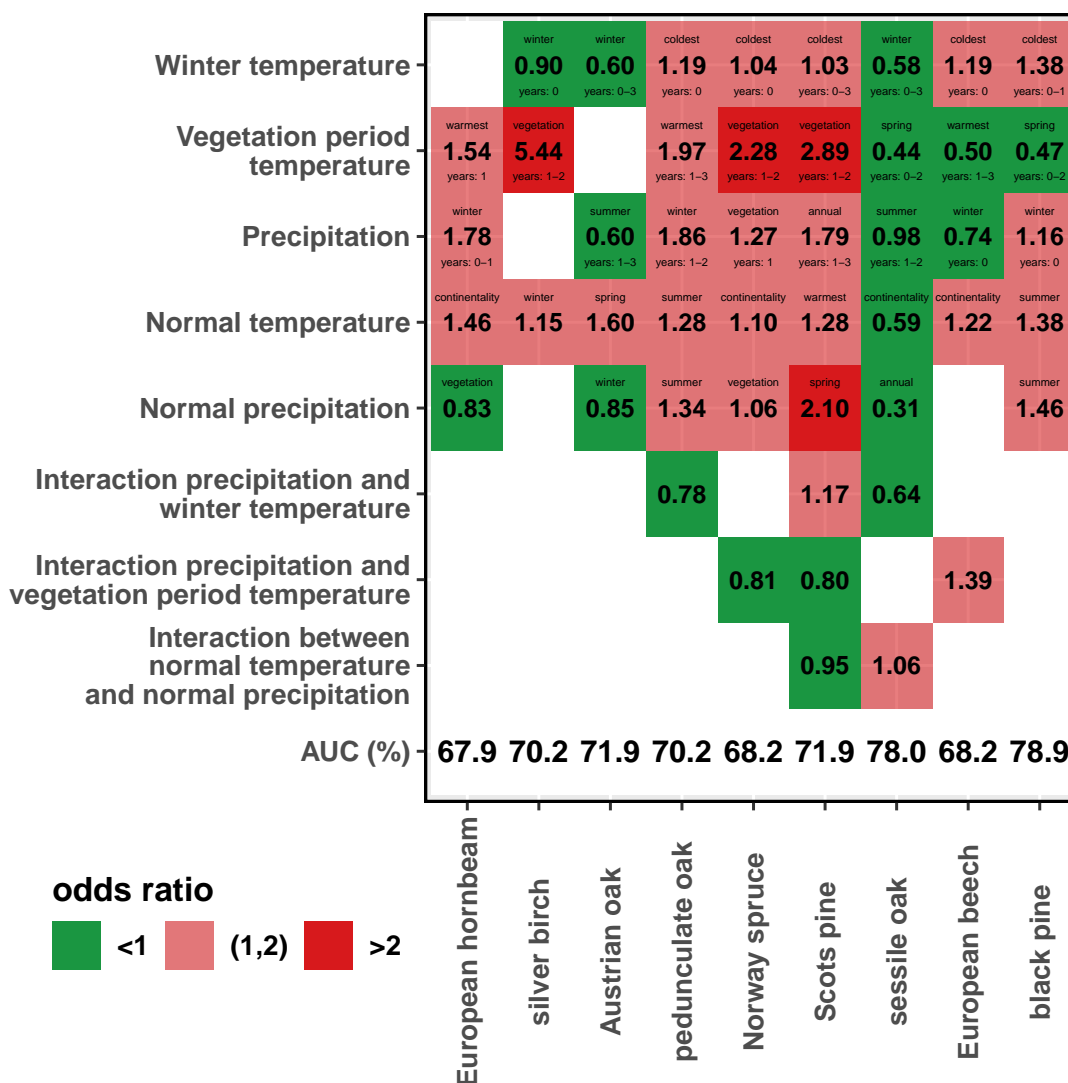


**Figure 4.4:** Odds ratio (OR) estimates based on stand and weather characteristics of all species by variable groups. OR's above 1 indicate that the increasing values of the risk factor increase the risk of tree death, while OR's below 1 indicate increasing values of the risk factors decrease the risk of tree death. OR's equal to 1 indicate the risk factor has no impact on tree death. Normal indicates the average of the annual respective weather variable measurements during the 30 years 1981 to 2010. For variables without this prefix, the anomaly is calculated by subtracting the climate normal from the seasonal value at the plot level. Red indicates an increase in tree death odds; green a decrease. The area under the receiver operating characteristic curve (AUC) indicates discrimination of a risk model for predicting the outcome of tree death, with higher values indicating better discrimination of trees that experienced death compared to those that did not. All effects were significant ( $p < 0.05$ ) except winter temperature in Scots pine (OR=1.03) and precipitation for sessile oak (OR=0.98). The selected variable within the variable group (Table 4.3) is indicated with abbreviations beside the averaged years for annual variables. Further model details can be found in Tables 4.4 to 4.12.

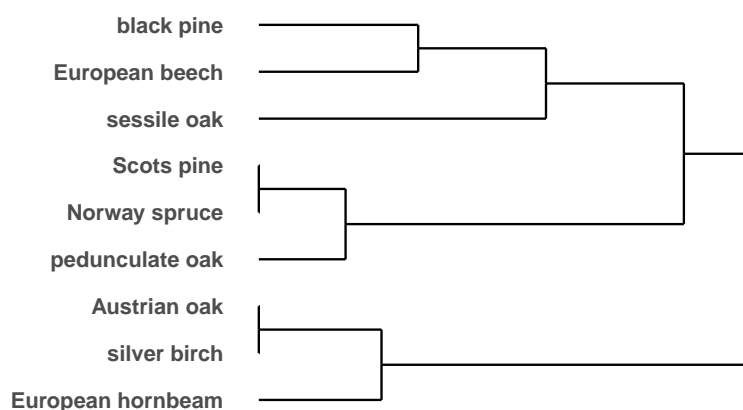


**Figure 4.5:** Dendrogram for similar tree species according to odds ratios of variable groups. Hierarchical cluster analysis was performed on the transformed model coefficients, whether they increased or decreased the odds of mortality.

### *European beech*

Among 148,349 European beech tree-year observations from 2011 to 2020, 419 trees died (Table 4.1). European beech had lower annual mortality rates than the other species during most years and was less affected by the droughts of 2013, 2015, and 2018 than the other species (Figure 4.1). Stand age of more than 120 years increased the odds of tree mortality by 53% compared to the reference age of 41 to 60 years (OR 1.53, Table 4.4). Compared with flat terrain, eastern exposition increased the odds of tree mortality by 58%, whereas south-western exposition decreased it by 48%. As a long-term climatic effect, plots with a one °C higher continentality, defined as the average of the difference between the warmest and coldest month average temperature over the 30 years from 1981 to 2010, experienced increased odds for tree mortality by 22%. Additionally, a one °C increase in the average temperature of the coldest month of the current winter increased the odds of tree mortality by 19%. This effect was confirmed by the results shown in Figure 4.6, where except for 2012 and 2013, years with a higher average temperature of the coldest month also had increased mortality. This can be seen especially in the drought year 2015. A 50 mm increase in winter precipitation of the current year decreased the odds of tree mortality by 26%. This association is seen in Figure 4.6 from 2018 onward, when winter precipitation decreased and mortality increased. One °C increase in the average temperature of the warmest month aggregated over the three previous years decreased the odds of tree mortality by 50%. This can be seen especially in the years 2016 to 2019, with less mortality following the temperature peaks in 2015 and 2018 (Figure 4.6). Combined, an increase in precipitation sum of winter and warmest month mean temperature led to 39% higher odds of tree mortality. The resulting model led to the evaluations shown in Figure 4.7, indicating higher mortality risks in northern and east-central Europe, with lower risks further west and in the south, depending on the year in question.



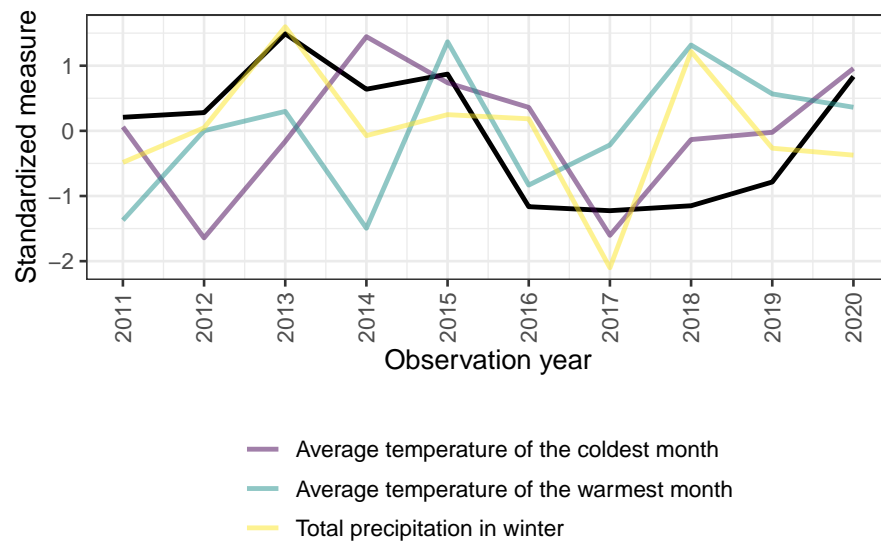


**Figure 4.6:** Annual values of weather variables and mortality (black line) for European beech. All variables have been standardized by subtraction of their means and divided by their standard deviations. Only variables from the final model in the pooled analysis over all years combined are shown.

**Table 4.4:** Logistic regression model estimates for European beech along with 95% confidence intervals and Likelihood ratio test p-values.

Variable	Odds ratio	Confidence interval	P-value
Mean stand age (Reference 41 - 60)			0.003
61 – 80	1.03	0.74 – 1.45	
81 – 100	0.85	0.60 – 1.21	
101 - 120	0.91	0.63 – 1.33	
>120	1.53	1.10 – 2.14	
Irregular stands	1.37	0.88 – 2.11	
Aspect (Reference Flat)			< 0.0001
North	1.31	0.89 – 1.98	
North-east	0.71	0.45 – 1.14	
East	1.58	1.04 – 2.42	
South-east	0.56	0.30 – 1.02	
South	0.78	0.47 – 1.27	
South-west	0.52	0.28 – 0.93	
West	0.85	0.54 – 1.33	
North-west	1.42	0.94 – 2.19	
Temperature difference between average temperature of the coldest and the warmest month (continentality) 30-years average (°C)	1.22	1.15 – 1.29	< 0.0001
Average temperature of the coldest month anomaly at reported tree mortality year (°C)	1.19	1.13 – 1.26	< 0.0001
Total precipitation in winter anomaly average of the reported tree mortality year (50mm)	0.74	0.56 – 0.96	0.02
Average temperature of the warmest month anomaly average of three previous years before reported tree mortality year (°C)	0.50	0.37 – 0.67	< 0.0001
Interaction between total precipitation in winter anomaly average of the reported tree mortality year and average temperature of the warmest month anomaly average of three previous years before reported tree mortality year (°C * 50mm)	1.39	1.15 – 1.66	0.0005

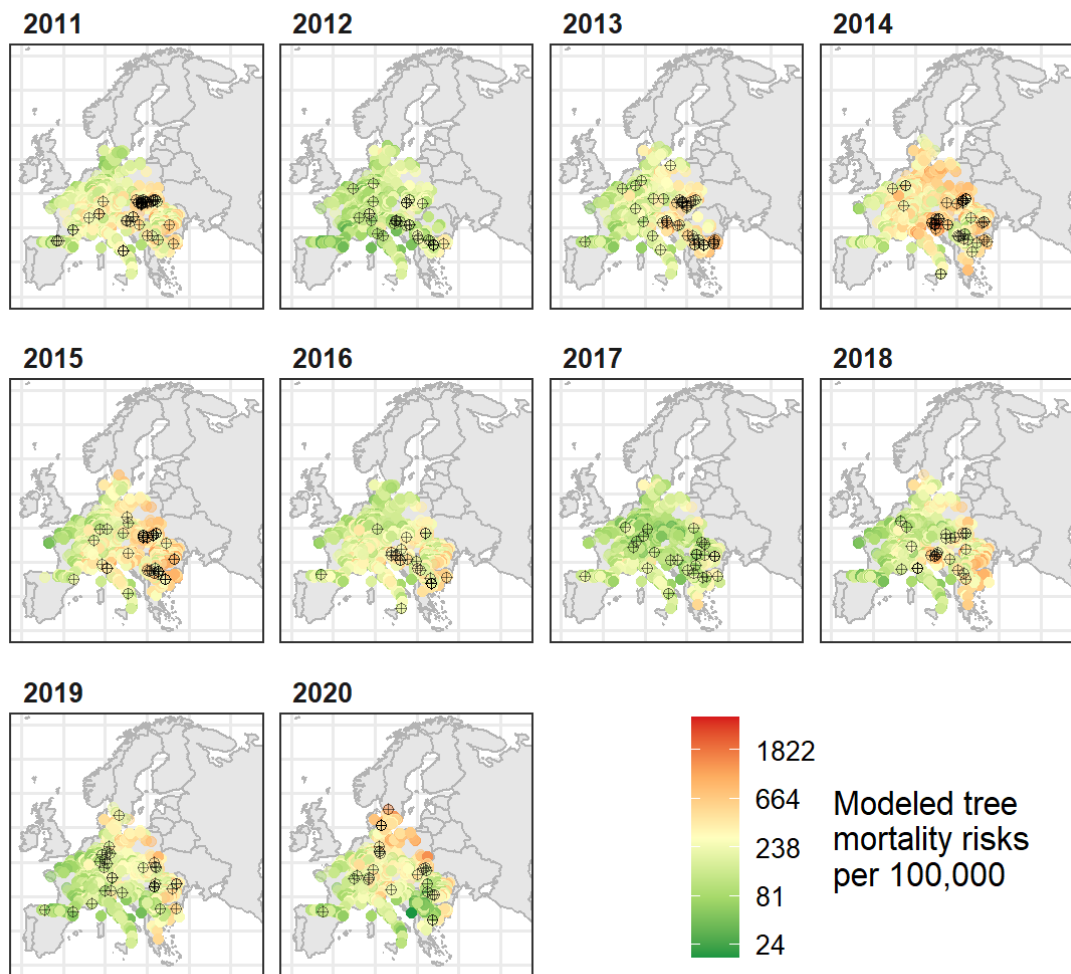


**Figure 4.7:** Spatial evaluation of modeled tree mortality for European beech for all analyzed ICP Forests plots on a logarithmic color scale. Black points indicate observations of dead trees ( $n=419$ ).

*Black pine*

Among 451,234 black pine tree-year observations from 2011 to 2020, 132 trees died (Table 4.1). Black pine had a peak in mortality in 2015 (Figure 4.1). Stand age of 41 to 60 years resulted in the highest odds of tree mortality, 67% to 55% higher than for other age groups (Table 4.5). For aspect, south, south-east and east exposition increased the mortality odds by up to 392% (OR 4.92 for south aspect). As a 30-year climatic long-term effect, plots with more summer precipitation and higher summer temperature had increased tree death odds by 38% and 46%, respectively. Additionally, a higher average temperature of the coldest month in the current and previous year increased the odds of tree death by 38%. This association cannot be observed in Figure 4.8. Higher winter precipitation in the current year increased the odds of tree death by 16% per 50 mm, which can be seen especially in 2015, but not in 2013 (Figure 4.8). Higher spring mean temperature of the current year and the two previous years decreased the odds of tree death by 53% per 1°C. This association can be seen in Figure 4.8, where mortality decreased after the 2018 peak in spring temperature, and the mortality peak in 2015 was preceded by lower spring temperatures in the three previous years. The model evaluations indicated higher mortality risks in central Europe, which is the edge of the distribution of this species in Europe (Figure 4.9).

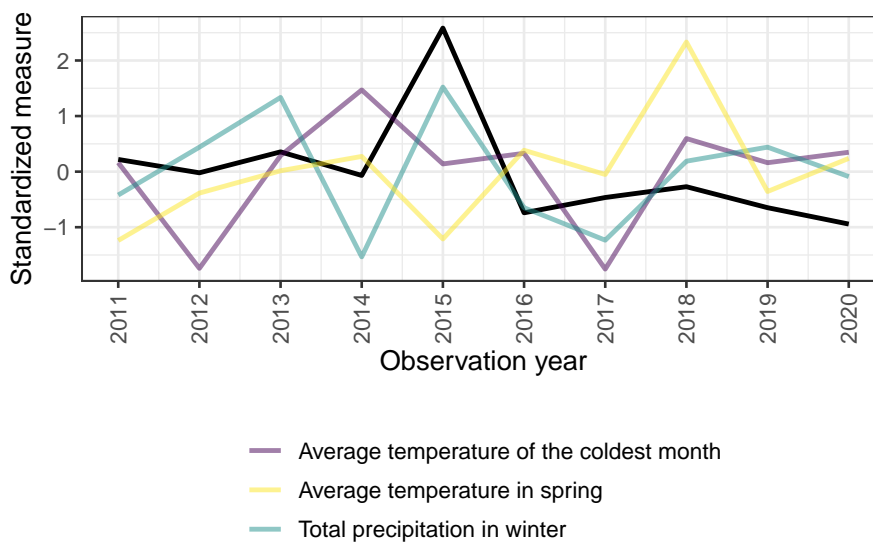


**Figure 4.8:** Annual values of weather variables and mortality (black line) for Black pine. All variables have been standardized by subtraction of their means and divided by their standard deviations. Only variables from the final model in the pooled analysis over all years combined are shown.

**Table 4.5:** Logistic regression model estimates for Black pine along with 95% confidence intervals and Likelihood ratio test p-values. Trees older than 120 years were excluded due to the lack of tree mortalities in this group.

Variable	Odds ratio	Confidence interval	P-value
Mean stand age (Reference 41 - 60)			< 0.0001
61 – 80	0.43	0.24 – 0.75	
81 – 100	0.33	0.15 – 0.63	
101 - 120	0.33	0.16 – 0.65	
Irregular stands	0.45	0.22 – 0.86	
Aspect (Reference Flat)			0.003
North	2.36	0.83 – 8.46	
North-east	2.96	1.07 – 10.51	
East	4.42	1.69 – 15.13	
South-east	3.95	1.27 – 14.70	
South	4.92	1.83 – 17.12	
South-west	1.64	0.55 – 6.00	
West	1.95	0.58 – 7.55	
North-west	2.26	0.76 – 8.19	
Average temperature in summer 30-years average (°C)	1.38	1.22 – 1.55	< 0.0001
Total precipitation in summer 30-years average (50mm)	1.46	1.34 – 1.59	< 0.0001
Average temperature of the coldest month anomaly average of the reported tree mortality and one previous year (°C)	1.38	1.19 – 1.61	< 0.0001
Average temperature in spring anomaly average of the reported tree mortality year and two previous years (°C)	0.47	0.30 – 0.73	0.0007
Total precipitation in winter anomaly of the reported tree mortality year (50mm)	1.16	1.04 – 1.29	0.008

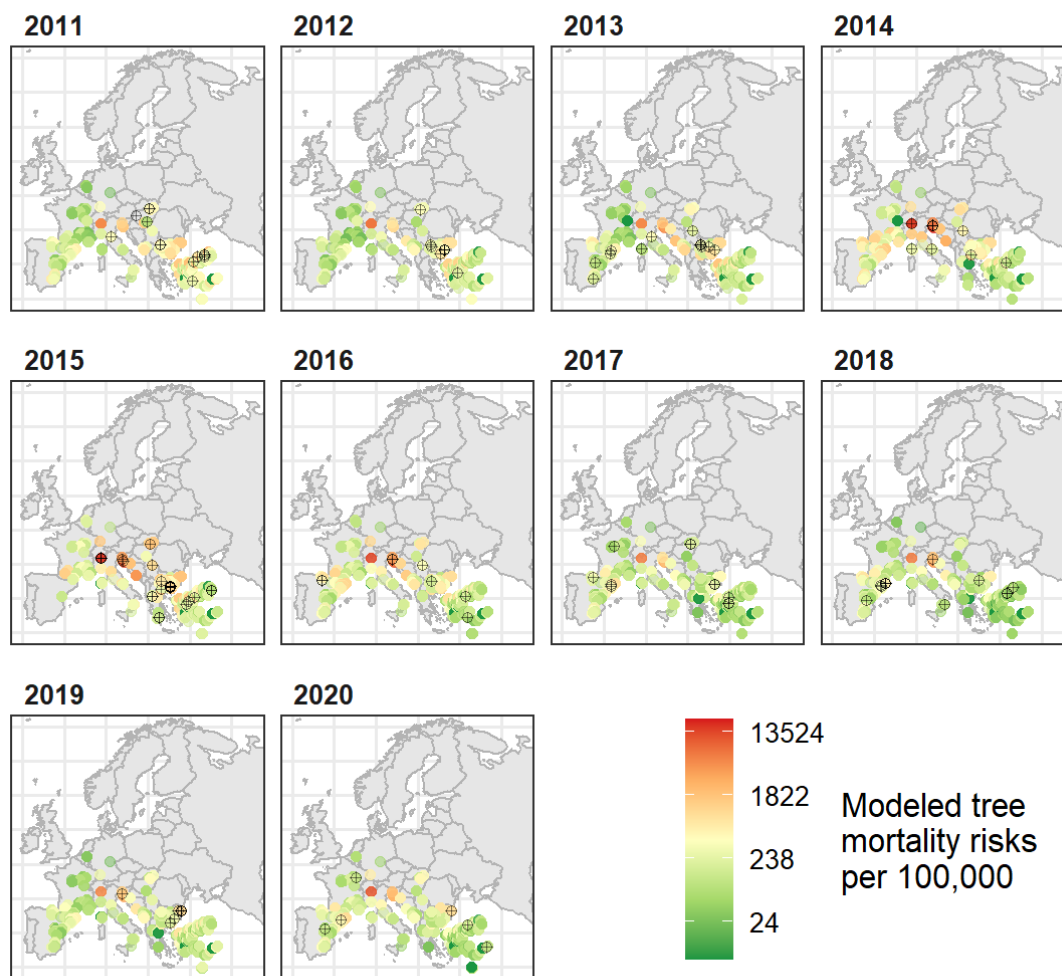


**Figure 4.9:** Spatial evaluation of modeled tree mortality for Black pine for all analyzed ICP Forests plots on a logarithmic color scale. Black points indicate observations of dead trees (n=132).

*Norway spruce*

Among 156,740 Norway spruce tree-year observations from 2011 to 2020, 1,399 trees died (Table 4.1). Norway spruce had higher mortality rates than most other species in 2011 and from 2018 to 2020 (Figure 4.1). This effect was strong in central Europe and even southern Sweden (Figure 4.11). Stand age 61 to 80 years resulted in the lowest odds of tree mortality, being 33% lower than other age groups (Table 4.6). Norway spruce showed lower odds for south-west, west, and north-west aspects (27% - 45%) and higher odds for all other expositions (17% - 70%). As a 30-year climatic long-term effect, plots with more precipitation in the vegetation period and higher continentality had increased tree mortality odds by 6% and 10%, respectively. Additionally, a higher average temperature of the coldest month in the current year increased the odds of tree mortality by 4% for a one °C increase, driven by the years 2018 to 2020 (Figure 4.10). During the vegetation period, higher average temperature in two previous years and more precipitation in the previous year led to higher tree mortality odds (128% and 27%, respectively) and their interaction to 19% lower tree mortality odds. Figure 4.10 shows a peak in vegetation period temperature in 2018 accompanied by low precipitation with increased mortality in the following years. Model evaluations indicated high mortality risks over the whole of Europe in recent years (Figure 4.11).

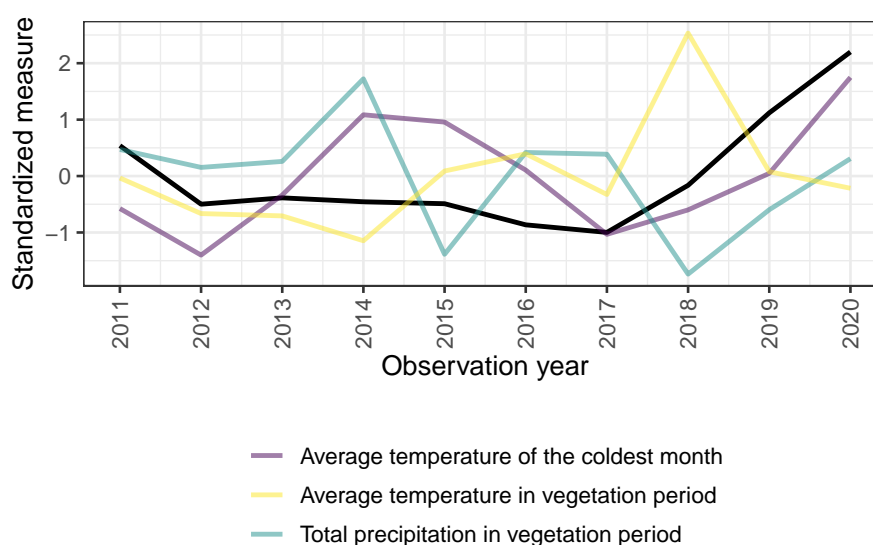


**Figure 4.10:** Annual values of weather variables and mortality (black line) for Norway spruce. All variables have been standardized by subtraction of their means and divided by their standard deviations. Only variables from the final model in the pooled analysis over all years combined are shown.

**Table 4.6:** Logistic regression model estimates for Norway spruce along with 95% confidence intervals and Likelihood ratio test p-values.

Variable	Odds ratio	Confidence interval	P-value
Mean stand age (Reference 41 - 60)			< 0.0001
61 – 80	0.67	0.55 – 0.80	
81 – 100	0.90	0.76 – 1.08	
101 - 120	1.06	0.88 – 1.27	
>120	0.79	0.64 – 0.96	
Irregular stands	1.19	0.89 – 1.56	
Aspect (Reference Flat)			< 0.0001
North	1.47	1.22 – 1.76	
North-east	1.31	1.05 – 1.63	
East	1.17	0.94 – 1.45	
South-east	1.47	1.19 – 1.80	
South	1.71	1.41 – 2.06	
South-west	0.73	0.56 – 0.95	
West	0.68	0.53 – 0.87	
North-west	0.55	0.42 – 0.72	
Total precipitation in vegetation period 30-years average (50mm)	1.06	1.04 – 1.08	< 0.0001
Temperature difference between average temperature of the coldest and the warmest month (continentality) 30-years average (°C)	1.10	1.07 – 1.13	< 0.0001
Average temperature of the coldest month anomaly at reported tree mortality year (°C)	1.04	1.01 – 1.06	0.004
Average temperature in vegetation period anomaly average of two previous years before reported tree mortality (°C)	2.28	2.01 – 2.60	< 0.0001
Total precipitation in vegetation period anomaly of the previous year before reported tree mortality (50mm)	1.27	1.22 – 1.33	< 0.0001
Interaction between average temperature in vegetation period anomaly average of two previous years before reported tree mortality and total precipitation in vegetation period anomaly of the previous year before reported tree mortality (°C * 50mm)	0.81	0.77 – 0.85	< 0.0001



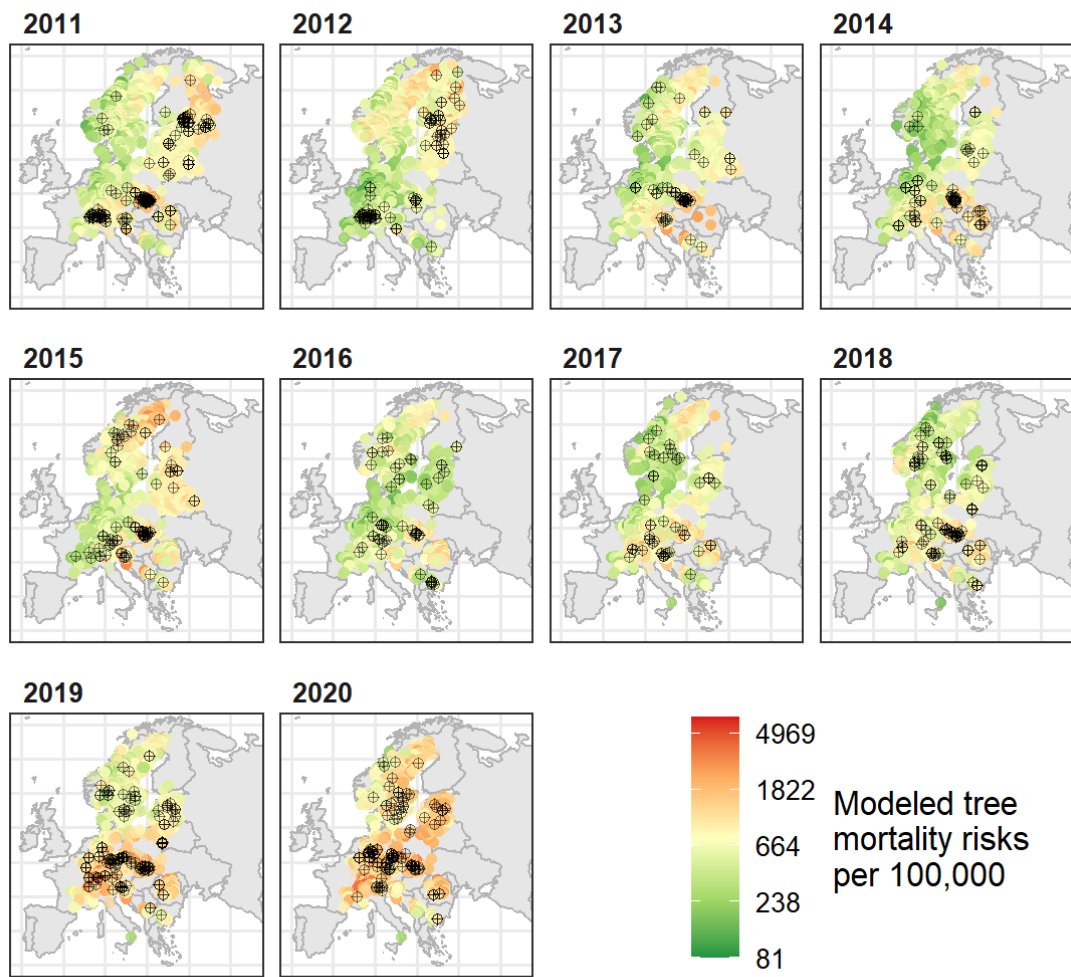


**Figure 4.11:** Spatial evaluation of modeled tree mortality for Norway spruce for all analyzed ICP Forests plots on a logarithmic color scale. Black points indicate observations of dead trees ( $n=1,399$ ).

Scots pine

Among 225,722 Scots pine tree-year observations from 2011 to 2020, 953 trees died (Table 4.1). Scots pine had consistently increasing mortality rates from 2014 to 2020 (Figure 4.1). Stand age 41 to 60 years resulted in the highest odds of tree mortality (Table 4.7). North-west aspect had 593% higher tree mortality odds compared to flat plots. As a 30-year climatic long-term effect, plots with more spring precipitation and a higher average temperature of the warmest month had increased tree mortality odds by 109% and 28%, respectively. However, their interaction reduced tree mortality odds by 5%. The higher average temperature in the vegetation period of two previous years increased the odds of tree mortality by 189%. Figure 4.12 shows mainly increasing mortality with increasing vegetation period temperature. The temperature peak in 2018 was also seemingly associated with 2020 mortality. The higher average temperature of the coldest month during the three previous years increased the odds of tree mortality by 3%. This association can be seen in Figure 4.12, where the winter temperature rose from 2012 to 2015, whereas the mortality increased from 2014 to 2020. More precipitation in the three previous years led to 79% higher tree mortality odds. Figure 4.12 shows high precipitation from 2012 to 2014, 2016, and 2017 and increasing mortalities from 2014 onward. The interaction between mean vegetation period temperature and precipitation decreased the tree mortality odds by 20%. The model evaluations indicated no spatial pattern (Figure 4.13).

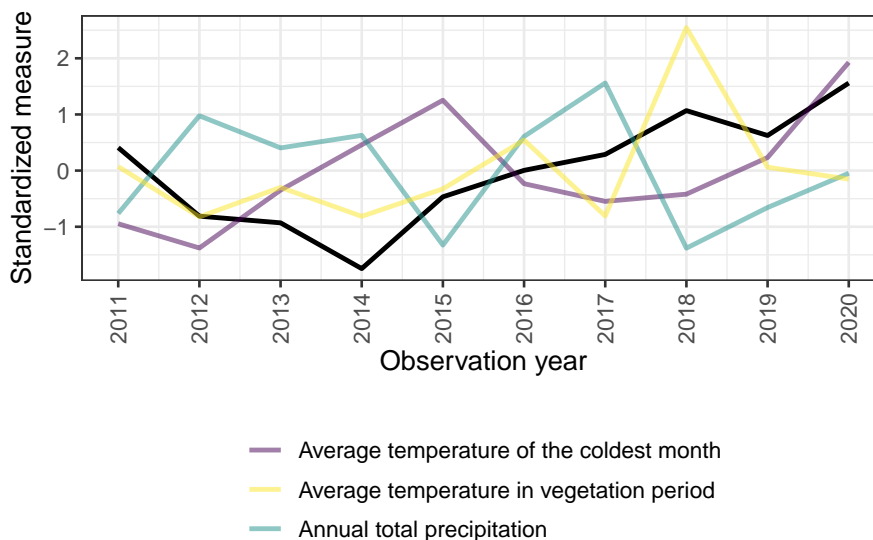


**Figure 4.12:** Annual values of weather variables and mortality (black line) for Scots pine. All variables have been standardized by subtraction of their means and divided by their standard deviations. Only variables from the final model in the pooled analysis over all years combined are shown.

**Table 4.7:** Logistic regression model estimates for Scots pine along with 95% confidence intervals and Likelihood ratio test p-values.

Variable	Odds ratio	Confidence interval	P-value
Mean stand age (Reference 41 - 60)			< 0.0001
61 – 80	0.58	0.49 – 0.69	
81 – 100	0.64	0.53 – 0.77	
101 - 120	0.56	0.43 – 0.72	
>120	0.73	0.55 – 0.96	
Irregular stands	0.81	0.55 – 1.15	
Aspect (Reference Flat)			< 0.0001
North	1.29	0.95 – 1.72	
North-east	6.93	5.61 – 8.54	
East	2.10	1.44 – 2.97	
South-east	1.13	0.71 – 1.71	
South	1.56	1.18 – 2.03	
South-west	1.21	0.83 – 1.69	
West	2.76	2.11 – 3.55	
North-west	2.73	2.10 – 3.52	
Average temperature of the warmest month 30-years average (°C)	1.28	1.15 – 1.43	< 0.0001
Total precipitation in spring 30-years average (50mm)	2.10	1.27 – 3.42	0.004
Interaction between average temperature of the warmest month 30-years average and total precipitation in spring 30-years average (°C * 50mm)	0.95	0.92 – 0.98	0.0004
Average temperature in vegetation period anomaly average of two previous years to the reported tree mortality year (°C)	2.89	2.45 – 3.42	< 0.0001
Annual total precipitation anomaly average of three previous years to the reported tree mortality year (50mm)	1.79	1.57 – 2.05	< 0.0001
Average temperature of the coldest month anomaly average of the reported tree mortality and three previous years (°C)	1.03	0.96 – 1.11	0.4
Interaction between average temperature in vegetation period anomaly average of two previous years to the reported tree mortality year and annual total precipitation anomaly average of three previous years to the reported tree mortality year (°C * 50mm)	0.80	0.70 – 0.91	0.0008
Interaction between average temperature of the coldest month anomaly average of the reported tree mortality and three previous years and annual total precipitation anomaly average of three previous years to the reported tree mortality year (°C * 50mm)	1.17	1.11 – 1.24	< 0.0001

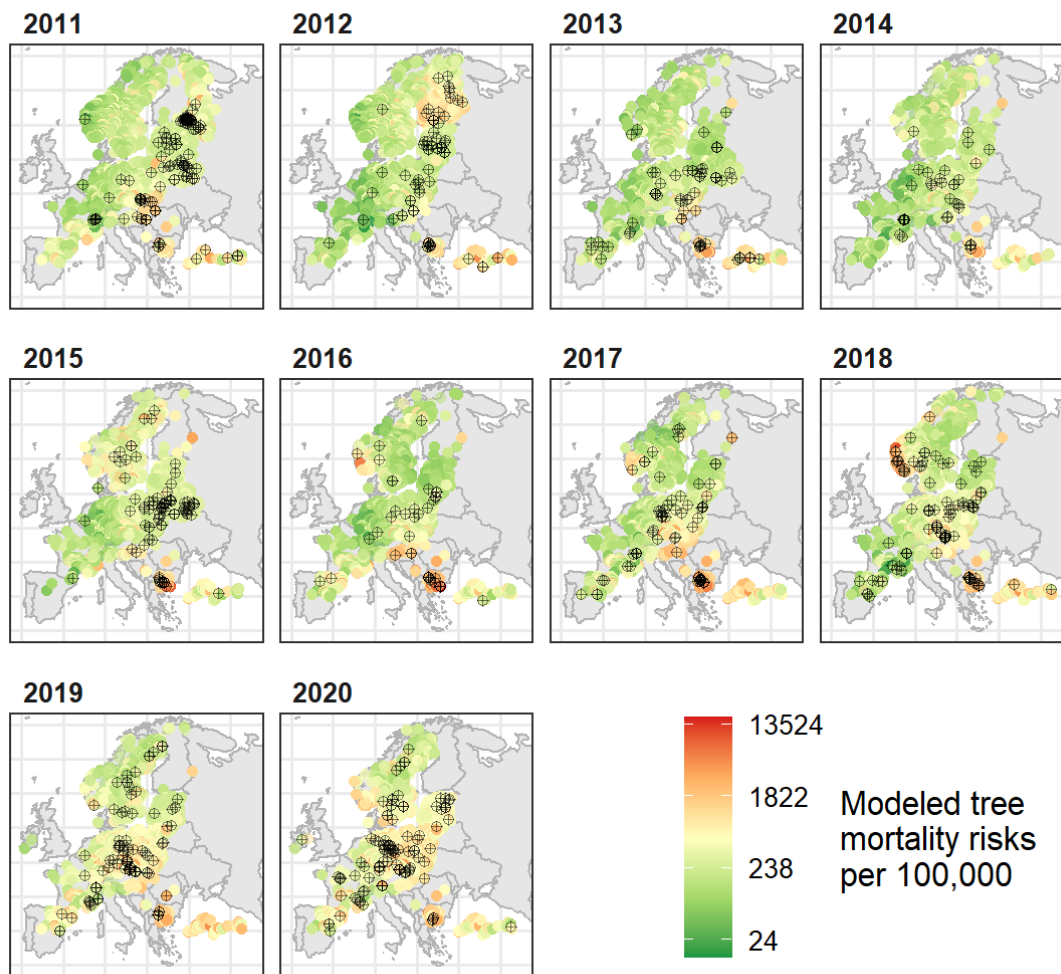


**Figure 4.13:** Spatial evaluation of modeled tree mortality for Scots pine for all analyzed ICP Forests plots on a logarithmic color scale. Black points indicate observations of dead trees (n=953).

### Silver birch

Among 21,694 silver birch tree-year observations from 2011 to 2020, 145 trees died (Table 4.1). Silver birch has had increasing mortality since 2015 (Figure 4.1). The older the tree stands, the higher their odds of tree mortality (Table 4.8). As a 30-year long-term effect, plots with higher average winter temperatures had increased tree mortality odds by 15%. Higher average vegetation period temperatures in the previous two years increased tree mortality odds by 444%. This association can be seen in Figure 4.14, where increased vegetation period temperature in 2018 was accompanied by increased mortality in 2019 and 2020. The high temperature in 2018 seems to have had a negative effect until 2020. The average winter temperature in the current year decreased the tree mortality odds by 10%. This association could be seen from 2014 to 2016, when the winter temperature increased, and mortality decreased. The model evaluations indicated a higher mortality risk in southern Europe, with an increasing trend over the years (Figure 4.15).

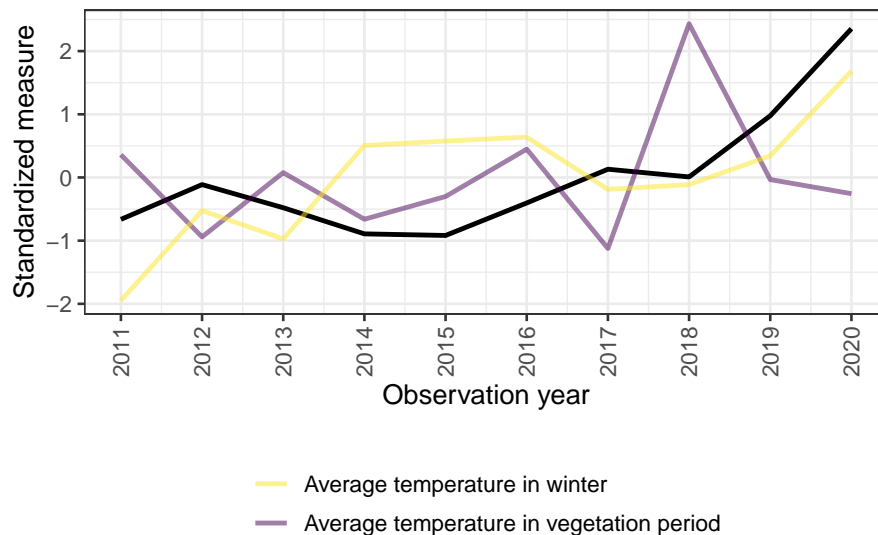


**Figure 4.14:** Annual values of weather variables and mortality (black line) for Silver birch. All variables have been standardized by subtraction of their means and divided by their standard deviations. Only variables from the final model in the pooled analysis over all years combined are shown.

**Table 4.8:** Logistic regression model estimates for Silver birch along with 95% confidence intervals and Likelihood ratio test p-values.

Variable	Odds ratio	Confidence interval	P-value
Mean stand age (Reference 41 - 60)			0.0004
61 – 80	1.77	1.16 – 2.74	
81 – 100	1.87	1.01 – 3.33	
101 - 120	3.53	1.58 – 7.12	
>120	4.74	2.25 – 9.27	
Irregular stands	1.68	0.82 – 3.36	
Average temperature in winter 30-years average (°C)	1.15	1.08 – 1.23	< 0.0001
Average temperature in vegetation period anomaly average of two previous years before reported tree mortality (°C)	5.44	3.38 – 8.91	< 0.0001
Average temperature in winter anomaly at reported tree mortality year (°C)	0.90	0.82 – 0.99	0.03

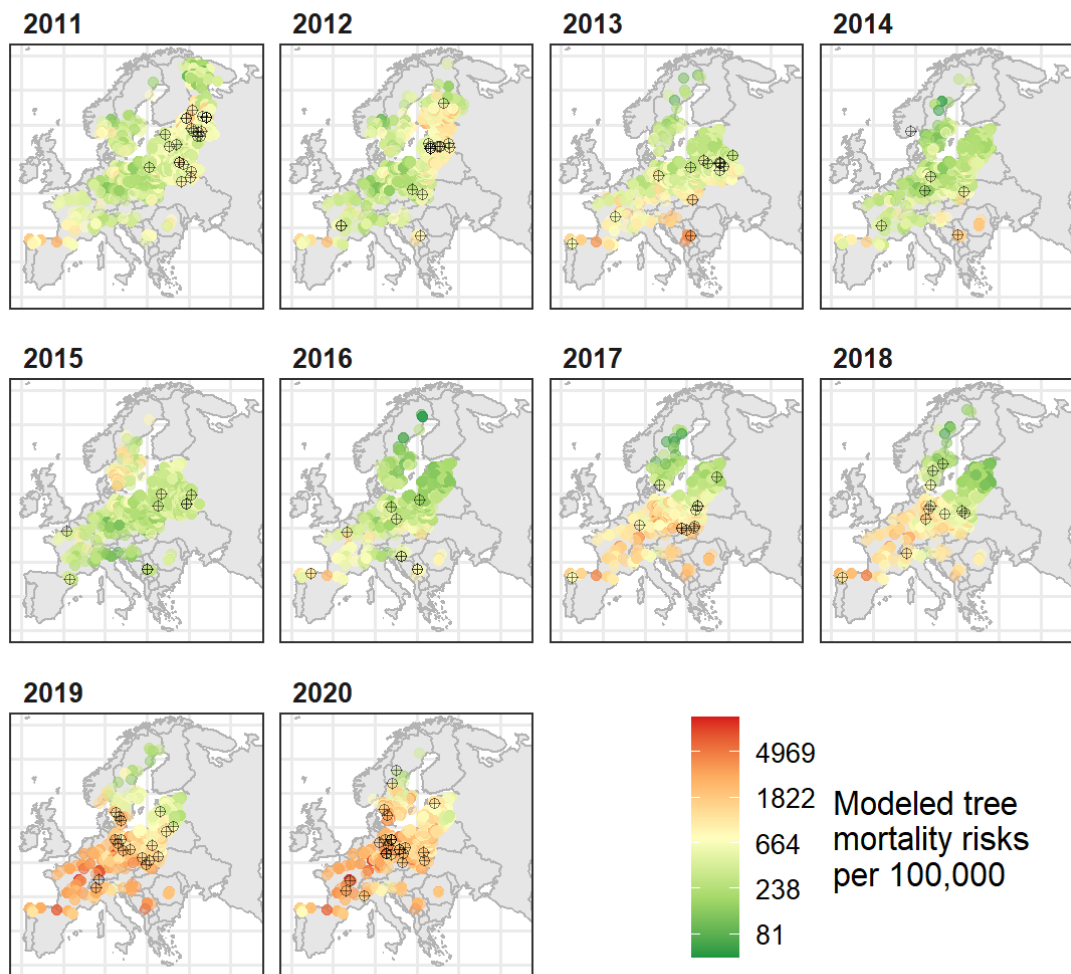


**Figure 4.15:** Spatial evaluation of modeled tree mortality for silver birch for all analyzed ICP Forests plots on a logarithmic color scale. Black points indicate observations of dead trees (n=145).

Austrian oak

Among 28,637 Austrian oak tree-year observations from 2011 to 2020, 101 trees died (Table 4.1). Austrian oak had the highest mortality in 2014 and a smaller peak in 2018 (Figure 4.1). This species is spread in south-eastern Europe (Figure 4.17). 30-year long-term higher average spring temperature increased tree mortality odds by 60%, and more winter precipitation decreased tree mortality odds by 15% (Table 4.9). Higher average winter temperature and higher summer precipitation during the three previous years decreased the odds of tree mortality by 40%. These opposing trends can be observed, for example, in 2014, when a temperature and precipitation peak was followed by a mortality decrease during the following years (Figure 4.16). The model evaluations indicated higher mortality risks in 2013 and 2014 in central Europe (Figure 4.17).

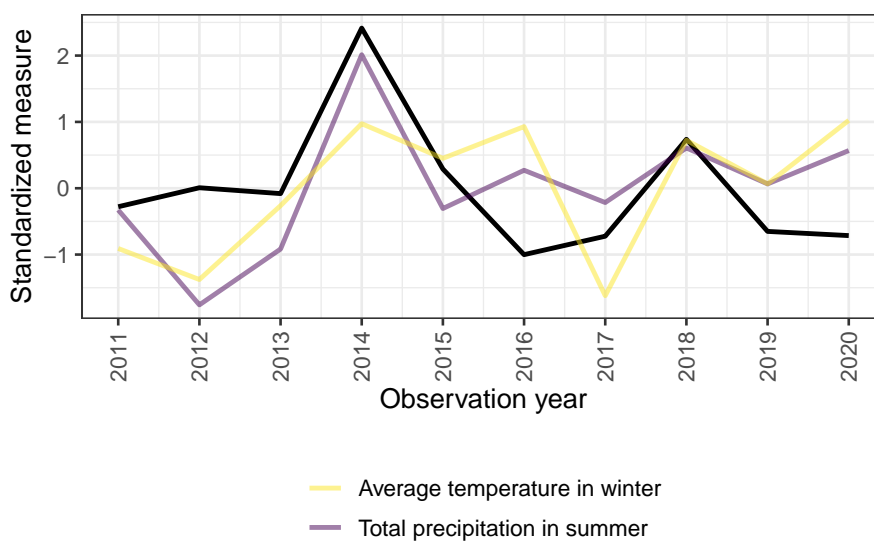


**Figure 4.16:** Annual values of weather variables and mortality (black line) for Austrian oak. All variables have been standardized by subtraction of their means and divided by their standard deviations. Only variables from the final model in the pooled analysis over all years combined are shown.



**Table 4.9:** Logistic regression model estimates for Austrian oak along with 95% confidence intervals and Likelihood ratio test p-values.

Variable	Odds ratio	Confidence interval	P-value
Mean temperature of spring 30-years average (°C)	1.60	1.35 – 1.92	< 0.0001
Precipitation sum of winter 30-years average (50mm)	0.85	0.72 – 0.98	0.02
Average temperature in winter anomaly average of the reported tree mortality year and three previous years(°C)	0.60	0.42 – 0.86	0.005
Total precipitation in summer anomaly average of three previous years to the reported tree mortality year (50mm)	0.60	0.43 – 0.86	0.005

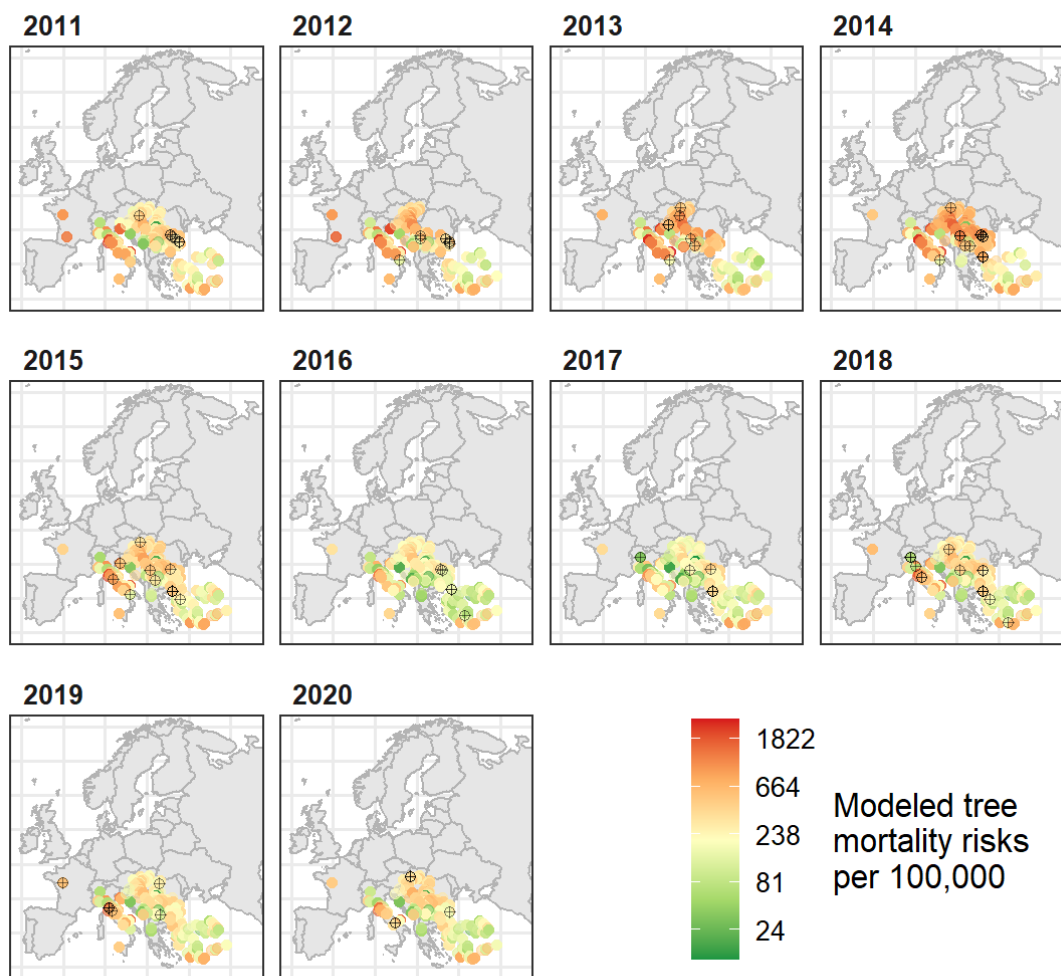


**Figure 4.17:** Spatial evaluation of modeled tree mortality for Austrian oak for all analyzed ICP Forests plots on a logarithmic color scale. Black points indicate observations of dead trees (n=101).

### European hornbeam

Among 17,653 European hornbeam tree-year observations from 2011 to 2020, 103 trees died (Table 4.1). Mortality for European hornbeam was strongly affected in 2011 and 2019 (Figure 4.1). Tree stands older than 120 years had the highest tree mortality, with odds 376% higher than those of 41 to 60-year-old stands (Table 4.10). 30-year long-term higher continentality increased tree death odds by 46%, and more precipitation in the vegetation period decreased tree death odds by 17% per 50 mm. The higher average temperature of the warmest month of the previous year and more winter precipitation in the current year increased the odds of tree mortality by 54% and 78%, respectively. The temperature association can be seen mainly for the years 2017 to 2019 when an increase in temperature increased mortality the following year (Figure 4.18). For precipitation, this increasing effect can be seen in all other years except 2011 and 2019. The model evaluations indicated a higher risk in eastern Europe (Figure 4.19).

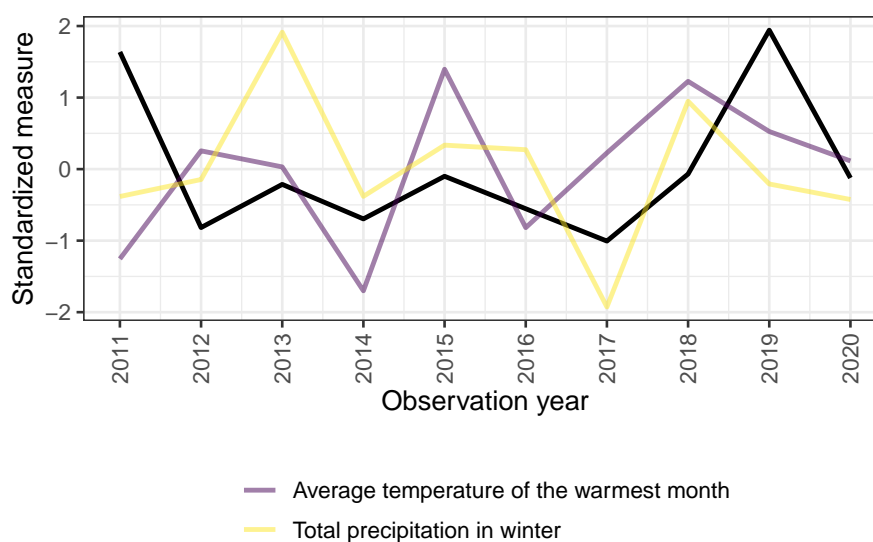


**Figure 4.18:** Annual values of weather variables and mortality (black line) for European hornbeam. All variables have been standardized by subtraction of their means and divided by their standard deviations. Only variables from the final model in the pooled analysis over all years combined are shown.

**Table 4.10:** Logistic regression model estimates for European hornbeam along with 95% confidence intervals and Likelihood ratio test p-values. Irregular-aged trees were excluded due to lack of tree mortalities in this group.

Variable	Odds ratio	Confidence interval	P-value
Mean stand age (Reference 41 - 60)			0.0003
61 – 80	1.32	0.77 – 2.28	
81 – 100	1.25	0.64 – 2.39	
101 - 120	1.46	0.68 – 2.97	
>120	4.76	2.49 – 8.98	
Temperature difference between average temperature of the coldest and the warmest month (continentality) 30-years average (°C)	1.46	1.26 – 1.73	< 0.0001
Total precipitation in vegetation period 30-years average (50mm)	0.83	0.70 – 0.97	0.02
Total precipitation in winter anomaly average of the reported tree mortality year and the previous year (50mm)	1.78	1.25 – 2.49	0.002
Average temperature of the warmest month previous year to reported tree mortality (°C)	1.54	1.15 – 2.09	0.003

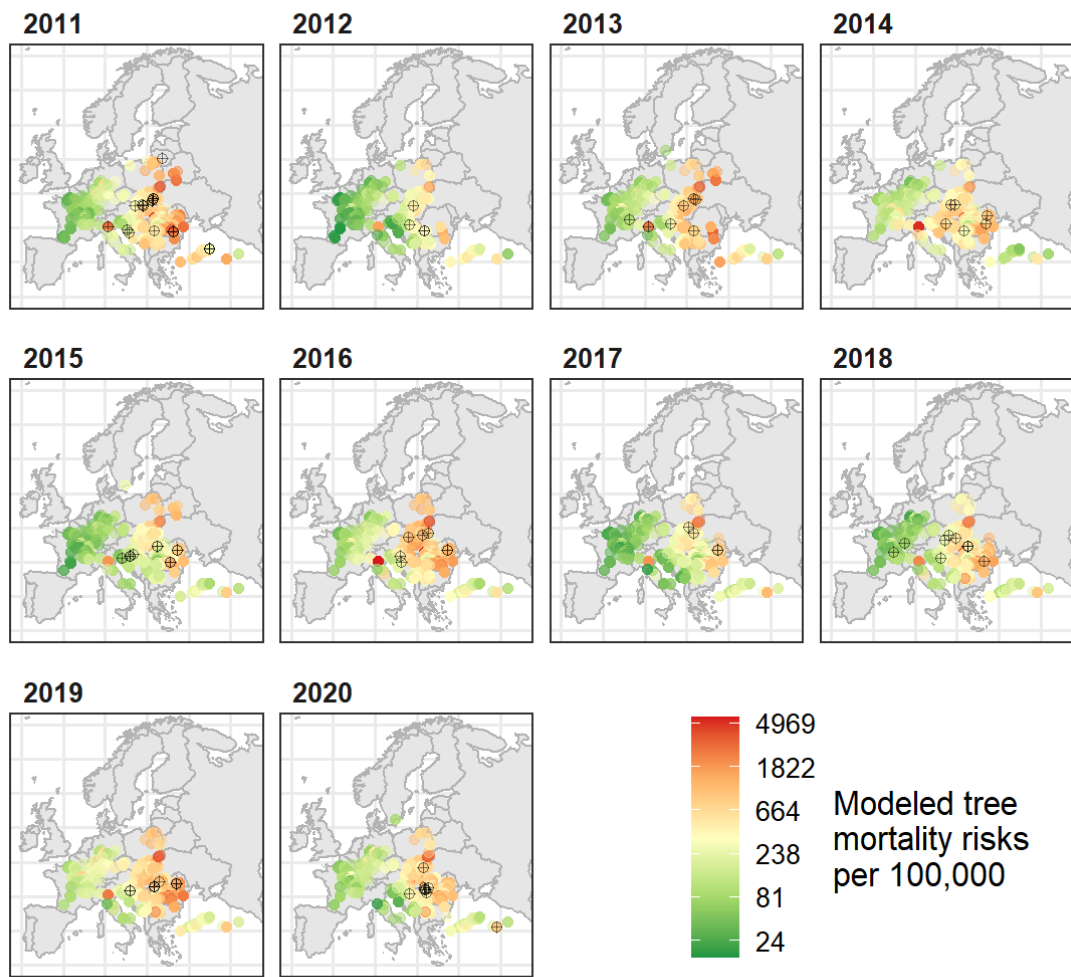


**Figure 4.19:** Spatial evaluation of modeled tree mortality for European hornbeam for all analyzed ICP Forests plots on a logarithmic color scale. Black points indicate observations of dead trees (n=103).

*Pedunculate oak*

Among 48,222 pedunculate oak tree-year observations from 2011 to 2020, 277 trees died (Table 4.1). Pedunculate oak exhibited the highest mortality in 2011, 2015, and 2020 with the strongest effects in south-eastern parts of central Europe (Figure 4.21). 30-year long-term higher summer temperature and precipitation increased tree mortality odds by 28% and 34%, respectively (Table 4.11). Higher average temperature of the warmest month during the previous three years increased the odds of tree mortality by 97%. Figure 4.20 shows the immediate association between the warmest month temperature for 2015 and the 2018 high-temperature association with a two-year delay increase in mortality in 2020. The higher average temperature of the coldest month in the reported year and more winter precipitation during the two previous years increased tree mortality odds by 19% and 86%, respectively, whereas their interaction decreased the mortality odds by 22%. Figure 4.20 indicates the direct association of coldest month temperature except for 2014, which seemed to influence 2015 mortality. The winter precipitation association appears to be driven by the higher precipitation in 2013 and 2018, with higher mortality in 2015 and 2020.

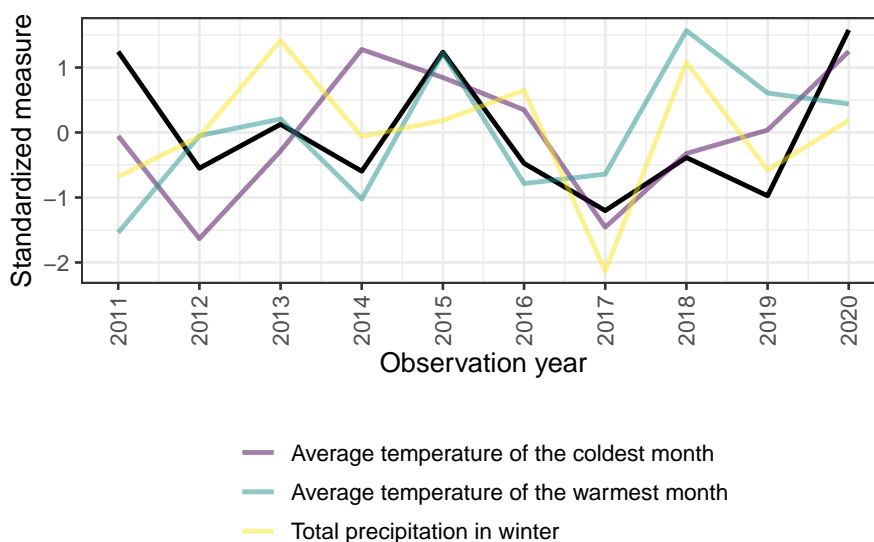


**Figure 4.20:** Annual values of weather variables and mortality (black line) for Pedunculate oak. All variables have been standardized by subtraction of their means and divided by their standard deviations. Only variables from the final model in the pooled analysis over all years combined are shown.

**Table 4.11:** Logistic regression model estimates for Pedunculate oak along with 95% confidence intervals and Likelihood ratio test p-values.

Variable	Odds ratio	Confidence interval	P-value
Average temperature in summer 30-years average (°C)	1.28	1.19 – 1.39	< 0.0001
Total precipitation in summer 30-years average (50mm)	1.34	1.19 – 1.48	< 0.0001
Average temperature of the warmest month anomaly average of the three previous year to reported tree mortality (°C)	1.97	1.42 – 2.73	< 0.0001
Average temperature of the coldest month anomaly average of the reported tree mortality year (°C)	1.19	1.09 – 1.30	< 0.0001
Total precipitation in winter anomaly average of two previous years to the reported tree mortality year (50mm)	1.86	1.39 – 2.46	< 0.0001
Interaction between average temperature of the coldest month anomaly average of the reported tree mortality year and total precipitation in winter anomaly average of two previous years to the reported tree mortality year (°C * 50mm)	0.78	0.66 – 0.91	0.002

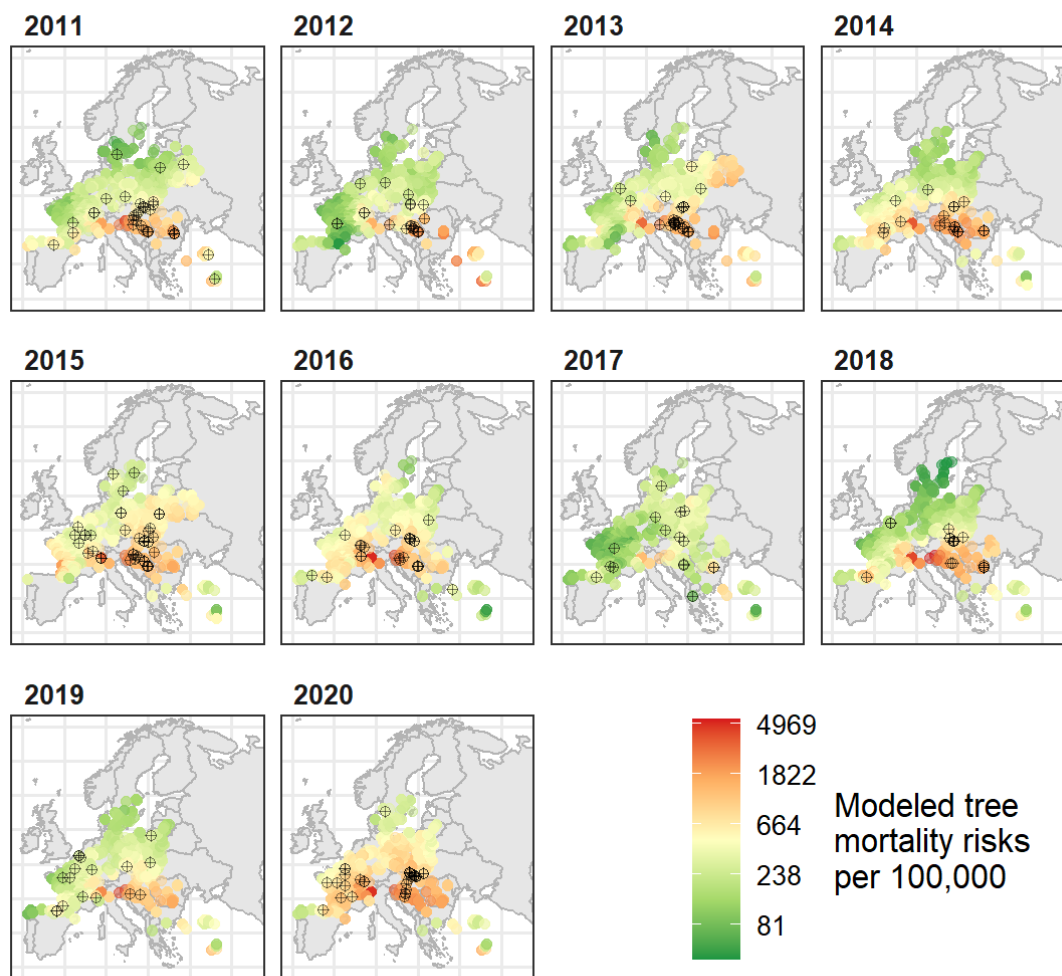


**Figure 4.21:** Spatial evaluation of modeled tree mortality for Pedunculate oak for all analyzed ICP Forests plots on a logarithmic color scale. Black points indicate observations of dead trees (n=277).



*Sessile oak*

Among 51,875 sessile oak tree-year observations from 2011 to 2020, 232 trees died (Table 4.1). Sessile oak experienced decreasing mortality from 2011 to 2016 and a slight increase from 2016 to 2020 (Figure 4.1). Tree stands between 41 and 60 years, and plots with north aspects showed the highest tree mortality (Table 4.12). 30-year long-term higher continentality and annual precipitation decreased tree mortality odds by 41% and 69%, respectively, whereas their interaction increased the odds by 6%. The higher average temperature in spring during the previous two years decreased the odds of tree mortality by 56%. Higher average winter temperature during the three previous years and more summer precipitation during the two previous years reduced the mortality odds by 42% and 2%, respectively, and their interaction reduced the odds by a further 36%. These associations are mostly seen after all three variable peaks in 2014, followed by a mortality decrease in the following years (Figure 4.22). The model evaluations indicated a higher mortality risk in central parts of Europe, especially from 2013 to 2015 (Figure 4.23).

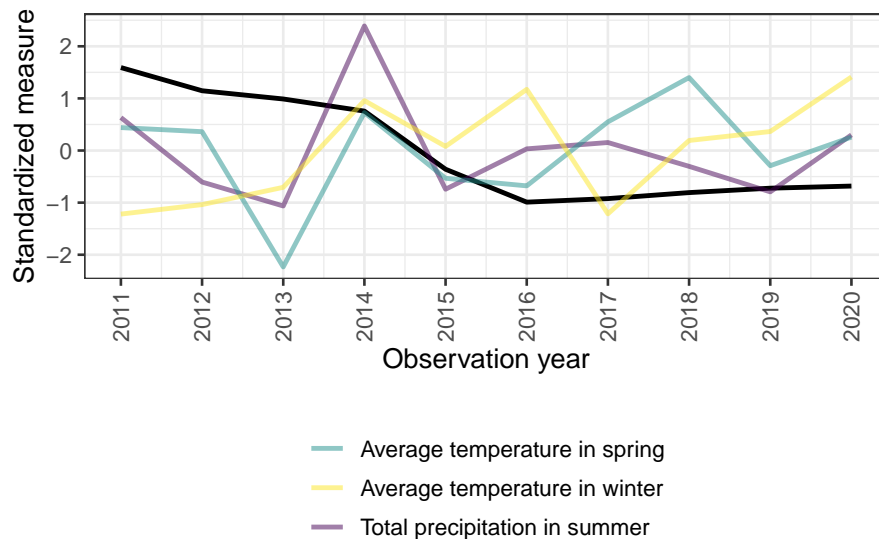


**Figure 4.22:** Annual values of weather variables and mortality (black line) for Sessile oak. All variables have been standardized by subtraction of their means and divided by their standard deviations. Only variables from the final model in the pooled analysis over all years combined are shown.

**Table 4.12:** Logistic regression model estimates for Sessile oak along with 95% confidence intervals and Likelihood ratio test p-values.

Variable	Odds ratio	Confidence interval	P-value
Mean stand age (Reference 41 - 60)			< 0.0001
61 – 80	0.73	0.50 – 1.05	
81 – 100	0.39	0.25 – 0.57	
101 - 120	0.37	0.20 – 0.63	
>120	0.48	0.25 – 0.84	
Irregular stands	0.43	0.21 – 0.82	
Aspect (Reference Flat)			0.0001
North	2.42	1.46 – 4.06	
North-east	1.29	0.71 – 2.31	
East	1.48	0.87 – 2.54	
South-east	1.50	0.83 – 2.70	
South	0.74	0.34 – 1.50	
South-west	0.78	0.42 – 1.42	
West	1.11	0.59 – 2.02	
North-west	0.93	0.44 – 1.85	
Temperature difference between average temperature of the coldest and the warmest month (continentality) 30-years average (°C)	0.59	0.41 – 0.82	0.002
Annual total precipitation 30-years average (50mm)	0.31	0.19 – 0.49	< 0.0001
Interaction between temperature difference between average temperature of the coldest and the warmest month 30-years average and annual total precipitation 30-years average (°C * 50mm)	1.06	1.04 – 1.09	< 0.0001
Average temperature in spring anomaly average of the reported tree mortality year and two previous years (°C)	0.44	0.29 – 0.67	0.0001
Average temperature in winter anomaly average of the reported tree mortality year and three previous years (°C)	0.58	0.47 – 0.70	< 0.0001
Total precipitation in summer anomaly average of two previous years to the reported tree mortality year (50mm)	0.98	0.80 – 1.19	0.8
Interaction between average temperature in winter anomaly average of the reported tree mortality year and three previous years and total precipitation in summer anomaly average of two previous years to the reported tree mortality year (°C * 50mm)	0.64	0.50 – 0.83	0.001

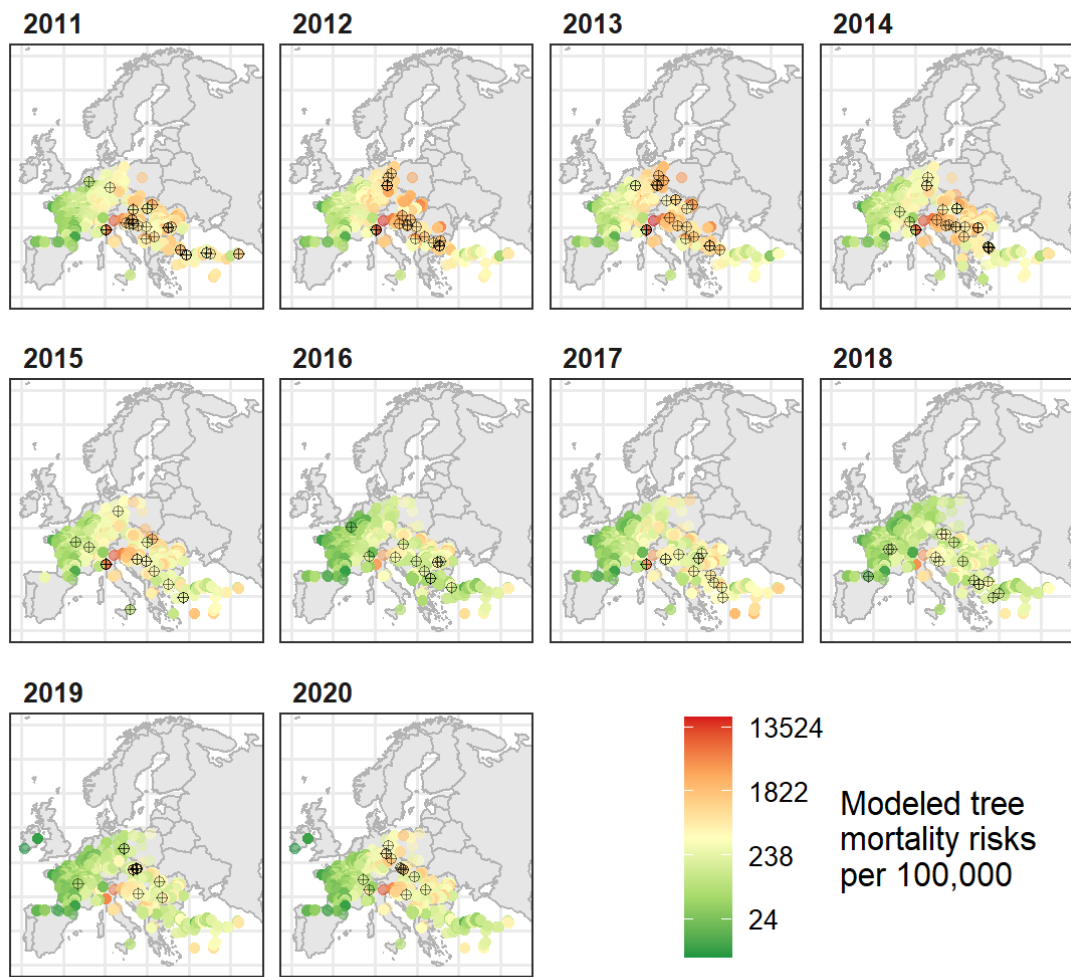


**Figure 4.23:** Spatial evaluation of modeled tree mortality for Sessile oak for all analyzed ICP Forests plots on a logarithmic color scale. Black points indicate observations of dead trees ( $n=232$ ).

## 4.5 Discussion

The analysis presented here, based on annual assessments of common tree species in European forests from 2011 to 2020, showed individual tree mortality to be impacted by long-term climate averages and weather factors. This aligns with previous findings (Brandl et al. 2020; Neumann et al. 2017), forming this study's first hypothesis.

Long-term climate averages and their change rate (evolution) over time showed importance for a broad range of species to explain background mortality in France (Taccoen et al. 2019). Likewise, Brandl et al. (2020) found long-term climate variables influencing mortality with higher temperature and lower precipitation increasing mortality risks. Generally, higher temperatures within growing seasons are related to higher evaporative demand and, therefore, might lead to drought stress (Eamus et al. 2013). Additionally, they are favored by pests. For example, in the case of bark beetles, more generations can fully develop within the season (Marini et al. 2012). Northward and altitudinal spread of forest insects was shown to have a strong temperature dependency, as reviewed in Pureswaran et al. (2018). The high risk of losing climatic niches for many species due to climate warming was also indicated by studies on the predictive distribution of species (Bombi et al. 2017; Dyderski et al. 2018; Thurm et al. 2018) and studies on vegetation samples (Gottfried et al. 2012; Schmidtlein et al. 2013). Brandl et al. (2020) additionally discussed the effect of increased growth and faster development under warmer temperatures so that trees moved faster along their life trajectories and died at younger ages with constant self-thinning lines.

In the data of this study, higher temperature normals (winter, spring, summer, warmest month, continentality) were related to higher mortality for all species except sessile oak. Results were comparable with Brandl et al. (2020) for spruce, beech, and Scots pine; their study did not separate oak species. This study found higher long-term summer temperatures related to higher mortality for pedunculate oak. Whereas, in the case of sessile oak, higher continentality reduced mortality. The ability of pedunculate oak to withstand continental conditions was well reflected in its eastern distribution range far into Russia. Still, sessile oak was not distributed to that extent, so the result was not evident. Oak decline has been reported to be associated with human, environmental and biotic factors, such as lowering groundwater table, absence of flooding, pollution, non-adapted silvicultural practices, and climate change (Eaton et al. 2016). Furthermore, pedunculate oak also grows on heavier soils in wet lowlands and damp areas by streams and rivers, tolerating periodic flooding. Thus, this species's vitality might depend more on soil conditions and water table (Kostić et al. 2021). The overall relation pattern between sessile oak and climate variables differed from the rest of the species set, possibly due to decreasing mortality trends in the decade studied.

Long-term averages for precipitation either increased (pedunculate oak, spruce, Scots pine, and black pine) or decreased (hornbeam, Austrian and sessile oak) odds ratios for mortality. We can only speculate why higher summer precipitation is related to higher mortality in the case of pedunculate oak, a drought-tolerant species (Eaton et al. 2016; Niinemets and Valladares 2006). A common problem for oaks is a combination of mildew of the second leaf flushing after massive defoliation (Eaton et al. 2016). The effect for spruce is very weak, which is in line with Brandl et al. (2020), who found no precipitation

effect for this species. Black pine provenances might suffer from fungal diseases (winter temperature and summer rain were both positively correlated with *Diplodia* colonization on cones in France and become virulent after drought periods (Fabre et al. 2011)). The results of this study support these findings. Higher spring precipitation showed an odds ratio above 2 for Scots pine. This, again, might be linked to *Diplodia* or other fungi or to wet snow (most likely in late autumn and early spring) and subsequent crown breakage that starts a decline spiral (Nykänen et al. 1997).

Besides long-term climate data (predisposing factors) that are related to diffuse background mortality, climate anomalies (pulse events) showed important effects on mortality and can be seen as inciting factors (Manion 1992, 1991; Senf et al. 2020; Sturrock et al. 2011). Anomalies are known to reduce growth (Thurm et al. 2018; Vanoni et al. 2016) or vitality measured, for example, as annual defoliation (Eickenscheidt et al. 2019). Mortality occurs when physiological thresholds are exceeded (Schuldt et al. 2020; Senf et al. 2020; Vanoni et al. 2016), which is likely under extremes as “plants have limited physiological potential to respond to rapid changes in the environment” (Choat et al. 2018). Climate and weather also promote systemic effects linked to vitality decline, such as pests or diseases that favor warmer temperatures (Sturrock et al. 2011). The impact of weather anomalies on forest insects is complex, but anomalies such as unusually warm or dry conditions can serve as initial eliciting factors for pest outbreaks (Raffa et al. 2008).

Except for European hornbeam, two to three-year averages of temperature anomalies for the warmest month, summer, spring, and vegetation periods primarily influenced the models, indicating lag effects, longer-lasting stress and favorable weather conditions for insects or fungi. Summer, vegetation period, or annual precipitation sum anomalies were significantly selected as two to three-year averages except for spruce. In contrast, the effects of winter anomalies (temperature and precipitation) had shorter periods. Therefore, they often had a more direct relation with mortality of the subsequent assessment in summer. This might indicate different processes: stress via heat and drought, which starts a decline and an immediate effect on insects or pathogens, but also a change in phenology that increases the risk for late frost damage or insect damage. A review on the phenological form of pedunculate oak states that there are two phenological types – early and late flushing – and that the late form of oak is more resistant to spring frosts and insect damage (Utkina and Rubtsov 2017).

This study found that warmer than average winters reduced mortality for birch, Austrian and sessile oak. At the same time, warmer coldest month temperatures increased the risk for pedunculate oak, spruce, Scots pine, beech, and black pine. Neumann et al. (2017) found that a warmer than average maximum temperature of the winter season increased mortality. In contrast, a warmer than average minimum temperature of the winter season decreased mortality in Europe's 2000 to 2012 period, which was interpreted as a reduction in cold-induced mortality. Warmer winters, earlier flushing, higher risk of late frost, higher survival of insects (Allen et al. 2010), and reduced cold-induced mortality under harsh environments might be related to this study's findings. Still, it is unclear why birch, an extremely cold hard species, is harmed by harsher winters. Austrian and sessile oak show lower cold hardiness and might benefit (hardiness ranking according to Roloff and Grundmann (2008)). Dietze and Moorcroft (2011) found differing responses for minimum winter temperature for differing plant functional types in North America,

highlighting the regional and species-specific differences between effect and response found here. Northern types showed higher mortality under colder winter (ice damage or freeze embolism), a result found in this study for birch, Austrian and sessile oak, the latter two not growing in Northern Europe.

In line with several studies (Allen et al. 2015, 2010; Brandl et al. 2020; Ciais et al. 2005; Maringer et al. 2021) and expectations of this study, warmer temperatures in the previous year increased mortality risk dramatically for five out of nine species. This was strongest for species that dominate Northern European forests (birch, spruce, Scots pine) either because they are not adapted to this situation or the link to insects and pests, which benefit from reduced temperature limitation. The overall effect of the coupling of stress and population dynamics driven by drought and heat is well documented in bark beetle infesting spruce (Anderegg et al. 2015; Marini et al. 2012; Raffa et al. 2008). This study found a contrasting result for sessile oak, beech, and black pine (higher temperatures in spring or warmest month related to reduced mortality). This effect should be expected in regions where warming reduces stress. For instance, Jolly et al. (2005) described how an extended vegetation period resulted in better tree growth in the Swiss Alps. Black pine growth improves with positive spring water balance (Marqués et al. 2016), so positive spring anomalies might reduce mortality when accompanied by precipitation or when growth limits due to low temperatures are reduced. Findings for spruce and beech but not for Scots pine are in line with the results of Nothdurft (2013), though the latter study focused on only one region in Germany and was based on a small data set and a different period.

Effects of precipitation anomalies split up between winter and non-winter periods (vegetation period, summer, or annual precipitation). Three of four species (hornbeam, pedunculate oak, black pine) suffered from higher winter precipitation. A result typically related to wind throw risk due to water-saturated soils when it coincides with high winds (reviewed by Mitchell (2013)), which was excluded from the data set of this study. Annual, summer, or vegetation period precipitation anomalies had to be taken as variables of the previous years, as the crown condition survey takes place in summer. Therefore, results do not reflect only direct drought effects but also lagged consequences, which was apparent from the steep increase of mortality following 2018 for spruce and birch in data of this study (Brun et al. (2020) and Senf et al. (2020)). Neumann et al. (2017)) pointed out that variability between summer and spring anomalies of the previous period are drivers of mortality (wet summer and dry spring). A reason for this might be the timing of bud formation in mid-summer so that the number of leaves is higher after a wet period which increases water demand in a subsequent drought in the following spring or summer (Meier and Leuschner 2008). Only Austrian oak witnessed a clear beneficial effect of higher precipitation, which is in accordance with drought susceptibility of this species (Colangelo et al. 2018). Effects of interaction between temperature and precipitation variables for spruce and Scots pine could be interpreted in the way that rising temperatures in the vegetation period can be compensated by higher precipitation.

Interpretation of observed results regarding the impact of aspect on mortality has limitations. Aspect and slope were not significant in other studies (Maringer et al. 2021). The data on aspect did not incorporate information on the slope. However, steep slopes in southern directions are understood to be warmer (Reger et al. 2011). Effects of aspect

could be hypothesized that southwest slopes are drier and warmer, and north-facing slopes are colder and even prone to frost-drought (Tranquillini 1982). In the models, beech and oaks tended to have lower mortality on the south and west-facing sites, whereas spruce exhibited this pattern only for western slopes. For black pine, the highest mortality estimates were calculated for sites facing east and west, while it was northeast and northwest for Scots pine. These are, of course, just generalized results of the models under the caveat that each species will favor different aspects, depending on altitude and latitude.

Neumann et al. (2017) found that warm summers and high seasonal precipitation variability increased the likelihood of tree death and that age was an important driver of mortality for European tree species. Brandl et al. (2020) found an increasing mortality risk with age for spruce and beech, but not so clear dependencies for oaks and Scots pine. This study found decreasing mortality with age for pine and oak species and a similar but weak trend for spruce. For beech, risk first diminished and then increased with age. Age increased mortality considerably for the short-lived pioneer species silver birch and short-lived hornbeam (Leuschner and Ellenberg 2017). Trees in uneven-aged stands had higher mortality compared to the reference group 41-60 years for Norway spruce, European beech, and silver birch but lower mortality for Scots pine and sessile and pedunculate oak. Age effects might be related to the development stages of stands, and age effects were leveled out between species when survival probabilities were displayed over tree height in the study by Maringer et al. (2021).

According to the second hypothesis, the effects of extreme and long-lasting droughts and heat waves on mortality are related to the short-term effects of annual anomalies. Europe has experienced a series of extremely hot and dry summers (2003, 2010, 2013, 2015, 2018) (Buras et al. 2020; Hanel et al. 2018). Heatwaves drove droughts and precipitation deficits in the vegetation period and affected certain parts of Europe. The effects on vegetation were modulated by the weather conditions in the preceding winter or subsiding seasons. For example, the 2015 summer was the hottest since 1950 across a large part of eastern and south-western Europe. Still, in terms of annual precipitation deficit, the severity of the 2015 drought was possibly limited due to the preceding wet winter over a large part of Europe (Hanel et al. 2018). Buras et al. (2020) described 2018 as characterized by a climatic dipole, “featuring extremely hot and dry weather conditions north of the Alps but comparably cool and moist conditions across large parts of the Mediterranean”. These spatio-temporal patterns affect mortality as species are not evenly distributed and are affected in single events. This was reflected in data here that exhibited a steep increase in annual mortality after 2018 for spruce, birch, and beech but showed no signs of increased mortality for species with a Mediterranean distribution like Austrian oak and black pine, or species that encompass at least considerable distributions in the Mediterranean like sessile oak. The effects of the drought in 2018 on spruce and beech in Germany were enhanced by consecutive drought years and led to increased mortality rates (Obladen et al. 2021). This aggravating effect of consecutive unfavorable weather conditions with an increase in soil moisture drought (Hanel et al. 2018) explains the absence of a drop in annual mortality for Norway spruce or birch after 2018. Strong drought-legacy effects in 2019, with missing physiological recovery, that leave trees highly vulnerable to secondary insect or fungal pathogen attacks were also reported (Moravec et al. 2021; Schuldt et al. 2020). In contrast, there was no effect of the hot and dry

summer of 2013 (Hanel et al. 2018) visible in the data of this study. Apart from Austrian oak, there was no increased annual mortality in 2013 or 2014. Thus, we can conclude that short-term effects of annual anomalies influence tree mortality. Still, the severity of the effects is also shaped by previous (Hanel et al. 2018) and subsequent (Schuldt et al. 2020) weather conditions.

The third hypothesis is difficult to judge as it is somewhat contradicting the assumption of an individual response of species to environmental stress. Nevertheless, this hypothesis was formulated due to spatial aspects in species distribution. Figure 4.4 can be interpreted for the grouping of species according to effects. It revealed similarities between some broadleaved species of warmer climates and lowlands (Austrian and sessile oaks) and species that also occur in higher elevations and colder climates (spruce, pine, and pedunculated oak) with distinct cold hardiness, as described by Kreyling et al. (2012) for *P. nigra*. *Q. cerris* forms mixed stands together with *Q. petraea* in Austria and southern Slovakia as outposts in the Pannonian region (Leuschner and Ellenberg 2017). Beech and hornbeam appear to fall between those two groups. The pioneer species silver birch, with only three significant climate or weather variables impacting its mortality, is hard to classify with other species. Species tolerating warmer conditions possess mechanisms to withstand heat and drought to a certain degree. Oak seedlings, for example, exposed to drought have been shown to have adapted their growth and xylem structure to improve drought resistance, for instance, via reduction of latewood vessel size (Vander Mijnsbrugge et al. 2020). Grouping according to distribution was also performed for North American species into plant functional traits with subsequent mortality patterns analyzed by Dietze and Moorcroft (2011), who distinguished between angiosperms and gymnosperms. Shade tolerance and abundant species groups were further separated into Northern and Southern ranges according to established differences in climatic tolerances. Only the distributional aspect of this classification might be appropriate for this study.

The lowland and higher elevation groups differed clearly in the effects of winter temperature anomalies. Broadleaved species of warmer climates might benefit from a lower risk of severe frost damage and a longer vegetation period with earlier flushing to allow for the use of soil water stocks from winter precipitation (e. g. in Mediterranean ecosystems). The negative effect of warmer (and wetter) winters for conifers is often related to wind throw (Maringer et al. 2021), an effect we excluded from our data set. Still, trees can be injured by snow break, and there is feedback on pathogens and pests with winter anomalies. Besides that, warmer winters are known to increase the likelihood of late spring frost damage in frost-prone regions as trees begin wood formation, leaf release, and flowering weeks earlier compared to the mid-twentieth century (Puchałka et al. 2017, 2016). The greater frequency of late spring frosts is related to climate warming (Sangüesa-Barreda et al. 2021).

A limitation of the study was the low event rate of mortality that affects the power for complex multivariable statistical models to detect weather and climate impacts, particularly concerning interactions among risk factors. These limitations are common to any study of rare events. Mortality is assessed annually, necessitating logistic regression methods for interval-censored data as described in the methods. While exact mortality dates are available for humans and animals and allow more accurate modeling, such as by the Cox proportional regression model, they do not exist for trees, where annual



assessment might be considered the least coarse option available for mortality assessments. The logistic regression methods outlined in this study for binary outcomes are easily transportable to other forest monitoring scenarios. They produce interpretable odds ratios that provide quantitative effect sizes and statistical significance.

## 4.6 Conclusion

Different types of mortality – background or disturbances - are related to different variables and time scales. Multi-year stress events hit managed forests with tremendous economic loss and hamper fulfillment of ecosystem services, for example, carbon storage. This study's tree mortality models and predictions, combined with climate change projections, could be used to improve forest management planning. It is important to stress that climate warming increases the risk of mortality of all studied tree species with less severity in the case of sessile oak, and this understanding should be the baseline of future forest management plans throughout Europe. Optimal tree species may be selected for planting, dependent on regional climates. Still, it is vital to understand the differences in mortality between managed or hugely human-influenced forests and natural forests. The individual tree logistic regression models should be updated annually with new mortality data, including precise age estimates. This would be especially beneficial for increasing the statistical power to detect effects for other tree species and incorporate recent weather events, thus maximally preparing for an uncertain future under climate change. Remote sensing techniques add additional value for future data on individual tree mortality.



## 5 Future outlook

The three applications of this thesis assess only possible associations with the available data. As already stated in the individual conclusions, there have been limitations to the studies regarding the data quality. Increasing the data quality would increase the number of observations and hence the power to detect significant associations, resulting in better interpretation, understanding, and predictions. This could reduce unnecessary surgeries, improve forest management, and make mountain sports safer. The main concerns are the realization and handiness of suggested improvements, which are discussed in the following.

### 5.1 Prostate cancer risk tool

Human medicine is improving continuously. This includes new medical instruments, techniques, and drugs. Further, the population is changing continually, as seen in the demography. These changes apply to prostate cancer and lead to the need for currently updated risk calculators. The biopsy method has improved from 10-12 core biopsies to Magnetic Resonance Imaging (MRI)-assisted biopsies. Prostate Biopsy Collaborative Group (PBCG) biopsy data from the new method is currently collected as part of an international PBCG headed by investigators in Australia. The international PBCG now additionally includes center in Asia, expanding the demographic scope from North America, Europe, and the Caribbean. The new data collection is an excellent opportunity to overcome the missingness problem learned from the PBCG. To improve predictions, clinics should be urged to collect all variables. Using a standardized input form, as the international PBCG currently does, secures data quality and consistency. With more outcomes collected, expanded definitions of prostate cancer can be investigated beyond clinically significant prostate cancer (csPCA) in the PBCG.

The future of prostate biopsies will further improve with automated techniques. Currently, extracted tissues are viewed by a pathologist who decides on the score according to a scale. These results depend on the pathologist's experience (Varma et al. 2018). Machine learning approaches for image recognition can be used to obtain consistent scores (Dov et al. 2022), which could also be on a finer scale and improve the accuracy of risk prediction.

Another challenge to develop risk tools is the data transfer, which must pass the approval process of several ethical offices, taking time and slowing down research. One solution is to take the analysis to the data and use meta-analyses to combine the individual cohort results (Gaye et al. 2014). Since only model coefficients have to be transferred, no extended ethics approval is necessary. On the other hand, analyses are out of the hand of a central statistical group. Classical statistical and data quality checks for outliers or suspicious cases need to be performed individually.

Lessons learned from the PBCG project endorse the following four data-science-driven strategies for improving clinical risk prediction. Firstly, to actively design prospective data collection, monitoring, analysis, and validation of risk tools using the same standards as for clinical trials. Secondly, to post risk tools and model formulas online to maximize doctor-patient decision-making and multiple external validations. Thirdly, the proposal is to dynamically update risk tools and tailor them to individual clinical centers to adapt to changing demographic and clinical landscapes. Fourthly, to accommodate missing data to optimize model training and flexibility in online tools for users who do not have all information. Following these strategies will lead to more effective risk prediction tools to assist clinical practice, as high-quality data will lead to high-quality risk predictions. Lessons of the PBCG are not limited to prostate cancer. Risk tools for breast cancer (Kanimozhi et al. 2019), psychosis onset (Studerus et al. 2020), diabetes (Dunkler et al. 2015), and many more can be improved by actively designed studies.

## 5.2 Austrian mountain sports

The Alpine Safety Board collects data on mountain accidents and fatalities to publish reports regularly. The extent of the data highly depends on the information collected by the rescue service about the victim at the accident site, the hospital, and from other witnesses who observed the accident or knew the victim. This is currently collected in text form, leading to many similar but different phrased entries. For optimized data collection, a standardized entry form should be used, as recommended by the PBCG.

Currently, the time is not usable since it is only rarely provided, and a system time is often entered. The exact time is important since the weather changes quickly in these regions, especially extreme weather events, which are only apparent for a certain time. Additionally, an exact position is necessary for more accurate analyses of fatal accidents. The topography changes quickly in the mountains, changing the weather association to the accident. As for firefighters, radio communication between the control station and rescue team occurs. This communication service was changed in recent years from analog to digital. Firefighters have to press a button as soon as they arrive at the emergency location such that the control station is informed about the progress. This is easy and does not disturb the rescue process. We are unsure if the Alpine rescue team has to follow the same procedure but could do so easily. In addition, they could transmit the GPS position when pressing this button. As a proxy for the time, one would have the rescue time, which could differ a lot from the accident time if the victim was alone or mobile service was unavailable. The exact time and position could refine association analyses and be relatively easy to implement.

Further helpful information would be personal information about the victim. This is an easier task if it is an ordinary accident but becomes more complicated if it is fatal. However, in both cases, it would improve the understanding as one can adjust analyses for personal factors. This information should include but is not limited to age, gender, personal fitness, experience level, safety equipment used (depending on sport type), and known potential human risk factors, such as hypertension. To improve the data collection process, one could introduce an App with drop-down menus for ease of use, as every

investigator could type in the information with their mobile phone. These drop-down menus can also allow missing factors if the field can not be answered. The prostate cancer application has shown appropriate analyses accommodating potentially missing data.

Data collection strategies apply after an accident, but what can be done to prevent fatal accidents or accidents? To reduce fatal accidents, the key measures are faster rescue and better help. Different people and personalities participate in mountain sports, ranging from people who like to have nice foto for social media with no experience and improper equipment to experts with a lot of knowledge but also a high willingness for risks. Due to the wide range of participants, safety policies need to be addressed for all of them. Another difficulty is the fact that changes take time. As an example, one can consider the introduction of helmets for skiing. They are not mandatory in Austria, but people choose to wear them, so it took almost one generation to reach the point where almost everyone wears one. The problem was not that older people did not realize helmets would be safer. It was that they had learned and performed skiing all their life without one. But when it came to the safety of their children, they equipped them with a helmet from the start. Another challenge is finding solutions that can be applied to many mountain sports types to reach as many people as possible.

As already outlined in the conclusion of Chapter 3, the Austrian Board of Trustees for Alpine Safety and cooperators established an emergency App in 2019 for parts of Austria, Italy, and Germany to improve the rescue speed. An issue with the App is that hardly anyone knows about it. So advertisement is necessary until the App becomes standard, like the helmet achieved for skiing. Another issue with the App is that its primary purpose is to transmit GPS coordinates to the rescue service, which is nowadays a functionality of a regular emergency call on mobile phones. Therefore, the App needs to be improved with additional functionality. We suggest it becomes accessible offline directly at the accident to walk the injured person or helper through first aid steps, otherwise performed by emergency teams via phone. Additionally, the App could provide short first aid tutorials once a month not to overwhelm users while preparing them for safety in the mountains.

Another safety feature could be registration before participating in a sport. For hiking, something similar exists for multi-day trips via guest books at the huts. If someone gets lost, one can follow their route. While more critical for people doing sports alone, accidents involving more than one person also happen. Such a feature must be easy to use; otherwise, it would not be used. At the starting point, one could do check-in and give the route a name, for example, the summit. The App could suggest close summits or titles other users have used. Additionally, the expected time should be included to account for when lack of check-in becomes suspicious. For popular hikes, one could set up QR codes at the starting point with all information and checkpoints in between, as in the huts for longer routes. As the batteries improve, GPS coordinates can be transmitted more continuously. If tracked continuously, the App could also recognize accidents by the moving profile and for severe accidents, immediately call emergency services. Something similar exists already for smart watches for certain sports types. Professionals, in particular, participate in mountain sports more often alone and need these adaptations.

An App becomes more valuable the more it can connect features from other existing Apps. Apps helping to plan a sports day have become more commonly used, as well as those incorporating weather forecasts specialized for mountainous regions. Such planning Apps as Komoot and Bergfex can also lead hikers through chosen routes. Combining these features into the App or linking the safety App to other GPS Apps would increase safety. Further, the inclusion of webcams could assist in improving the planning process and assessments of current risks of routes. With the weather forecast included, one could estimate risks for a planned tour on a specific day, which could then be distributed by tourist information offices, web pages, huts, and other accommodations.

For better planning, it is necessary to account for the number of people at risk, which is currently lacking. The App's before-mentioned check-in function could also provide a number of people at risk, allowing models to adjust for that. On the one hand, more people at risk means more potential accidents and more people to help on the spot of the accident. On the other hand, for some sports, such as skiing, more people also means that the sport becomes more prone to a higher risk of crashes from other participants.

Finally, we must say that preventing accidents will not be possible altogether. With better equipment and knowledge, mountain sports continue to become safer. This also leads to more willingness to risk and makes it accessible to a broader range of people. Hence, safety improvement will always be an issue.

Mountain suicides and work accidents were not discussed so far, as they have different mechanisms. Safety at work improved in the past and should continue to do so. Suicide requires preventive measures unrelated to the mountains since people often live in the valleys. But safety Apps could at least expedite the rescue process and increase survival. One could set up signs for help hotlines and recreational sites at suicide hotspots, with the aim to deter life-threatening decisions.

### **5.3 Climate-based forest management**

A common issue of the presented studies was that events were rarely observed. To overcome this issue, cooperations were built to overcome the small sample size with data from different sites. The International Co-operative Programme on Assessment and Monitoring of Air Pollution Effects on Forests (ICP Forests) were founded to create a European-wide data set of tree damage and mortality. Before, every country selected its own variables of interest, and no standard existed between countries. This can still be observed as countries collect more variables and submit only mandatory variables. More variables should be compulsory to improve the data quality. For instance, the consistent collection of the slope would improve the predictions as it most likely would interact with aspects. The beauty of such stand-level variables is that they must be collected only once for a plot and updated now and then. More improvement of models could be reached by collecting more information on the individual tree level. Tree age is an example managed by some countries by exact tree age instead of the age classes used by ICP Forests. Changing the requirement to actual age will incur guesses and inaccuracies for older trees, but will become more accurate with time, as the exact

age is only accessible if the planting date is known. With precise age, models could better distinguish between mortality due to age versus environmental influences. Data collection should be further standardized across ICP Forests countries to ensure a robust data basis for future management decisions. The standardization process should follow the recommendations from the prostate cancer study.

One limitation of tree mortality studies is that tree death is not standardized as for human death. A tree that is declared dead could recover after years. Further, a tree with breakage could bud and build a new crown. Tree death is thus subjective with criteria that likely differed among the ICP Forests countries. Therefore, standard definitions for the event of tree death need to be implemented. Again in the spirit of the prostate cancer application of this thesis, standardized entry forms are needed for all outcomes and risk factors that can be implemented in user-friendly interfaces to correct data upon entry. Currently, it is possible that a tree is classified as dead in one year but would be classified dead in a different year with another investigator or in an other country. One approach which circumvents the issues is remote sensing techniques, whereby dead trees could be identified with image recognition with machine learning. By this approach, only the dominant canopy could be investigated as in this application. Competition effects within the lower canopy could not be detected. Maps of tree vitality could be overlaid with weather and topographic maps. Weather needs to be aggregated to the same time scale as the tree data, which is currently only annually. Daily measurements would lead to an enormous database that could be handled by machine learning.

Classical and interpretable approaches, such as logistic regression, could be further improved by adjusting for spatial effects. These can, for example, be exponential functions peaking in a center and declining with further distance, as shown in Figure 5.1. Using multiple of these over whole Europe can model spatial patterns over time. For our study, we implemented this approach but experienced some shortcomings. To overlap Europe with spatial functions requires a sufficient amount of mortalities to have enough power to find significant effects. Further, as the weather is highly correlated with spatial locations, spatial functions obfuscate weather effects, as spatial soil and background information is confounded with the weather. We focused on interpretable results for this study and used classical logistic regression due to lack of power.

This study focused on the most common tree species as sufficient data was available. Still, more uncommon tree species could be more resistant to climate change conditions and, therefore, interesting for forest management. For the ICP Forests data, more of these species could be selected and analyzed. But these trees grow in environments with other tree species dominant. Therefore, exploring these tree species in regions where they are the dominant species and transferring the results to Europe under climate change scenarios makes sense. For the common species, further investigation would be interesting into how they react to stress, such as single drought events. Field experiments under harsh conditions to investigate time delay effects or precipitation thresholds for common species are complex. It takes years to accumulate data, and only some trees die after a particular time. Control groups are needed leading to large areas of study. Grown trees exposed to experimental conditions are also required. Tree mortality risks could serve as warnings for regions in danger, instigating prevention, such as irrigation.

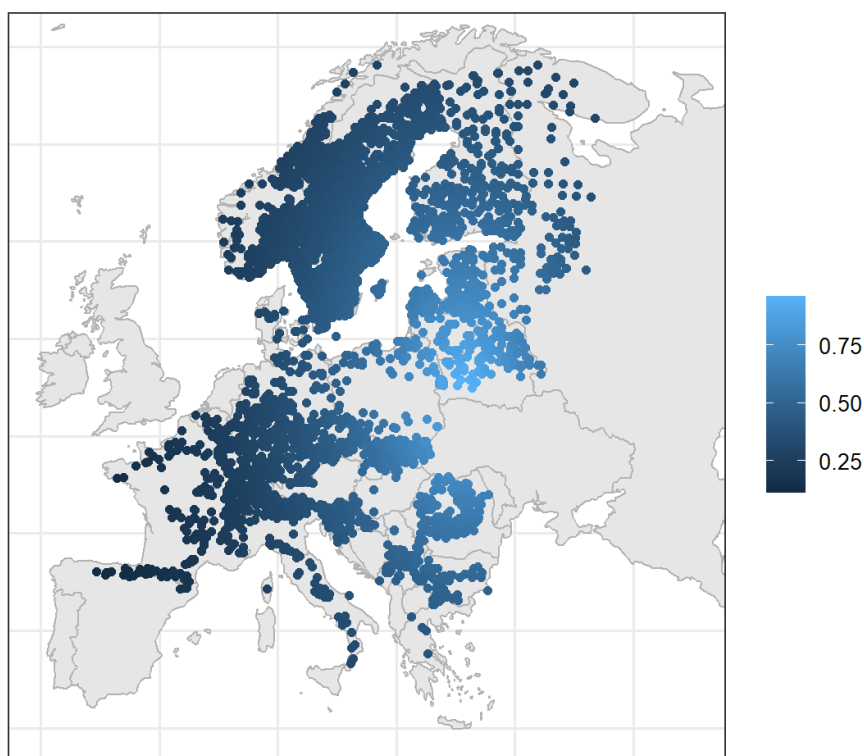


**Figure 5.1:** One selected exponential spatial basis function. In this example, twelve basis functions peaking at different locations were overlaid on Europe to cover it completely. These basis functions can be used to investigate spatial effects in regression models.

Weather is measured at stations and interpolated to continuous maps, which depends on the topography, such as mountains or oceans. Often weather data are not interpolated in great detail as this brings high uncertainty. Other weather data sets may lack information regarding different indices and only provide a few characteristics. Another issue is that weather needs to mirror the same time scale as the outcomes for the association analyses. All data sets need to be updated regularly, as has been argued for the prostate cancer application, which could be expedited by extracting information from satellite images. This way, essential variables like precipitation could be assessed and updated daily.

Several indices exist for further investigation of drought effects, including the the Standardized Precipitation Evapotranspiration Index (SPEI). These indices are combinations of individual weather variables and aim for thresholds for drought identification. The German weather institute defines a drought for a specific location if the SPEI value is smaller than minus one standard deviation. An issue with this definition is that it depends on the data used. The same SPEI value can indicate a drought in one data set but not in another. It is questionable whether a drought in wet regions means the same as in dry areas. Since defining a European-wide drought threshold is complex and as the drought indices are combinations and transformations of individual variables, it can be more efficient to develop risk models directly from the individual variables, as performed in this thesis application. Many weather variables and multicollinearity lead to problems



for estimation but not for prediction.

Trees play an essential role in climate change and fighting against it. Dying and harvested trees reduce the number of trees over decades. Trees are related to climate change in a direct manner as oxygen providers and air cleaners, but also indirectly as carbon stores or air coolers. Therefore, many organizations plant trees to reduce climate change effects. But to a certain degree, climate change effects will be observed in the future. To assist tree planting and commercial forest harvesting, tree species that are more resistant to coming conditions are needed. Understanding tree mortality processes build the basis to transfer knowledge to predictions for a future world that faces climate change.



## 6 Acknowledgment

First, I would like to thank Prof. Donna Ankerst for her dedicated supervision, patience, and productive discussions. Thank you for your great professional and personal support for my work throughout my Ph.D. student time. I especially appreciated your leading in publication processes and pushing projects forward. Further, I like to thank you for the opportunity and the support for going to international conferences and working in international collaborations.

Great thanks go to Prof. Jon Gelfond and Prof. Aurélien Tellier for serving on my Ph.D. committee.

I like to thank Dr. Hannes Petermeier for mentoring, thoughtful comments, encouraging conversations, time together in the office, and great work together in teaching.

I would also greatly thank all co-authors and project partners, especially Wolfgang Falk and Prof. Annette Menzel, for their support and scientific contributions.

Finally, the greatest thanks go to my parents for supporting me during studying and making it possible for me to do my Ph.D. Further, I like to thank my family and friends for supporting me during this time.



## 7 References

- Abbott, R. D. (1985). "Logistic regression in survival analysis". In: *American journal of epidemiology* 121.3, pp. 465–471. ISSN: 0002-9262. DOI: 10.1093/oxfordjournals.aje.a114019..
- Abraham, B. and J. Ledolter (2006). *Introduction to regression modeling*. Duxbury applied series. Belmont, Calif.: Thomson Brooks/Cole. ISBN: 9780534420758. URL: <http://www.loc.gov/catdir/enhancements/fy1215/2004109839-d.html>.
- Adam-Poupart, A., A. Smargiassi, M.-A. Busque, P. Duguay, M. Fournier, J. Zayed, and F. Labrèche (2015). "Effect of summer outdoor temperatures on work-related injuries in Quebec (Canada)". In: *Occupational and environmental medicine* 72.5, pp. 338–345. DOI: 10.1136/oemed-2014-102428.
- Adams, H. D., M. J. B. Zeppel, W. R. L. Anderegg, H. Hartmann, S. M. Landhäuser, et al. (2017). "A multi-species synthesis of physiological mechanisms in drought-induced tree mortality". In: *Nature ecology & evolution* 1.9, pp. 1285–1291. DOI: 10.1038/s41559-017-0248-x.
- Ajdacic-Gross, V., C. Lauber, R. Sansossio, M. Bopp, D. Eich, M. Gostynski, F. Gutzwiller, and W. Rössler (2007). "Seasonal associations between weather conditions and suicide—evidence against a classic hypothesis". In: *American journal of epidemiology* 165.5, pp. 561–569. ISSN: 0002-9262. DOI: 10.1093/aje/kwk034.
- Allen, C. D., D. D. Breshears, and N. G. McDowell (2015). "On underestimation of global vulnerability to tree mortality and forest die-off from hotter drought in the Anthropocene". In: *Ecosphere* 6.8, art129. ISSN: 2150-8925. DOI: 10.1890/ES15-00203.1.
- Allen, C. D., A. K. Macalady, H. Chenchouni, D. Bachelet, N. McDowell, M. Vennetier, T. Kitzberger, A. Rigling, D. D. Breshears, E. H. Hogg, P. Gonzalez, R. Fensham, Z. Zhang, J. Castro, N. Demidova, J.-H. Lim, G. Allard, S. W. Running, A. Semerci, and N. Cobb (2010). "A global overview of drought and heat-induced tree mortality reveals emerging climate change risks for forests". In: *Forest Ecology and Management* 259.4, pp. 660–684. ISSN: 03781127. DOI: 10.1016/j.foreco.2009.09.001.
- Amaya-Fragoso, E. and C. M. García-Pérez (2021). "Improving prostate biopsy decision making in Mexican patients: Still a major public health concern". In: *Urologic oncology* 39.12, 831.e11–831.e18. DOI: 10.1016/j.urolonc.2021.05.022.
- Anderegg, W. R. L., J. A. Hicke, R. A. Fisher, C. D. Allen, J. Aukema, B. Bentz, S. Hood, J. W. Lichstein, A. K. Macalady, N. McDowell, Y. Pan, K. Raffa, A. Sala, J. D. Shaw, N. L. Stephenson, C. Tague, and M. Zeppel (2015). "Tree mortality from drought, insects, and their interactions in a changing climate". In: *The New phytologist* 208.3, pp. 674–683. DOI: 10.1111/nph.13477.
- Ankerst, D. P., A. Boeck, S. J. Freedland, I. M. Thompson, A. M. Cronin, et al. (2012). "Evaluating the PCPT risk calculator in ten international biopsy cohorts: results from the Prostate Biopsy Collaborative Group". In: *World journal of urology* 30.2, pp. 181–187. DOI: 10.1007/s00345-011-0818-5.

- Ankerst, D. P., J. Hoefler, S. Bock, P. J. Goodman, A. Vickers, J. Hernandez, L. J. Sokoll, M. G. Sanda, J. T. Wei, R. J. Leach, and I. M. Thompson (2014). "Prostate Cancer Prevention Trial risk calculator 2.0 for the prediction of low- vs high-grade prostate cancer". In: *Urology* 83.6, pp. 1362–1367. DOI: 10.1016/j.urology.2014.02.035.
- Ankerst, D. P., J. Straubinger, K. Selig, L. Guerrios, A. de Hoedt, J. Hernandez, M. A. Liss, R. J. Leach, S. J. Freedland, M. W. Kattan, R. Nam, A. Haese, F. Montorsi, S. A. Boorjian, M. R. Cooperberg, C. Poyet, E. Vertosick, and A. J. Vickers (2018). "A Contemporary Prostate Biopsy Risk Calculator Based on Multiple Heterogeneous Cohorts". In: *European urology* 74.2, pp. 197–203. DOI: 10.1016/j.eururo.2018.05.003.
- Aschauer, E., E. Ritter, H. Resch, H. Thoeni, and H. Spatzenegger (2007). "Verletzungen und Verletzungsrisiko beim Ski- und Snowboardsport". In: *Der Unfallchirurg* 110.4, pp. 301–306. ISSN: 0177-5537. DOI: 10.1007/s00113-007-1263-1.
- Austrian Board of Trustees for Alpine Safety (2021). *Slope rules*. URL: <https://www.alpinesicherheit.at/de/Pisten-Ordnungs-Entwurf/> (visited on 11/13/2021).
- Bennett, D. A. (2001). "How can I deal with missing data in my study?" In: *Australian and New Zealand Journal of Public Health* 25.5, pp. 464–469. ISSN: 13260200. DOI: 10.1111/j.1467-842X.2001.tb00294.x.
- Bergrettung (2022a). *Daten - Zahlen - Fakten*. URL: <https://bergrettung.at/medien/statistik/> (visited on 05/05/2022).
- (2022b). *geborgene Personen*. URL: <https://bergrettung.at/medien/statistik/> (visited on 05/05/2022).
- Bodner, T. E. (2008). "What Improves with Increased Missing Data Imputations?" In: *Structural Equation Modeling: A Multidisciplinary Journal* 15.4, pp. 651–675. ISSN: 1070-5511. DOI: 10.1080/10705510802339072.
- Boeck, A., J. Dieler, P. Biber, H. Pretzsch, and D. P. Ankerst (2014). "Predicting Tree Mortality for European Beech in Southern Germany Using Spatially Explicit Competition Indices". In: *Forest Science* 60.4, pp. 613–622. ISSN: 0015-749X. DOI: 10.5849/forsci.12-133.
- Bombi, P., E. D'Andrea, N. Rezaie, M. Cammarano, and G. Matteucci (2017). "Which climate change path are we following? Bad news from Scots pine". In: *PloS one* 12.12, e0189468. DOI: 10.1371/journal.pone.0189468.
- Brandl, S., C. Paul, T. Knoke, and W. Falk (2020). "The influence of climate and management on survival probability for Germany's most important tree species". In: *Forest Ecology and Management* 458, p. 117652. ISSN: 03781127. DOI: 10.1016/j.foreco.2019.117652.
- Breunig, C. (2019). "Testing Missing at Random Using Instrumental Variables". In: *Journal of Business & Economic Statistics* 37.2, pp. 223–234. ISSN: 0735-0015. DOI: 10.1080/07350015.2017.1302879.
- Brown, M. L. and J. F. Kros (2003). "Data mining and the impact of missing data". In: *Industrial Management & Data Systems* 103.8, pp. 611–621. ISSN: 0263-5577. DOI: 10.1108/02635570310497657.
- Brun, P., A. Psomas, C. Ginzler, W. Thuiller, M. Zappa, and N. E. Zimmermann (2020). "Large-scale early-wilting response of Central European forests to the 2018 extreme drought". In: *Global change biology* 26.12, pp. 7021–7035. DOI: 10.1111/gcb.15360.
- Buras, A., A. Rammig, and C. S. Zang (2020). "Quantifying impacts of the 2018 drought on European ecosystems in comparison to 2003". In: *Biogeosciences* 17.6, pp. 1655–1672. DOI: 10.5194/bg-17-1655-2020.

- 
- Burkart, K. G., M. Brauer, A. Y. Aravkin, W. W. Godwin, S. I. Hay, J. He, V. C. Iannucci, S. L. Larson, S. S. Lim, J. Liu, C. J. L. Murray, P. Zheng, M. Zhou, and J. D. Stanaway (2021). "Estimating the cause-specific relative risks of non-optimal temperature on daily mortality: a two-part modelling approach applied to the Global Burden of Disease Study". In: *The Lancet* 398.10301, pp. 685–697. ISSN: 01406736. DOI: 10.1016/S0140-6736(21)01700-1.
- Carbunaru, S., O. S. Nettey, P. Gogana, I. B. Helenowski, B. Jovanovic, M. Ruden, C. M. P. Hollowell, R. Sharifi, R. A. Kittles, E. Schaeffer, P. Gann, and A. B. Murphy (2019). "A comparative effectiveness analysis of the PBCG vs. PCPT risks calculators in a multi-ethnic cohort". In: *BMC urology* 19.1, p. 121. DOI: 10.1186/s12894-019-0553-6.
- Carnicer, J., M. Coll, M. Ninyerola, X. Pons, G. Sánchez, and J. Peñuelas (2011). "Widespread crown condition decline, food web disruption, and amplified tree mortality with increased climate change-type drought". In: *Proceedings of the National Academy of Sciences of the United States of America* 108.4, pp. 1474–1478. DOI: 10.1073/pnas.1010070108.
- Caudullo, G., W. Tinner, and D. de Rigo (2016). "Picea abies in Europe: distribution, habitat, usage and threats". In:
- Chakraborty, D., L. Dobor, A. Zolles, T. Hlásny, and S. Schueler (2021). "High-resolution gridded climate data for Europe based on bias-corrected EURO-CORDEX: The ECLIPS dataset". In: *Geoscience Data Journal* 8.2, pp. 121–131. ISSN: 2049-6060. DOI: 10.1002/gdj3.110.
- Choat, B., T. J. Brodribb, C. R. Brodersen, R. A. Duursma, R. López, and B. E. Medlyn (2018). "Triggers of tree mortality under drought". In: *Nature* 558.7711, pp. 531–539. DOI: 10.1038/s41586-018-0240-x.
- Chow, F. K., S. F. de Wekker, and B. J. Snyder (2013). *Mountain Weather Research and Forecasting*. Dordrecht: Springer Netherlands. ISBN: 978-94-007-4097-6. DOI: 10.1007/978-94-007-4098-3.
- Ciais, P., M. Reichstein, N. Viovy, A. Granier, J. Ogee, et al. (2005). "Europe-wide reduction in primary productivity caused by the heat and drought in 2003". In: *Nature* 437.7058, pp. 529–533. DOI: 10.1038/nature03972.
- Colangelo, M., J. J. Camarero, M. Borghetti, T. Gentilesca, J. Oliva, M.-A. Redondo, and F. Ripullone (2018). "Drought and Phytophthora Are Associated With the Decline of Oak Species in Southern Italy". In: *Frontiers in plant science* 9, p. 1595. ISSN: 1664-462X. DOI: 10.3389/fpls.2018.01595.
- DAV (2015). *Bergunfallstatistik 2014-2015*. URL: [https://www.alpenverein.de/chameleon/public/5eed899e-039b-f088-9a71-c8a26c25e440/Unfallstatistik-2014-15\\_28235.pdf](https://www.alpenverein.de/chameleon/public/5eed899e-039b-f088-9a71-c8a26c25e440/Unfallstatistik-2014-15_28235.pdf). (visited on 11/13/2021).
- Deisenhammer, E. A., G. Kemmler, and P. Parson (2003). "Association of meteorological factors with suicide". In: *Acta psychiatrica Scandinavica* 108.6, pp. 455–459. ISSN: 0001-690X. DOI: 10.1046/j.0001-690X.2003.00219.x.
- Dietze, M. C. and P. R. Moorcroft (2011). "Tree mortality in the eastern and central United States: patterns and drivers". In: *Global change biology* 17.11, pp. 3312–3326. ISSN: 13541013. DOI: 10.1111/j.1365-2486.2011.02477.x.
- Doan, P., P. Graham, J. Lahoud, S. Remmers, M. J. Roobol, L. Kim, and M. I. Patel (2021). "A comparison of prostate cancer prediction models in men undergoing both magnetic resonance imaging and transperineal biopsy: Are the models still relevant?" In: *BJU international* 128 Suppl 3, pp. 36–44. DOI: 10.1111/bju.15554.

- Domínguez-Castro, F., F. Reig, S. M. Vicente-Serrano, E. Aguilar, D. Peña-Angulo, I. Noguera, J. Revuelto, G. van der Schrier, and A. M. El Kenawy (2020). "A multidecadal assessment of climate indices over Europe". In: *Scientific data* 7.1, p. 125. DOI: 10.1038/s41597-020-0464-0.
- Donders, A. R. T., G. J. M. G. van der Heijden, T. Stijnen, and K. G. M. Moons (2006). "Review: a gentle introduction to imputation of missing values". In: *Journal of clinical epidemiology* 59.10, pp. 1087–1091. DOI: 10.1016/j.jclinepi.2006.01.014.
- Dov, D., S. Assaad, A. Syedibrahim, J. Bell, J. Huang, J. Madden, R. Bentley, S. McCall, R. Henao, L. Carin, and W.-C. Foo (2022). "A Hybrid Human-Machine Learning Approach for Screening Prostate Biopsies Can Improve Clinical Efficiency Without Compromising Diagnostic Accuracy". In: *Archives of pathology & laboratory medicine* 146.6, pp. 727–734. DOI: 10.5858/arpa.2020-0850-0A.
- Dunkler, D., P. Gao, S. F. Lee, G. Heinze, C. M. Clase, S. Tobe, K. K. Teo, H. Gerstein, J. F. E. Mann, and R. Oberbauer (2015). "Risk Prediction for Early CKD in Type 2 Diabetes". In: *Clinical journal of the American Society of Nephrology : CJASN* 10.8, pp. 1371–1379. DOI: 10.2215/CJN.10321014.
- Dyderski, M. K., S. Paż, L. E. Frelich, and A. M. Jagodziński (2018). "How much does climate change threaten European forest tree species distributions?" In: *Global change biology* 24.3, pp. 1150–1163. DOI: 10.1111/gcb.13925.
- Eamus, D., N. Boulain, J. Cleverly, and D. D. Breshears (2013). "Global change-type drought-induced tree mortality: vapor pressure deficit is more important than temperature per se in causing decline in tree health". In: *Ecology and evolution* 3.8, pp. 2711–2729. ISSN: 2045-7758. DOI: 10.1002/ece3.664.
- Eaton, E., G. Caudullo, S. Oliveira, and D. de Rigo (2016). "Quercus robur and Quercus petraea in Europe: distribution, habitat, usage and threats." In: *San-Miguel-Ayanz, J., de Rigo, D., Caudullo, G., Houston Durrant, T., Mauri, A. (Eds.), European Atlas of Forest Tree Species. Publ. Off. EU, Luxembourg, pp. e01c6df+*.
- Eickenscheidt, N., H. Puhmann, W. Riek, P. Schmidt-Walter, N. Augustin, and N. Wellbrock (2019). "Spatial Response Patterns in Biotic Reactions of Forest Trees and Their Associations with Environmental Variables in Germany". In: *Status and Dynamics of Forests in Germany*. Ed. by N. Wellbrock and A. Bolte. Vol. 237. Ecological Studies. Cham: Springer International Publishing, pp. 311–354. ISBN: 978-3-030-15732-6. DOI: 10.1007/978-3-030-15734-0\_11.
- Ekeland, A., S. R. Larsen, A. G. Tuxen, and P. Nygaard (1989). "Organization of Skiing Safety in Norway". In: *Skiing Trauma and Safety: Seventh International Symposium*. Ed. by R. J. Johnson, C. D. Mote, and M.-H. Binet. 100 Barr Harbor Drive, PO Box C700, West Conshohocken, PA 19428-2959: ASTM International, pp. 342-342–12. ISBN: 978-0-8031-1197-4. DOI: 10.1520/STP19482S.
- Fabre, B., D. Piou, M.-L. Desprez-Loustau, and B. Marçais (2011). "Can the emergence of pine Diplodia shoot blight in France be explained by changes in pathogen pressure linked to climate change?" In: *Global change biology* 17.10, pp. 3218–3227. ISSN: 13541013. DOI: 10.1111/j.1365-2486.2011.02428.x.
- Faulhaber, M., E. Pocecco, M. Posch, and G. Ruedl (2020). "Accidents during mountain hiking and alpine skiing – epidemiological data from the Austrian Alps". In: *Deutsche Zeitschrift für Sportmedizin/German Journal of Sports Medicine* 71.11-12, pp. 293–299. ISSN: 03445925. DOI: 10.5960/dzsm.2020.465.



- 
- Fick, S. E. and R. J. Hijmans (2017). "WorldClim 2: new 1-km spatial resolution climate surfaces for global land areas". In: *International Journal of Climatology* 37.12, pp. 4302–4315. ISSN: 08998418. DOI: 10.1002/joc.5086.
- Forzieri, G., M. Girardello, G. Ceccherini, J. Spinoni, L. Feyen, H. Hartmann, P. S. A. Beck, G. Camps-Valls, G. Chirici, A. Mauri, and A. Cescatti (2021). "Emergent vulnerability to climate-driven disturbances in European forests". In: *Nature communications* 12.1, p. 1081. DOI: 10.1038/s41467-021-21399-7.
- Gaye, A., Y. Marcon, J. Isaeva, P. LaFlamme, A. Turner, et al. (2014). "DataSHIELD: taking the analysis to the data, not the data to the analysis". In: *International journal of epidemiology* 43.6, pp. 1929–1944. DOI: 10.1093/ije/dyu188.
- George, D. J. (1993). "Weather and mountain activities". In: *Weather* 48.12, pp. 404–410. ISSN: 00431656. DOI: 10.1002/j.1477-8696.1993.tb05829.x.
- Gottfried, M., H. Pauli, A. Futschik, M. Akhalkatsi, P. Barančok, et al. (2012). "Continent-wide response of mountain vegetation to climate change". In: *Nature Climate Change* 2.2, pp. 111–115. ISSN: 1758-678X. DOI: 10.1038/nclimate1329.
- Groenwold, R. H. H., I. R. White, A. R. T. Donders, J. R. Carpenter, D. G. Altman, and K. G. M. Moons (2012). "Missing covariate data in clinical research: when and when not to use the missing-indicator method for analysis". In: *CMAJ : Canadian Medical Association journal = journal de l'Association medicale canadienne* 184.11, pp. 1265–1269. DOI: 10.1503/cmaj.110977.
- Hanel, M., O. Rakovec, Y. Markonis, P. Máca, L. Samaniego, J. Kysely, and R. Kumar (2018). "Revisiting the recent European droughts from a long-term perspective". In: *Scientific reports* 8.1, p. 9499. DOI: 10.1038/s41598-018-27464-4.
- Hanewinkel, M., D. A. Cullmann, M.-J. Schelhaas, G.-J. Nabuurs, and N. E. Zimmermann (2013). "Climate change may cause severe loss in the economic value of European forest land". In: *Nature Climate Change* 3.3, pp. 203–207. ISSN: 1758-678X. DOI: 10.1038/nclimate1687.
- Hanley, J. A. and B. J. McNeil (1982). "The meaning and use of the area under a receiver operating characteristic (ROC) curve". In: *Radiology* 143.1, pp. 29–36. ISSN: 0033-8419. DOI: 10.1148/radiology.143.1.7063747.
- Haylock, M. R., N. Hofstra, A. M. G. Klein Tank, E. J. Klok, P. D. Jones, and M. New (2008). "A European daily high-resolution gridded data set of surface temperature and precipitation for 1950–2006". In: *Journal of Geophysical Research* 113.D20. ISSN: 0148-0227. DOI: 10.1029/2008JD010201.
- Heo, S., W. Lee, and M. L. Bell (2021). "Suicide and Associations with Air Pollution and Ambient Temperature: A Systematic Review and Meta-Analysis". In: *International journal of environmental research and public health* 18.14. DOI: 10.3390/ijerph18147699..
- Hock, R., G. Rasul, C. Adler, B. Cáceres, S. Gruber, Y. Hirabayashi, M. Jackson, A. Käab, S. Kang, S. Kutuzov, A. Milner, U. Molau, S. Morin, B. Orlove, and H. Steltzer (2019). "High Mountain Areas". In: *IPCC Special Report on the Ocean and Cryosphere in a Changing Climate*.
- Hoogland, J., M. van Barneveld, T. P. A. Debray, J. B. Reitsma, T. E. Verstraelen, M. G. W. Dijkgraaf, and A. H. Zwinderman (2020). "Handling missing predictor values when validating and applying a prediction model to new patients". In: *Statistics in medicine* 39.25, pp. 3591–3607. DOI: 10.1002/sim.8682.
- Hughes, R. A., J. Heron, J. A. C. Sterne, and K. Tilling (2019). "Accounting for missing data in statistical analyses: multiple imputation is not always the answer".

- In: *International journal of epidemiology* 48.4, pp. 1294–1304. DOI: 10.1093/ije/dyz032.
- ICP Forests (2022). *Plots and Data*. URL: <http://icp-forests.net/> (visited on 06/07/2022).
- IPCC (2018). *Global Warming of 1.5°C: An IPCC Special Report on the impacts of global warming of 1.5°C above pre-industrial levels and related global greenhouse gas emission pathways, in the context of strengthening the global response to the threat of climate change, sustainable development, and efforts to eradicate poverty* [Masson-Delmotte, V., P. Zhai, H.-O. Pörtner, D. Roberts, J. Skea, P.R. Shukla, A. Pirani, W. Moufouma-Okia, C. Péan, R. Pidcock, S. Connors, J.B.R. Matthews, Y. Chen, X. Zhou, M.I. Gomis, E. Lonnoy, T. Maycock, M. Tignor, and T. Waterfield (eds.)] URL: <https://www.ipcc.ch/sr15/> (visited on 11/13/2021).
- (2014). “Synthesis Report. Contribution of Working Groups I, II and III to the Fifth Assessment Report of the Intergovernmental Panel on Climate Change”. In: 151 pp.
- Issa, M. A., F. Chebana, P. Masselot, C. Campagna, É. Lavigne, P. Gosselin, and T. B. M. J. Ouarda (2021). “A heat-health watch and warning system with extended season and evolving thresholds”. In: *BMC public health* 21.1, p. 1479. DOI: 10.1186/s12889-021-10982-8.
- Jaeger, M. (2006). “On Testing the Missing at Random Assumption”. In: *Machine Learning: ECML 2006*. Ed. by D. Hutchison, T. Kanade, J. Kittler, J. M. Kleinberg, F. Mattern, J. C. Mitchell, M. Naor, O. Nierstrasz, C. Pandu Rangan, B. Steffen, M. Sudan, D. Terzopoulos, D. Tygar, M. Y. Vardi, G. Weikum, J. Fürnkranz, T. Scheffer, and M. Spiliopoulou. Vol. 4212. Lecture Notes in Computer Science. Berlin, Heidelberg: Springer Berlin Heidelberg, pp. 671–678. ISBN: 978-3-540-45375-8. DOI: 10.1007/11871842\_66.
- Jalali, A., R. W. Foley, R. M. Maweni, K. Murphy, D. J. Lundon, T. Lynch, R. Power, F. O’Brien, K. J. O’Malley, D. J. Galvin, G. C. Durkan, T. B. Murphy, and R. W. Watson (2020). “A risk calculator to inform the need for a prostate biopsy: a rapid access clinic cohort”. In: *BMC medical informatics and decision making* 20.1, p. 148. DOI: 10.1186/s12911-020-01174-2.
- Janssen, K. J. M., A. R. T. Donders, F. E. Harrell, Y. Vergouwe, Q. Chen, D. E. Grobbee, and K. G. M. Moons (2010). “Missing covariate data in medical research: to impute is better than to ignore”. In: *Journal of clinical epidemiology* 63.7, pp. 721–727. DOI: 10.1016/j.jclinepi.2009.12.008.
- Jentsch, A. and P. White (2019). “A theory of pulse dynamics and disturbance in ecology”. In: *Ecology* 100.7, e02734. DOI: 10.1002/ecy.2734.
- Jolly, W. M., M. Dobbertin, N. E. Zimmermann, and M. Reichstein (2005). “Divergent vegetation growth responses to the 2003 heat wave in the Swiss Alps”. In: *Geophysical Research Letters* 32.18, n/a–n/a. ISSN: 00948276. DOI: 10.1029/2005gl023252.
- Jornet, K. (2022). *History of Competitions in the mountains*. URL: <https://mtnath.com/history-competitions/> (visited on 05/04/2022).
- Kanimozhi, U., S. Ganapathy, D. Manjula, and A. Kannan (2019). “An Intelligent Risk Prediction System for Breast Cancer Using Fuzzy Temporal Rules”. In: *National Academy Science Letters* 42.3, pp. 227–232. ISSN: 0250-541X. DOI: 10.1007/s40009-018-0732-0.
- Kollanus, V., P. Tiittanen, and T. Lanki (2021). “Mortality risk related to heatwaves in Finland - Factors affecting vulnerability”. In: *Environmental research* 201, p. 111503. DOI: 10.1016/j.envres.2021.111503..

- 
- Kostić, S., L. Kesić, B. Matović, S. Orlović, S. Stojnić, and D. B. Stojanović (2021). "Soil properties are significant modifiers of pedunculate oak (*Quercus robur* L.) radial increment variations and their sensitivity to drought". In: *Dendrochronologia* 67, p. 125838. ISSN: 11257865. DOI: 10.1016/j.dendro.2021.125838.
- Koszevska, I., E. Walawender, A. Baran, J. Zieliński, and Z. Ustrnul (2019). "Foehn wind as a seasonal suicide risk factor in amountain region". In: *Psychiatria i Psychologia Kliniczna* 19.1, pp. 48–53. ISSN: 16446313. DOI: 10.15557/PiPK.2019.0007.
- Krawczyk, B. (2016). "Learning from imbalanced data: open challenges and future directions". In: *Progress in Artificial Intelligence* 5.4, pp. 221–232. ISSN: 2192-6352. DOI: 10.1007/s13748-016-0094-0.
- Kreyling, J., G. L. Wiesenberger, D. Thiel, C. Wohlfart, G. Huber, J. Walter, A. Jentsch, M. Konnert, and C. Beierkuhnlein (2012). "Cold hardiness of *Pinus nigra* Arnold as influenced by geographic origin, warming, and extreme summer drought". In: *Environmental and Experimental Botany* 78, pp. 99–108. ISSN: 00988472. DOI: 10.1016/j.envexpbot.2011.12.026.
- Ladenbauer, W. (2006). "Die Bergrettung, die älteste alpine Rettungsorganisation der Welt". In: *Der Gebirgsfreund* 117.
- Leard B, R. K. (2015). "Weather, Traffic Accidents, and Climate Change: Discussion paper". In: *Washington, DC: Resources for the future (RFF)*, pp. 15–19.
- Leuschner, C. and H. Ellenberg (2017). *Ecology of Central European Forests*. Cham: Springer International Publishing. ISBN: 978-3-319-43040-9. DOI: 10.1007/978-3-319-43042-3.
- Li, C. (2013). "Little's Test of Missing Completely at Random". In: *The Stata Journal: Promoting communications on statistics and Stata* 13.4, pp. 795–809. ISSN: 1536-867X. DOI: 10.1177/1536867X1301300407.
- Lischke, V., C. Byhahn, K. Westphal, and P. Kessler (2001). "Mountaineering accidents in the European Alps: have the numbers increased in recent years?" In: *Wilderness & Environmental Medicine* 12.2, pp. 74–80. ISSN: 10806032. DOI: 10.1580/1080-6032(2001)012[0074:maitea]2.0.co;2.
- Little, R. J. A. (1988). "A Test of Missing Completely at Random for Multivariate Data with Missing Values". In: *Journal of the American Statistical Association* 83.404, pp. 1198–1202. ISSN: 0162-1459. DOI: 10.1080/01621459.1988.10478722.
- Ma, S., P. J. Schreiner, E. R. Seaquist, M. Ugurbil, R. Zmora, and L. S. Chow (2020). "Multiple predictively equivalent risk models for handling missing data at time of prediction: With an application in severe hypoglycemia risk prediction for type 2 diabetes". In: *Journal of biomedical informatics* 103, p. 103379. DOI: 10.1016/j.jbi.2020.103379.
- Machado Nunes Romeiro, J., T. Eid, C. Antón-Fernández, A. Kangas, and E. Trømborg (2022). "Natural disturbances risks in European Boreal and Temperate forests and their links to climate change – A review of modelling approaches". In: *Forest Ecology and Management* 509, p. 120071. ISSN: 03781127. DOI: 10.1016/j.foreco.2022.120071.
- Mandrekar, J. N. (2010). "Receiver operating characteristic curve in diagnostic test assessment". In: *Journal of thoracic oncology : official publication of the International Association for the Study of Lung Cancer* 5.9, pp. 1315–1316. DOI: 10.1097/JTO.0b013e3181ec173d.
- Manion, P. D., ed. (1992). *Forest decline concepts: Based, in part, on presentations from a symposium held in conjunction with the joint meeting of the American*

- Phytopathological Society and the Canadian Phytopathological Society on August 7, 1990, in Grand Rapids, Michigan*. St. Paul, Minn.: APS Press. ISBN: 0890541434.
- Manion, P. D. (1991). *Tree disease concepts*. 2. ed. Englewood Cliffs, N.J.: Prentice-Hall. ISBN: 0139294236.
- Marchi, M., D. Castellanos-Acuña, A. Hamann, T. Wang, D. Ray, and A. Menzel (2020). "ClimateEU, scale-free climate normals, historical time series, and future projections for Europe". In: *Scientific data* 7.1, p. 428. DOI: 10.1038/s41597-020-00763-0.
- Maringer, J., A.-S. Stelzer, C. Paul, and A. T. Albrecht (2021). "Ninety-five years of observed disturbance-based tree mortality modeled with climate-sensitive accelerated failure time models". In: *European Journal of Forest Research* 140.1, pp. 255–272. ISSN: 1612-4669. DOI: 10.1007/s10342-020-01328-x.
- Marini, L., M. P. Ayres, A. Battisti, and M. Faccoli (2012). "Climate affects severity and altitudinal distribution of outbreaks in an eruptive bark beetle". In: *Climatic Change* 115.2, pp. 327–341. ISSN: 0165-0009. DOI: 10.1007/s10584-012-0463-z.
- Marqués, L., J. J. Camarero, A. Gazol, and M. A. Zavala (2016). "Drought impacts on tree growth of two pine species along an altitudinal gradient and their use as early-warning signals of potential shifts in tree species distributions". In: *Forest Ecology and Management* 381, pp. 157–167. ISSN: 03781127. DOI: 10.1016/J.FORECO.2016.09.021.
- Martínez-Solanas, È., M. Quijal-Zamorano, H. Achebak, D. Petrova, J.-M. Robine, F. R. Herrmann, X. Rodó, and J. Ballester (2021). "Projections of temperature-attributable mortality in Europe: a time series analysis of 147 contiguous regions in 16 countries". In: *The Lancet Planetary Health* 5.7, e446–e454. ISSN: 25425196. DOI: 10.1016/S2542-5196(21)00150-9.
- Matoso, A. and J. I. Epstein (2019). "Defining clinically significant prostate cancer on the basis of pathological findings". In: *Histopathology* 74.1, pp. 135–145. DOI: 10.1111/his.13712.
- McDowell, N. G. and C. D. Allen (2015). "Darcy's law predicts widespread forest mortality under climate warming". In: *Nature Climate Change* 5.7, pp. 669–672. ISSN: 1758-678X. DOI: 10.1038/nclimate2641.
- McInnes, J. A., E. M. MacFarlane, M. R. Sim, and P. Smith (2018). "The impact of sustained hot weather on risk of acute work-related injury in Melbourne, Australia". In: *International journal of biometeorology* 62.2, pp. 153–163. DOI: 10.1007/s00484-017-1435-9.
- McIntosh, S. E., A. D. Campbell, J. Dow, and C. K. Grissom (2008). "Mountaineering fatalities on Denali". In: *High altitude medicine & biology* 9.1, pp. 89–95. ISSN: 1527-0297. DOI: 10.1089/ham.2008.1047..
- Mealli, F. and D. B. Rubin (2015). "Clarifying missing at random and related definitions, and implications when coupled with exchangeability: Table 1". In: *Biometrika* 102.4, pp. 995–1000. ISSN: 0006-3444. DOI: 10.1093/biomet/asv035.
- Meier, I. C. and C. Leuschner (2008). "Leaf Size and Leaf Area Index in *Fagus sylvatica* Forests: Competing Effects of Precipitation, Temperature, and Nitrogen Availability". In: *Ecosystems* 11.5, pp. 655–669. ISSN: 1432-9840. DOI: 10.1007/s10021-008-9135-2.
- Mellert, K. H., V. Fensterer, H. Küchenhoff, B. Reger, C. Kölling, H. J. Klemmt, and J. Ewald (2011). "Hypothesis-driven species distribution models for tree species in the Bavarian Alps". In: *Journal of Vegetation Science* 22.4, pp. 635–646. ISSN: 11009233. DOI: 10.1111/j.1654-1103.2011.01274.x.

- 
- Michel, A. K., A.-K. Prescher, W. Seidling, and M. Ferretti (2018). "A policy-relevant infrastructure for long-term, large-scale assessment and monitoring of forest ecosystems". In: *Thünen-Institute of Forest Ecosystems*. DOI: 10.3220/ICP1520841254000.
- Mitchell, S. J. (2013). "Wind as a natural disturbance agent in forests: a synthesis". In: *Forestry* 86.2, pp. 147–157. ISSN: 0015-752X. DOI: 10.1093/forestry/cps058.
- Moravec, V., Y. Markonis, O. Rakovec, M. Svoboda, M. Trnka, R. Kumar, and M. Hanel (2021). "Europe under multi-year droughts: how severe was the 2014–2018 drought period?" In: *Environmental Research Letters* 16.3, p. 034062. DOI: 10.1088/1748-9326/abe828.
- Moreno, A. and H. Hasenauer (2016). "Spatial downscaling of European climate data". In: *International Journal of Climatology* 36.3, pp. 1444–1458. ISSN: 08998418. DOI: 10.1002/joc.4436.
- Mortezavi, A., T. Palsdottir, M. Eklund, V. Chellappa, S. K. Murugan, K. Saba, D. P. Ankerst, E. S. Haug, and T. Nordström (2021). "Head-to-head Comparison of Conventional, and Image- and Biomarker-based Prostate Cancer Risk Calculators". In: *European urology focus* 7.3, pp. 546–553. DOI: 10.1016/j.euf.2020.05.002.
- Mourey, J., M. Marcuzzi, L. Ravel, and F. Pallandre (2019). "Effects of climate change on high Alpine mountain environments: Evolution of mountaineering routes in the Mont Blanc massif (Western Alps) over half a century". In: *Arctic, Antarctic, and Alpine Research* 51.1, pp. 176–189. ISSN: 1523-0430. DOI: 10.1080/15230430.2019.1612216.
- Mueller, R. C., C. M. Scudder, M. E. Porter, R. Talbot Trotter, C. A. Gehring, and T. G. Whitham (2005). "Differential tree mortality in response to severe drought: evidence for long-term vegetation shifts". In: *Journal of Ecology* 93.6, pp. 1085–1093. ISSN: 00220477. DOI: 10.1111/j.1365-2745.2005.01042.x.
- Mueller, T., G. Ruedl, M. Ernstbrunner, F. Plachel, S. Fröhlich, T. Hoffelner, H. Resch, and L. Ernstbrunner (2019). "A Prospective Injury Surveillance Study on Ski Touring". In: *Orthopaedic journal of sports medicine* 7.9, p. 2325967119867676. ISSN: 2325-9671. DOI: 10.1177/2325967119867676..
- Netherer, S., B. Panassiti, J. Pennerstorfer, and B. Matthews (2019). "Acute Drought Is an Important Driver of Bark Beetle Infestation in Austrian Norway Spruce Stands". In: *Frontiers in Forests and Global Change* 2. DOI: 10.3389/ffgc.2019.00039.
- Neumann, M., V. Mues, A. Moreno, H. Hasenauer, and R. Seidl (2017). "Climate variability drives recent tree mortality in Europe". In: *Global change biology* 23.11, pp. 4788–4797. ISSN: 13541013. DOI: 10.1111/gcb.13724.
- Neves, G., N. Gallardo, and F. Vecchia (2017). "A Short Critical History on the Development of Meteorology and Climatology". In: *Climate* 5.1, p. 23. DOI: 10.3390/cli5010023.
- Niinemets, Ü. and F. Valladares (2006). "Tolerance to shade, drought, and waterlogging of temperate northern hemisphere trees and shrubs". In: *Ecological Monographs* 76.4, pp. 521–547. ISSN: 0012-9615. DOI: 10.1890/0012-9615(2006)076[0521:TTSDAW]2.0.CO;2.
- Nijman, S. W. J., T. K. J. Groenhof, J. Hoogland, M. L. Bots, M. Brandjes, J. J. L. Jacobs, F. W. Asselbergs, K. G. M. Moons, and T. P. A. Debray (2021). "Real-time imputation of missing predictor values improved the application of prediction models in daily practice". In: *Journal of clinical epidemiology* 134, pp. 22–34. DOI: 10.1016/j.jclinepi.2021.01.003.

- Nothdurft, A. (2013). "Spatio-temporal prediction of tree mortality based on long-term sample plots, climate change scenarios and parametric frailty modeling". In: *Forest Ecology and Management* 291, pp. 43–54. ISSN: 03781127. DOI: 10.1016/j.foreco.2012.11.028.
- Nykänen, M.-L., H. Peltola, C. Quine, S. Kellomäki, and M. Broadgate (1997). "Factors affecting snow damage of trees with particular reference to European conditions." In: *The Finnish Society of Forest Science and The Finnish Forest Research Institute*. URL: <http://hdl.handle.net/1975/8519>.
- Obladen, N., P. Dechering, G. Skiadaresis, W. Tegel, J. Keßler, S. Höllerl, S. Kaps, M. Hertel, C. Dulamsuren, T. Seifert, M. Hirsch, and A. Seim (2021). "Tree mortality of European beech and Norway spruce induced by 2018-2019 hot droughts in central Germany". In: *Agricultural and Forest Meteorology* 307, p. 108482. ISSN: 01681923. DOI: 10.1016/j.agrformet.2021.108482.
- Österreichisches Kuratorium für Alpine Sicherheit (2022). *Geschichte*. URL: <https://alpinesicherheit.at/das-oeakas/geschichte/> (visited on 05/05/2022).
- Park Williams, A., C. D. Allen, A. K. Macalady, D. Griffin, C. A. Woodhouse, D. M. Meko, T. W. Swetnam, S. A. Rauscher, R. Seager, H. D. Grissino-Mayer, J. S. Dean, E. R. Cook, C. Gangodagamage, M. Cai, and N. G. McDowell (2013). "Temperature as a potent driver of regional forest drought stress and tree mortality". In: *Nature Climate Change* 3.3, pp. 292–297. ISSN: 1758-678X. DOI: 10.1038/nclimate1693.
- Pascual and Callado (2010). "Mountain accidents associated with winter northern flows in the Mediterranean Pyrenees". In: *Tethys, Journal of Weather and Climate of the Western Mediterranean*. ISSN: 16971523. DOI: 10.3369/tethys.2010.7.04.
- Potthoff, R. F., G. E. Tudor, K. S. Pieper, and V. Hasselblad (2006). "Can one assess whether missing data are missing at random in medical studies?" In: *Statistical methods in medical research* 15.3, pp. 213–234. ISSN: 0962-2802. DOI: 10.1191/0962280206sm448oa.
- Presti, J. C., S. Alexeeff, B. Horton, S. Prausnitz, and A. L. Avins (2021). "Prospective validation of the Kaiser Permanente prostate cancer risk calculator in a contemporary, racially diverse, referral population". In: *Urologic oncology* 39.11, 783.e11–783.e19. DOI: 10.1016/j.urolonc.2021.03.023.
- Pretis, F., M. Schwarz, K. Tang, K. Hausteiner, and M. R. Allen (2018). "Uncertain impacts on economic growth when stabilizing global temperatures at 1.5°C or 2°C warming". In: *Philosophical transactions. Series A, Mathematical, physical, and engineering sciences* 376.2119. DOI: 10.1098/rsta.2016.0460.
- Przybylak, R., P. Oliński, M. Koprowski, J. Filipiak, A. Pospieszńska, W. Chorążyczewski, R. Puchałka, and H. P. Dąbrowski (2020). "Droughts in the area of Poland in recent centuries in the light of multi-proxy data". In: *Climate of the Past* 16.2, pp. 627–661. DOI: 10.5194/cp-16-627-2020.
- Puchałka, R., M. Koprowski, J. Gričar, and R. Przybylak (2017). "Does tree-ring formation follow leaf phenology in Pedunculate oak (*Quercus robur* L.)?" In: *European Journal of Forest Research* 136.2, pp. 259–268. ISSN: 1612-4669. DOI: 10.1007/s10342-017-1026-7.
- Puchałka, R., M. Koprowski, J. Przybylak, R. Przybylak, and H. P. Dąbrowski (2016). "Did the late spring frost in 2007 and 2011 affect tree-ring width and earlywood vessel size in Pedunculate oak (*Quercus robur*) in northern Poland?" In: *International journal of biometeorology* 60.8, pp. 1143–1150. DOI: 10.1007/s00484-015-1107-6.

- 
- Pureswaran, D. S., A. Roques, and A. Battisti (2018). "Forest Insects and Climate Change". In: *Current Forestry Reports* 4.2, pp. 35–50. DOI: 10.1007/s40725-018-0075-6.
- Quilodrán, C. S., M. Currat, and J. I. Montoya-Burgos (2021). "Air temperature influences early Covid-19 outbreak as indicated by worldwide mortality". In: *The Science of the total environment* 792, p. 148312. DOI: 10.1016/j.scitotenv.2021.148312.
- R Core Team (2021). *A language and environment for statistical computing*. Vienna, Austria. URL: <https://www.R-project.org/> (visited on 11/13/2021).
- Raffa, K. F., B. H. Aukema, B. J. Bentz, A. L. Carroll, J. A. Hicke, M. G. Turner, and W. H. Romme (2008). "Cross-scale Drivers of Natural Disturbances Prone to Anthropogenic Amplification: The Dynamics of Bark Beetle Eruptions". In: *BioScience* 58.6, pp. 501–517. ISSN: 0006-3568. DOI: 10.1641/B580607.
- Reger, B., C. Kölling, and J. Ewald (2011). "Modelling effective thermal climate for mountain forests in the Bavarian Alps: Which is the best model?" In: *Journal of Vegetation Science* 22.4, pp. 677–687. ISSN: 11009233. DOI: 10.1111/j.1654-1103.2011.01270.x.
- Robusto, C. C. (1957). "The Cosine-Haversine Formula". In: *The American Mathematical Monthly* 64.1, p. 38. ISSN: 00029890. DOI: 10.2307/2309088.
- Rodrigues, M., P. Santana, and A. Rocha (2020). "Modelling climate change impacts on attributable-related deaths and demographic changes in the largest metropolitan area in Portugal: A time-series analysis". In: *Environmental research* 190, p. 109998. DOI: 10.1016/j.envres.2020.109998.
- Roloff, A. and B. M. Grundmann (2008). "Waldbaumarten und ihre Verwendung im Klimawandel." In: *Archiv Forstwes. Landsch. Ökol.* 42, pp. 97–109.
- Roobol, M. J., H. A. van Vugt, S. Loeb, X. Zhu, M. Bul, C. H. Bangma, A. G. L. J. H. van Leenders, E. W. Steyerberg, and F. H. Schröder (2012). "Prediction of prostate cancer risk: the role of prostate volume and digital rectal examination in the ERSPC risk calculators". In: *European urology* 61.3, pp. 577–583. DOI: 10.1016/j.eururo.2011.11.012.
- Rosenzweig, C., D. Karoly, M. Vicarelli, P. Neofotis, Q. Wu, G. Casassa, A. Menzel, T. L. Root, N. Estrella, B. Seguin, P. Tryjanowski, C. Liu, S. Rawlins, and A. Imeson (2008). "Attributing physical and biological impacts to anthropogenic climate change". In: *Nature* 453.7193, pp. 353–357. DOI: 10.1038/nature06937.
- Rubin, D. B. (1978). "Multiple Imputations in Sample Surveys: A Phenomenological Bayesian Approach to Nonresponse". In: *Proceedings of the Survey Research Methods Section, Washington, DC: American Statistical Association*, pp. 20–34.
- Rubio-Briones, J., A. Borque-Fernando, L. M. Esteban, J. M. Mascarós, M. Ramírez-Backhaus, J. Casanova, A. Collado, C. Mir, A. Gómez-Ferrer, A. Wong, F. Aragón, A. Calatrava, J. A. López-Guerrero, J. Groskopf, J. Schalken, W. van Criekinge, and J. Domínguez-Escrig (2020). "Validation of a 2-gene mRNA urine test for the detection of  $\geq$ GG2 prostate cancer in an opportunistic screening population". In: *The Prostate* 80.6, pp. 500–507. DOI: 10.1002/pros.23964.
- Ruedl, G., C. Fink, A. Schranz, R. Sommersacher, W. Nachbauer, and M. Burtscher (2012). "Impact of environmental factors on knee injuries in male and female recreational skiers". In: *Scandinavian journal of medicine & science in sports* 22.2, pp. 185–189. DOI: 10.1111/j.1600-0838.2011.01286.x.
- Rugg, C., L. Tiefenthaler, S. Rauch, H. Gatterer, P. Paal, and M. Ströhle (2020). "Rock Climbing Emergencies in the Austrian Alps: Injury Patterns, Risk Analysis and

- Preventive Measures". In: *International journal of environmental research and public health* 17.20. DOI: 10.3390/ijerph17207596.
- Salgado, C. M., C. Azevedo, H. Proença, and S. M. Vieira (2016). *Secondary Analysis of Electronic Health Records: Missing Data*. Cham (CH). ISBN: 9783319437408. DOI: 10.1007/978-3-319-43742-2\_13.
- Sangüesa-Barreda, G., A. Di Filippo, G. Piovesan, V. Rozas, L. Di Fiore, M. García-Hidalgo, A. I. García-Cervigón, D. Muñoz-Garachana, M. Baliva, and J. M. Olano (2021). "Warmer springs have increased the frequency and extension of late-frost defoliations in southern European beech forests". In: *The Science of the total environment* 775, p. 145860. DOI: 10.1016/j.scitotenv.2021.145860.
- Saucy, A., M. S. Ragettli, D. Vienneau, K. de Hoogh, L. Tangermann, B. Schäffer, J.-M. Wunderli, N. Probst-Hensch, and M. Rösli (2021). "The role of extreme temperature in cause-specific acute cardiovascular mortality in Switzerland: A case-crossover study". In: *The Science of the total environment* 790, p. 147958. DOI: 10.1016/j.scitotenv.2021.147958.
- Schmidtlein, S., U. Faude, O. Rössler, H. Feilhauer, J. Ewald, and A. Meyn (2013). "Differences between recent and historical records of upper species limits in the northern European Alps". In: *Erdkunde* 67.4, pp. 345–354. ISSN: 00140015. DOI: 10.3112/erdkunde.2013.04.04.
- Schuldt, B., A. Buras, M. Arend, Y. Vitasse, C. Beierkuhnlein, et al. (2020). "A first assessment of the impact of the extreme 2018 summer drought on Central European forests". In: *Basic and Applied Ecology* 45, pp. 86–103. ISSN: 14391791. DOI: 10.1016/j.baae.2020.04.003.
- Schwarz, G. (1978). "Estimating the Dimension of a Model". In: *Annals of Statistics* 6.2, pp. 461–464. URL: [www.jstor.org/stable/2958889](http://www.jstor.org/stable/2958889).
- Senf, C., A. Buras, C. S. Zang, A. Rammig, and R. Seidl (2020). "Excess forest mortality is consistently linked to drought across Europe". In: *Nature communications* 11.1, p. 6200. DOI: 10.1038/s41467-020-19924-1.
- Senf, C. and R. Seidl (2021a). "Mapping the forest disturbance regimes of Europe". In: *Nature Sustainability* 4.1, pp. 63–70. DOI: 10.1038/s41893-020-00609-y.
- (2021b). "Persistent impacts of the 2018 drought on forest disturbance regimes in Europe". In: *Biogeosciences* 18.18, pp. 5223–5230. DOI: 10.5194/bg-18-5223-2021.
- Sim, K., Y. Kim, M. Hashizume, A. Gasparrini, B. Armstrong, F. Sera, C. F. S. Ng, Y. Honda, and Y. Chung (2020). "Nonlinear temperature-suicide association in Japan from 1972 to 2015: Its heterogeneity and the role of climate, demographic, and socioeconomic factors". In: *Environment international* 142, p. 105829. DOI: 10.1016/j.envint.2020.105829.
- Sisk, R., L. Lin, M. Sperrin, J. K. Barrett, B. Tom, K. Diaz-Ordaz, N. Peek, and G. P. Martin (2021). "Informative presence and observation in routine health data: A review of methodology for clinical risk prediction". In: *Journal of the American Medical Informatics Association : JAMIA* 28.1, pp. 155–166. DOI: 10.1093/jamia/ocaa242.
- Smith, G. A. and C. D. Kiesinger (2020). *mountaineering*. Ed. by Encyclopedia Britannica. URL: <https://www.britannica.com/sports/mountaineering> (visited on 05/04/2022).
- Soulé, B., B. Lefèvre, and E. Boutroy (2017). "The dangerousness of mountain recreation: A quantitative overview of fatal and non-fatal accidents in France". In: *European journal of sport science* 17.7, pp. 931–939. DOI: 10.1080/17461391.2017.1324525.



- 
- Spector, J. T., D. K. Bonauto, L. Sheppard, T. Busch-Isaksen, M. Calkins, D. Adams, M. Lieblich, and R. A. Fenske (2016). "A Case-Crossover Study of Heat Exposure and Injury Risk in Outdoor Agricultural Workers". In: *PLoS one* 11.10, e0164498. DOI: 10.1371/journal.pone.0164498.
- Sperrin, M., G. P. Martin, R. Sisk, and N. Peek (2020). "Missing data should be handled differently for prediction than for description or causal explanation". In: *Journal of clinical epidemiology* 125, pp. 183–187. DOI: 10.1016/j.jclinepi.2020.03.028.
- Stein, C. (1956). "Inadmissibility of the usual estimator for the mean of a multivariate distribution". In: *Proc. Third Berkeley Symp. Math. Statist.* 1, pp. 197–206.
- Stojadinovic, M., T. Trifunovic, and S. Jankovic (2020). "Adaptation of the prostate biopsy collaborative group risk calculator in patients with PSA less than 10 ng/ml improves its performance". In: *International urology and nephrology* 52.10, pp. 1811–1819. DOI: 10.1007/s11255-020-02517-8.
- Ströhle, M., B. Wallner, M. Lanthaler, S. Rauch, H. Brugger, and P. Paal (2018). "Lightning accidents in the Austrian alps - a 10-year retrospective nationwide analysis". In: *Scandinavian journal of trauma, resuscitation and emergency medicine* 26.1, p. 74. DOI: 10.1186/s13049-018-0543-9.
- Studerus, E., K. Beck, P. Fusar-Poli, and A. Riecher-Rössler (2020). "Development and Validation of a Dynamic Risk Prediction Model to Forecast Psychosis Onset in Patients at Clinical High Risk". In: *Schizophrenia bulletin* 46.2, pp. 252–260. DOI: 10.1093/schbul/sbz059.
- Sturrock, R. N., S. J. Frankel, A. V. Brown, P. E. Hennon, J. T. Kliejunas, K. J. Lewis, J. J. Worrall, and A. J. Woods (2011). "Climate change and forest diseases". In: *Plant Pathology* 60.1, pp. 133–149. ISSN: 00320862. DOI: 10.1111/j.1365-3059.2010.02406.x.
- Sung, H., J. Ferlay, R. L. Siegel, M. Laversanne, I. Soerjomataram, A. Jemal, and F. Bray (2021). "Global Cancer Statistics 2020: GLOBOCAN Estimates of Incidence and Mortality Worldwide for 36 Cancers in 185 Countries". In: *CA: a cancer journal for clinicians* 71.3, pp. 209–249. DOI: 10.3322/caac.21660.
- Taccoen, A., C. Piedallu, I. Seynave, A. Gégout-Petit, L.-M. Nageleisen, N. Bréda, and J.-C. Gégout (2021). "Climate change impact on tree mortality differs with tree social status". In: *Forest Ecology and Management* 489, p. 119048. ISSN: 03781127. DOI: 10.1016/j.foreco.2021.119048.
- Taccoen, A., C. Piedallu, I. Seynave, V. Perez, A. Gégout-Petit, L.-M. Nageleisen, J.-D. Bontemps, and J.-C. Gégout (2019). "Background mortality drivers of European tree species: climate change matters". In: *Proceedings. Biological sciences* 286.1900, p. 20190386. DOI: 10.1098/rspb.2019.0386.
- Techel, F., F. Jarry, G. Kronthaler, S. Mitterer, P. Nairz, M. Pavšek, M. Valt, and G. Darms (2016). "Avalanche fatalities in the European Alps: long-term trends and statistics". In: *Geographica Helvetica* 71.2, pp. 147–159. DOI: 10.5194/gh-71-147-2016.
- Thalheimer, L., F. Otto, and S. Abele (2021). "Deciphering Impacts and Human Responses to a Changing Climate in East Africa". In: *Frontiers in Climate* 3. DOI: 10.3389/fclim.2021.692114.
- Thom, D. and R. Seidl (2016). "Natural disturbance impacts on ecosystem services and biodiversity in temperate and boreal forests". In: *Biological reviews of the Cambridge Philosophical Society* 91.3, pp. 760–781. DOI: 10.1111/brv.12193.

- Thurm, E. A., L. Hernandez, A. Baltensweiler, S. Ayan, E. Rasztovits, K. Bielak, T. M. Zlatanov, D. Hladnik, B. Balic, A. Freudenschuss, R. Büchsenmeister, and W. Falk (2018). "Alternative tree species under climate warming in managed European forests". In: *Forest Ecology and Management* 430, pp. 485–497. ISSN: 03781127. DOI: 10.1016/j.foreco.2018.08.028.
- Tolksdorf, J., M. W. Kattan, S. A. Boorjian, S. J. Freedland, K. Saba, C. Poyet, L. Guerrios, A. de Hoedt, M. A. Liss, R. J. Leach, J. Hernandez, E. Vertosick, A. J. Vickers, and D. P. Ankerst (2019). "Multi-cohort modeling strategies for scalable globally accessible prostate cancer risk tools". In: *BMC medical research methodology* 19.1, p. 191. DOI: 10.1186/s12874-019-0839-0.
- Tranquillini, W. (1982). "Frost-Drought and Its Ecological Significance". In: *Physiological Plant Ecology II*. Ed. by O. L. Lange, P. S. Nobel, C. B. Osmond, and H. Ziegler. Berlin, Heidelberg: Springer Berlin Heidelberg, pp. 379–400. ISBN: 978-3-642-68152-3. DOI: 10.1007/978-3-642-68150-9\_12.
- Unguryanu, T. N., A. M. Grjibovski, T. A. Trovik, B. Ytterstad, and A. V. Kudryavtsev (2020). "Weather Conditions and Outdoor Fall Injuries in Northwestern Russia". In: *International journal of environmental research and public health* 17.17. DOI: 10.3390/ijerph17176096.
- Urban, A., C. Di Napoli, H. L. Cloke, J. Kyselý, F. Pappenberger, et al. (2021). "Evaluation of the ERA5 reanalysis-based Universal Thermal Climate Index on mortality data in Europe". In: *Environmental research* 198, p. 111227. DOI: 10.1016/j.envres.2021.111227.
- Utkina, I. A. and V. V. Rubtsov (2017). "Studies of Phenological Forms of Pedunculate Oak". In: *Contemporary Problems of Ecology* 10.7, pp. 804–811. ISSN: 1995-4255. DOI: 10.1134/S1995425517070101.
- van Buuren, S. and K. Groothuis-Oudshoorn (2011). "mice : Multivariate Imputation by Chained Equations in R". In: *Journal of Statistical Software* 45.3. DOI: 10.18637/jss.v045.i03.
- van Calster, B., D. J. McLernon, M. van Smeden, L. Wynants, and E. W. Steyerberg (2019). "Calibration: the Achilles heel of predictive analytics". In: *BMC medicine* 17.1, p. 230. DOI: 10.1186/s12916-019-1466-7.
- van der Heijden, G. J. M. G., A. R. T. Donders, T. Stijnen, and K. G. M. Moons (2006). "Imputation of missing values is superior to complete case analysis and the missing-indicator method in multivariable diagnostic research: a clinical example". In: *Journal of clinical epidemiology* 59.10, pp. 1102–1109. DOI: 10.1016/j.jclinepi.2006.01.015.
- van Riel, L. A. M. J. G., A. Jager, D. Meijer, A. W. Postema, R. S. Smit, A. N. Vis, T. M. de Reijke, H. P. Beerlage, and J. R. Oddens (2022). "Predictors of clinically significant prostate cancer in biopsy-naïve and prior negative biopsy men with a negative prostate MRI: improving MRI-based screening with a novel risk calculator". In: *Therapeutic advances in urology* 14, p. 17562872221088536. ISSN: 1756-2872. DOI: 10.1177/17562872221088536.
- Vander Mijnsbrugge, K., A. Turcsán, É. Erdélyi, and H. Beeckman (2020). "Drought Treated Seedlings of *Quercus petraea* (Matt.) Liebl., *Q. robur* L. and Their Morphological Intermediates Show Differential Radial Growth and Wood Anatomical Traits". In: *Forests* 11.2, p. 250. DOI: 10.3390/f11020250.
- Vanoni, M., H. Bugmann, M. Nötzli, and C. Bigler (2016). "Drought and frost contribute to abrupt growth decreases before tree mortality in nine temperate tree species". In:

- 
- Forest Ecology and Management* 382, pp. 51–63. ISSN: 03781127. DOI: 10.1016/j.foreco.2016.10.001.
- Varma, M., K. Narahari, M. Mason, J. D. Oxley, and D. M. Berney (2018). “Contemporary prostate biopsy reporting: insights from a survey of clinicians’ use of pathology data”. In: *Journal of clinical pathology* 71.10, pp. 874–878. DOI: 10.1136/jclinpath-2018-205093.
- Vickers, A. J., A. M. Cronin, M. J. Roobol, J. Hugosson, J. S. Jones, et al. (2010). “The relationship between prostate-specific antigen and prostate cancer risk: the Prostate Biopsy Collaborative Group”. In: *Clinical cancer research : an official journal of the American Association for Cancer Research* 16.17, pp. 4374–4381. DOI: 10.1158/1078-0432.CCR-10-1328.
- Wang, H., Z. Lu, and Y. Liu (2021). *Score test for missing at random or not*. DOI: 10.48550/arXiv.2105.12921.
- Wang, W., C. Peng, D. D. Kneeshaw, G. R. Larocque, and Z. Luo (2012). “Drought-induced tree mortality: ecological consequences, causes, and modeling”. In: *Environmental Reviews* 20.2, pp. 109–121. ISSN: 1181-8700. DOI: 10.1139/a2012-004.
- Wei, G., B. D. Kelly, B. Timm, M. Perera, D. J. Lundon, G. Jack, and D. M. Bolton (2021). “Clash of the calculators: External validation of prostate cancer risk calculators in men undergoing mpMRI and transperineal biopsy”. In: *BJUI compass* 2.3, pp. 194–201. DOI: 10.1002/bco2.58.
- White, I. R., P. Royston, and A. M. Wood (2011). “Multiple imputation using chained equations: Issues and guidance for practice”. In: *Statistics in medicine* 30.4, pp. 377–399. DOI: 10.1002/sim.4067.
- World Meteorological Organization (2017). *WMO Guidelines on the Calculation of Climate Normals*. URL: [https://library.wmo.int/doc\\_num.php?explnum\\_id=4453](https://library.wmo.int/doc_num.php?explnum_id=4453) (visited on 11/13/2021).
- Yildizhan, M., M. Balci, U. Eroğlu, E. Asil, S. Coser, A. Y. Özercan, B. Köseoğlu, O. Güzel, A. Asfuroğlu, and A. Tuncel (2022). “An analysis of three different prostate cancer risk calculators applied prior to prostate biopsy: A Turkish cohort validation study”. In: *Andrologia* 54.2, e14329. DOI: 10.1111/and.14329.
- Zacharias, S. (2012). “Literaturstudie zum Einfluss des Wetters auf die menschliche Gesundheit.” In: *Umweltforschungsplan des Bundesministeriums für Umwelt, Naturschutz, Bau und Reaktorsicherheit UFOPLAN no. 3711 61 238*.
- Zentralanstalt für Meteorologie und Geodynamik (2022). *Geschichte*. URL: <https://www.zamg.ac.at/cms/de/topmenu/ueber-uns/geschichte> (visited on 05/06/2022).
- Zhou, A. G., D. C. Salles, I. V. Samarska, and J. I. Epstein (2019). “How Are Gleason Scores Categorized in the Current Literature: An Analysis and Comparison of Articles Published in 2016-2017”. In: *European urology* 75.1, pp. 25–31. DOI: 10.1016/j.eururo.2018.07.021.

